(1)

NASA CR-165456

R81AEG393

National Aeronautics and
Space Administration

DO NOT DESTROY
RETURN TO LIBRARY

STRUCTURES PERFORMANCE, BENEFIT, COST - STUDY

by
Otto G. Woike

GENERAL ELECTRIC COMPANY

SEPTEMBER 1981

21 OCT 1981
RESEARCH ... LIBRARY

Prepared For
National Aeronautics and Space Administration

NASA-Lewis Research Center
NAS3-22049

NASA-CR-165456

MRI-17185

1. Report No.	2. Government Accession No.	3. Recipient's Catalog No.
NASA CR-165456		

4. Title and Subtitle	5. Report Date
STRUCTURES PERFORMANCE, BENEFIT, COST-STUDY ADVANCED STRUCTURES CONCEPTS FOR TURBOFANS	September 1981
	6. Performing Organization Code
7. Author(s)	8. Performing Organization Report No.
O.G. Woike, C.T. Salemme, E.M. Stearns, P. Oritz, M.L. Roberts	R81AEG393
	10. Work Unit No.
9. Performing Organization Name and Address	11. Contract or Grant No.
General Electric Company Aircraft Engine Business Group Cincinnati, Ohio 45215	NAS3-22049
	13. Type of Report and Period Covered
12. Sponsoring Agency Name and Address	Contract - 1 year
National Aeronautics and Space Administration Lewis Research Center 21000 Brookpark Road Cleveland, Ohio 44135	14. Sponsoring Agency Code

15. Supplementary Notes

Project Manager - L.J. Kiraly
NASA-Lewis Research Center
21000 Brookpark Road (Mail Stop 49-6)
Cleveland, Ohio 44135

16. Abstract

This systems study identifies new technology concepts and structural analysis development needs which could lead to improved life cycle cost for future high-bypass turbofans. The NASA-GE energy efficient engine (E^3) technology is used as a base to assess the concept benefits. Recommended programs are identified for attaining these generic structural and other beneficial technologies.

17. Key Words (Suggested by Author(s))	18. Distribution Statement
High Bypass Turbofans Advanced Engine Structures Concepts Energy Efficient Engine (E^3)	Unclassified Unlimited

19. Security Classif. (of this report)	20. Security Classif. (of this page)	21. No. of Pages	22. Price*
Unclassified	Unclassified	192	

* For sale by the National Technical Information Service, Springfield, Virginia 22161

NASA-C-168 (Rev. 10-75)

Page intentionally left blank

FOREWORD

The work was performed by the Technology Programs and Performance Technology Department of General Electric's Aircraft Engine Group. The program was conducted for the National Aeronautics and Space Administration, Lewis Research Center, Cleveland, Ohio under Contract NAS3-22049. Mr. L. J. Kiraly was the NASA Project Manager.

This report was prepared by O. G. Woike, General Electric Program Manager. Contributors included C. T. Salemme, E. M. Stearns, P. Ortiz, M. L. Roberts, J. L. Baughman, R. P. Johnston, H. F. Demel, R. G. Stabrylla, and G. A. Coffinberry.

Page intentionally left blank

TABLE OF CONTENTS

		Page
1.0	SUMMARY	1
2.0	INTRODUCTION	6
3.0	METHOD OF ANALYSIS	9
4.0	ADVANCED CONCEPT STUDIES	15
	4.1 Cycle Performance Improvement Studies	17
	4.2 HPT Metal Cooling Improvements	36
	4.3 HPT Modulated Cooling Flow	38
	4.4 HPT Metal Temperature Improvement	40
	4.5 Metal Coating Improvements	42
	4.6 Shortened Fan Configuration	44
	4.7 HPC Active Clearance Control	60
	4.8 Advanced Fan Blades	71
	4.9 Low-Emissions Single Annular Combustor	80
	4.10 Compressor Blisk	82
	4.11 Composite Vanes	83
	4.12 Composite Spinner	87
	4.13 Component Efficiency Improvement	91
	4.14 Variable-Area Nozzle, Mixed-Flow Exhaust	94
	4.15 Turbomachinery 3D Aero Analysis	96
	4.16 LPT Flared Flowpath	98
	4.17 LPT Orthogonal Blading	100
	4.18 Advanced Fuel Delivery System	102
	4.19 Advanced Secondary Power System, AEA	114
	4.20 Exhaust Nozzle Load Isolation and Alignment Joint	128
5.0	RECOMMENDED TECHNOLOGY PROGRAMS	130
	5.1 Summary	130
	5.2 HPT Metal Cooling Improvements	131
	5.3 HPT Modulated Cooling Flow	132
	5.4 HPT Metal Temperature Improvement	133
	5.5 Metal Coating Improvements	134
	5.6 Shortened Fan Flowpath	135
	5.7 HPC Active Clearance Control	136
	5.8 Advanced Fan Blades	137
	5.9 Low-Emissions Single Annular Combustor	138
	5.10 Compressor Blisk	139
	5.11 Composite Vanes	140
	5.12 Composite Spinner	141
	5.13 Component Efficiency Improvement	142
	5.14 Variable-Area Nozzle, Mixed-Flow Exhaust	143
	5.15 Turbomachinery 3D Aero Analysis	144
	5.16 LPT Flared Flowpath	145
	5.17 LPT Orthogonal Blading	146
	5.18 Advanced Fuel Delivery System	147
	5.19 Advanced Secondary Power System, AEA	148
	5.20 Exhaust Nozzle Load Isolation and Alignment Joint	149

TABLE OF CONTENTS (Concluded)

		Page
6.0	STRUCTURAL AND LIFE ANALYSIS PROGRAMS	150
	6.1 Improved Interface Between Heat Transfer and Stress Analysis	152
	6.2 Simplified Frame Analysis	155
	6.3 Verification of Airfoil Stresses and Deformations	157
	6.4 Dovetail Design Verification Program	159
	6.5 Analysis Tools for Predicting Fabrication Effects	161
	6.6 Structure, Life Analysis, and Test Techniques for Coatings	164
	6.7 Anisotropic Turbine Blade and Vane Life Prediction	166
	6.8 Component Fatigue and Rupture Damage Measurement	168
	6.9 Extend Manson-Halford Damage-Curve Life Analysis Methodology	171
	6.10 Incorporate Damping Into Vibration Analysis of Fan Blades	174
	6.11 Time-Sharing Program for the Analysis of Turbomachinery Vibration	176
	6.12 Transient Blade-Out Modal Analysis	179
	6.13 Transient Analysis and Design Criteria for Engine Seizure Loads	181
7.0	DISTRIBUTION	185

LIST OF ILLUSTRATIONS

Figure		Page
1-1	Task Flow Chart.	2
1-2	Advanced Technology Concepts.	3
1-3	Structural Analysis Needs.	5
2-1	Baseline Energy Efficient Engine.	7
2-2	Large U.S. Commercial Transport Engines Fuel Consumption Trend.	8
2-3	Trend in Engine Performance Parameter Technology.	8
3-1	Direct Operating Cost Variation with Fuel Price.	12
3-2	Aircraft Fleet Definition.	14
4.1-1	Uninstalled sfc at Max Climb vs. CPR and ΔT41 with Assumed Component Efficiency Improvements.	19
4.1-2	Uninstalled sfc at Max Climb vs. CPR and ΔT41 with Assumed Metal Temperature Improvement.	19
4.1-3	Uninstalled sfc at Max Climb vs. CPR and ΔT41 with Combined Component Efficiency and Metal Temperature Improvements.	19
4.1-4	Installed sfc at Max Climb vs. CPR and ΔT41 with Combined Component Efficiency and Metal Temperature Improvements.	21
4.1-5	Fan Corrected Flow Variation vs. CPR and ΔT41.	21
4.1-6	Compressor Corrected Flow Reduction vs. CPR and ΔT41.	21
4.1-7	Bypass Ratio vs. CPR and ΔT41.	22
4.1-8	Uninstalled sfc at Max Climb Thrust vs. CPR, ΔT41, and FPR - 35K/0.8M/Std. Day -18° F.	25
4.1-9	Fan and Compressor Corrected Flow Variation vs. CPR and FPR.	26
4.1-10	Installed sfc at Max Climb vs. CPR and FPR with Improvements in Component Efficiencies and Metal Temperatures.	27
4.1-11	Weight Comparison Between Lower-Fan-Pressure-Ratio Flowpath Configuration and Current FPS E^3 Configuration.	30
4.1-12	Effects of Variable Exhaust Nozzle Area for E^3 FPS.	33
4.2-1	HPT Metal Cooling Improvements.	37
4.3-1	Modulated Cooling Flow.	39
4.4-1	Metal Temperature Improvement - +100° F HPT Materials.	41
4.5-1	Metal Coating Improvement - Thermal Barrier Coatings in Combustor and HP Turbine.	43
4.6-1	Flowpath Configuration Comparison Between Shortened Fan and E^3 FPS.	45

LIST OF ILLUSTRATIONS (Continued)

Figure		Page
4.6-2	Shortened Fan Configuration.	45
4.6-3	E^3 Engine Component Noise Summary for Takeoff and Approach Conditions Using Boeing Twinjet Aircraft.	47
4.6-4	Change in Fan Component Noise with Rotor-OGV Spacing.	48
4.6-5	Variation in Total System Approach EPNL with Rotor-Stator Spacing.	49
4.6-6	Nonmodified MASS Model of FPS Fan Frame.	50
4.6-7	E^3 FPS Fan Synchronous Combined-Modes Frequency Response - No. 1 Bearing Load.	53
4.6-8	E^3 FPS Fan Synchronous Combined-Modes Frequency Response - Fan Relative Deflection.	53
4.6-9	E^3 FPS Fan Synchronous Combined-Modes Frequency Response - HP Compressor Stage 1 Relative Deflection.	54
4.6-10	E^3 FPS Fan Synchronous Combined-Modes Frequency Response - HP Turbine Stage 1 Relative Deflection.	54
4.6-11	E^3 FPS Fan Synchronous Combined-Modes Frequency Response - LP Turbine Stage 1 Relative Deflection.	55
4.6-12	E^3 FPS Fan Synchronous Combined-Modes Frequency Response - LP Turbine Stage 5 Relative Deflection.	55
4.6-13	E^3 FPS Fan Synchronous Combined-Modes Frequency Response - No. 1 Bearing Load - Baseline vs. Short Fan Flowpath.	57
4.6-14	E^3 FPS Fan Synchronous Combined-Modes Frequency Response - Fan Relative Deflection - Baseline vs. Short Fan Flowpath.	57
4.6-15	E^3 FPS Fan Synchronous Combined-Modes Frequency Response - HP Compressor Stage 1 Relative Deflection - Baseline vs. Short Fan Flowpath.	58
4.6-16	E^3 FPS Fan Synchronous Combined-Modes Frequency Response - HP Turbine Stage 1 Relative Deflection - Baseline vs. Short Fan Flowpath.	58
4.7-1	Mechanical Active Clearance Control Concepts.	61
4.7-2	Organic-Fluid Heat Pipe Cooling Concept.	63
4.7-3	Fan Air Cooling Baffle Configuration.	65
4.7-4	Current E^3 HPC Active Clearance Control Concept.	66
4.8-1	FOD Panel SPF/DB Process.	72
4.8-2	SiC/Ti Fiber-Reinforced Advanced Hollow Titanium (FRAHT) Fan Blade Conceptual Design.	76

LIST OF ILLUSTRATIONS (Continued)

Figure		Page
4.8-3	E^3 FRAHT Design No. 1.	76
4.8-4	E^3 FRAHT Design No. 3.	76
4.9-1	Single Annular Combustor.	81
4.11-1	E^3 FPS Composite Vane Applications.	84
4.11-2	Composite Vane Conceptual Design.	85
4.12-1	Composite Spinner Conceptual Design.	88
4.13-1	Benefits of Aggregate Component Efficiency Improvement (+1%).	93
4.14-1	Variable-Area Nozzle (A_8).	95
4.15-1	Low Pressure Turbine Aerodynamics - 3D Aero.	97
4.16-1	Low Pressure Turbine - Flared Flowpath.	99
4.17-1	Low Pressure Turbine Aerodynamics - Orthogonal Flowpath.	101
4.18-1	Advanced Lightweight Fuel Delivery System.	103
4.18-2	Conventional Fuel Delivery System.	103
4.18-3	Advanced Fuel System.	105
4.18-4	Environmental Control System (ECS) Waste Heat Recovery System.	105
4.18-5	Effects of Waste Heat Recovery, Synthetic Fuels, and Advanced Fuel System on Nozzle Fuel Inlet Temperatures.	107
4.18-6	Main Fuel Pump of LWFDS.	107
4.18-7	Vortex Nozzle Flow Characteristics.	109
4.18-8	Vortex Fuel Nozzle.	109
4.18-9	Fuel Metering Assembly with Shear-Type Valves .	111
4.18-10	ECS Waste Heat Recovery System Tank Heating with High-Freeze-Point Fuel.	112
4.19-1	Hybrid Electric Power System.	118
4.19-2	Integrated Engine Generator/Starter.	118
4.19-3	Mechanical Arrangement of Accessory Drive System.	120
4.19-4	Packaging of Generator/Starters and Engine Accessories.	120
4.19-5	Post-E^3 FPS Configuration for One Engine.	121
4.19-6	150 kVA SmCo Generator/Starter Cross Section.	123
4.19-7	Bleed Air and Shaft Power Extraction Penalties on sfc for E^3 FPS.	126

LIST OF ILLUSTRATIONS (Concluded)

Figure		Page
4.20-1	Spherical Flexure Joint for Three-Mount Engine System.	129
6.1.1	Automatic Interface Between Heat Transfer Program and Stress Analysis Program.	153
6.2-1	Frame Structural Analysis Model.	155
6.3-1	Prediction/Correlation of F101X Stage 1 Fan Blade End-Effect Stresses.	157
6.4-1	Comparison Between Analytic and Photoelastic Data.	159
6.5-1	Residual Stress Distributions in Shot-Peened Rene' 95 Surfaces.	162
6.5-2	Effect of Strain-Controlled Cyclic Load on Residual Stress Distribution.	162
6.6-1	CF6-6D and CF6-50 Stage 1 Blades - Cold Bridge Design Operating Strain-Temperature Conditions.	164
6.7-1	Low Cycle Fatigue of Conventionally Cast and Directionally Solidified Rene' 80 Alloys.	166
6.8-1	Microstructural Damage Assessment.	169
6.9-1	Manson-Halford Damage Curve.	172
6.10-1	Proposed Conceptual Design Fiber-Reinforced Titanium Blade.	174
6.11-1	Time-sharing Computer Program for the Analysis of Turbo-machinery Vibration.	177
6.13-1	Locus of Relative-Displacement Vector Between the Fan Rotor and the Case for the Demonstrator Model for Sudden 1000 gm-in. Fan Unbalance at 3000 rpm.	182

LIST OF TABLES

Table		Page
1-1	Concept Benefit Summary.	4
2-1	Comparison of Baseline E^3 to Reference CF6-50C.	7
3-1	Present-Worth Example Calculation.	14
4.0-1	Concept Benefit Summary.	16
4.1-1	E^3 FPS Cycle Definition.	18
4.1-2	Design Variable Matrix.	18
4.1-3	Parametric Study Assumptions.	18
4.1-4	Improved Efficiencies and Metal Temperature Capability - Cycle Selection Results at Minimum sfc.	22
4.1-5	Engine Sizing Benefits Resulting from Improved Metal Temperature Capability.	23
4.1-6	Fan Design Assumptions.	23
4.1-7	LP Turbine Design Variation with Fan Pressure Ratio.	28
4.1-8	Sfc Sensitivity to Component Efficiency - E^3 FPS Cycle Design Point.	28
4.1-9	Performance Comparison Between E^3 FPS and Reduced Fan-Pressure-Ratio Technologies.	31
4.1-10	Size Comparison Between E^3 FPS and Reduced Fan-Pressure-Ratio Technologies.	31
4.1-11	Mission Profile sfc Benefits of a 5% Variable Area Nozzle.	33
4.2-1	HPT Metal Cooling Improvements.	37
4.3-1	Modulated Cooling Flow.	39
4.4-1	Metal Temperature Improvement - +100° F HPT Materials.	41
4.5-1	Metal Coating Improvement - Thermal Barrier Coatings in Combustor and HP Turbine.	43
4.6-1	E^3 FPS and ICLS Frame Flexibilities.	49
4.6-2	E^3 FPS and ICLS Beam Bending Clearance Comparison for Static Loads.	52
4.6-3	E^3 FPS Baseline and Short Fan Flowpath - Beam-Bending Comparison for Static Loads.	56
4.6-4	E^3 Baseline and Short Fan Flowpath - Bearing Load Comparison for Static Loads.	56
4.6-5	Weight Savings Potential of Shortened Fan Configuration for the E^3 Engine.	59

LIST OF TABLES (Concluded)

Table		Page
4.6-6	Shortened Fan Flowpath.	59
4.7-1	Baffle Configuration Weight Savings.	68
4.7-2	Fan Air Baffle Configuration Summary (Compared to Current E^3 FPS).	70
4.7-3	HPC Active Clearance Control - Fan Air Cooling.	70
4.8-1	E^3 SiC/Ti Fan Blade Design Study.	74
4.8-2	Advanced Fan Blades.	78
4.9-1	Single Annular Combustor.	81
4.10-1	Compressor Bonded Blisk.	82
4.11-1	Vane Material Properties.	84
4.11-2	E^3 FPS Composite Vane Applications Weight Summary.	85
4.11-3	Composite Vanes.	86
4.12-1	40% Graphite, Chopped-Fiber-Filled Nylon 610 Thermoplastic (QC 1008).	88
4.12-2	Comparison of Spinner Stresses, Max Climb, Case 41 - 3539 rpm.	88
4.12-3	Life Requirements for Spinner at the Critical Mission Points.	89
4.12-4	Composite Spinner.	90
4.13-1	Benefits of Component Efficiency Improvements (+1%).	92
4.13-2	Combined Benefits of Component Efficiency Improvements.	93
4.14-1	Variable-Area Nozzle (A_8).	95
4.15-1	Low Pressure Turbine Aerodynamics - 3D Aero.	97
4.16-1	Low Pressure Turbine - Flared Flowpath.	99
4.17-1	Low Pressure Turbine - Orthogonal Blading.	101
4.18-1	Advanced Fuel Delivery System.	113
4.18-2	Advanced Fuel Delivery System Benefits.	113
4.19-1	Weight Summary, Baseline and EEG/S.	125
4.19-2	Reliability of E^3 FPS vs. E^3-EEG/S - Replacements per 10^6 Hours.	125
4.19-3	System Payoff Results - Comparison Between Baseline and E^3 EEG/S.	127
4.19-4	All-Electric Aircraft Engine SPS Benefits.	127
6.0-1	Advanced Design Concepts and Required Structural Analysis Programs.	151
6.13-1	Physical Global Degrees of Freedom and Direction Numbers for the Subsystems.	183

1.0 SUMMARY

The principal purpose of this study was to identify structural analysis capability developments needed in the design of post-E^3-generation turbine engines. Engine and structural design concepts were developed to identify the associated structural analysis development needs. These engine and structural design concepts are themselves valuable by-products of this study.

The study consisted of three tasks. New technology concepts were screened in Task 1. The benefits of the concepts were assessed in Task 2, and in Task 3 associated structural analysis development needs were identified. Technology programs and structures analysis programs were then outlined. This flow is shown in Figure 1-1.

A summary of the new technology concepts is shown in Figure 1-2. The NASA-GE Energy Efficient Engine (E^3) technology was used as a base to assess the concept benefits. Payoffs were evaluated for a domestic twin-engine aircraft, which is considered typical of the aircraft which would benefit from the technologies studied:

- 225 Seats
- 55% Load Factor
- 35,000 ft, 0.8 M_N
- 3,000 NMi Design Range
- 700 NMi Flight
- 282,670 Pounds TOGW

Specific fuel consumption (sfc), weight and cost effects were scaled from E^3 size to 40,590 pound thrust size, required for the twin aircraft. Direct operating cost, fuel burned, and present-worth effects were determined for each technology applied to the domestic twin.

The benefits of the technology concepts are summarized in Table 1-1. The potential fuel-burned advantage shown is for thousands of gallons of fuel saved per aircraft per year for each advanced concept. Costs are in 1980 dollars. Fuel prices of one and two dollars were used in the study to assess the effects of future fuel escalation independent of inflation. The two-dollar price was used in Table 1-1. The technologies are ranked in the order of:

$$\frac{\text{(Present Worth of Future Savings) X (Probability of Success)}}{\text{(Initial Development Cost)}}$$

This ratio indicates the payoff compared to the investment and should be used for relative ranking rather than as an absolute level because of the arbitrary (300 plane) fleet size and fuel prices selected. Additional payoffs for the generic concepts are attainable on other engine systems. A summary of the structural analysis development needs is presented in Figure 1-3. These needs are discussed in Section 6.

After the introduction, Section 2, this report covers the methods used in the analysis, Section 3. The advanced technology concepts are presented in Section 4. The recommended technology programs follow in Section 5, while the Structural and Life Analysis programs are presented in Section 6.

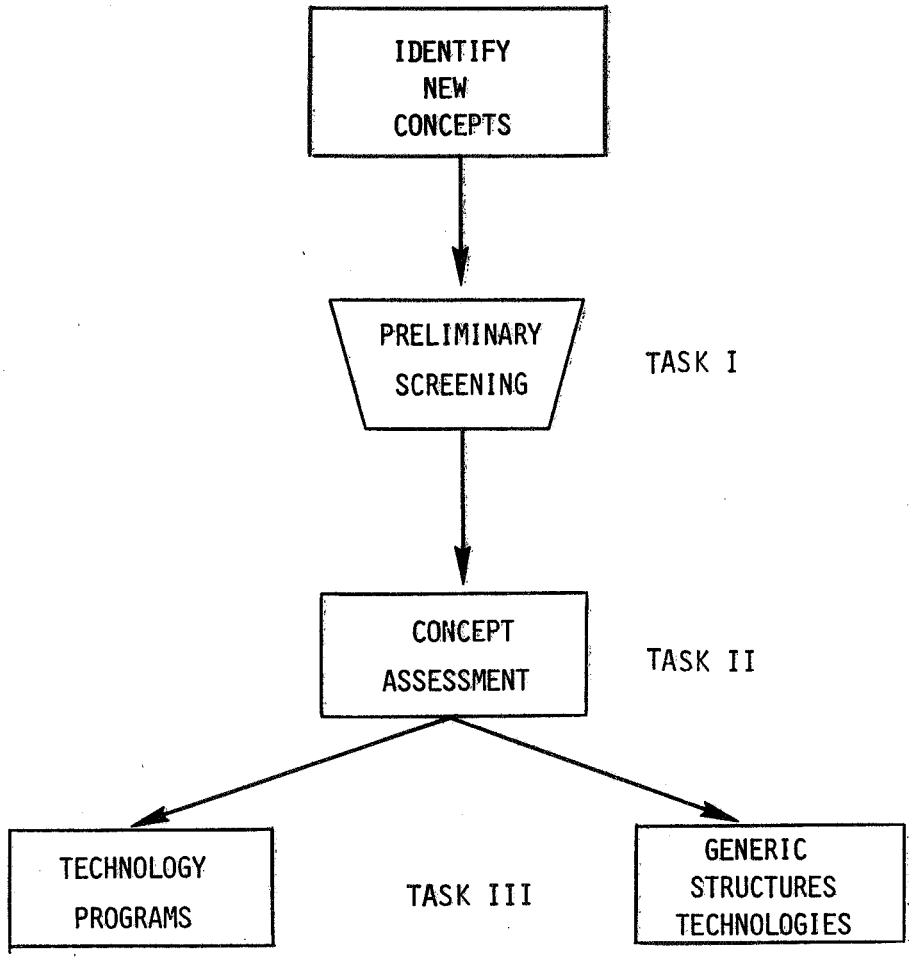

Figure 1-1. Task Flow Chart.

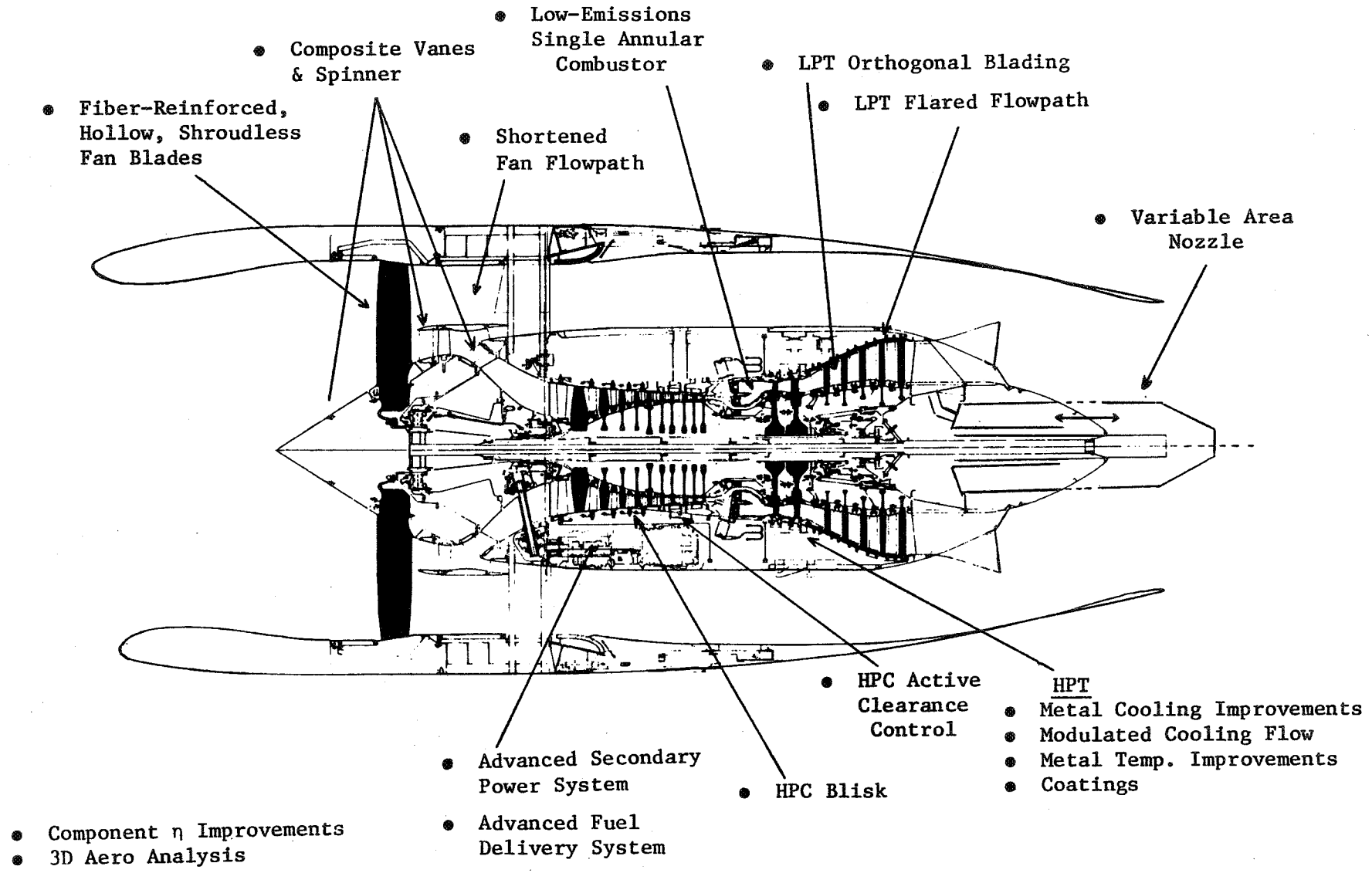

Figure 1-2. Advanced Technology Concepts.

Table 1-1. Concept Benefit Summary.

ITEM	△FUEL BURNED KG/AC/YR	△DOC %	PWxPS / IDC
HPT METAL COOL. IMPROV.	47	-1.2	58
ALL ELECTRIC AIRCRAFT	73	-1.5	57
HPT METAL TEMP. IMPROVE.	153	-4.7	41
MODULATED COOLING FLOW	36	-.80	40
HPT COATING IMPROVE.	31	-.75	17
SHORTENED FAN FLOWPATH	20	-.85	16
HPC ACC - FAN AIR	5.8	-.34	15
SINGLE ANNULAR COMB.	5.0	-.43	11
COMPONENT η IMPROVEMENT	197	-4.9	8.4
VARIABLE A_8 NOZZLE	18	-.12	7.6
3-D AERO ANALYSIS	11	-.26	6.9
ADV. FAN BLD, FIB. REIN. Ti, 1.5"	24	-.88	5.8
LPT - FLARED FLOWPATH	13	-.17	5.6
COMP. VANES	5.4	-.28	5.1
COMP. SPINNER	0.5	-.03	3.9
HPC, BLISK BONDED	23	-.56	3.2
LPT ORTHOGONAL BLADING	5.3	-.13	2.2
ADVANCED FUEL SYSTEM	2.0	-.11	1.1

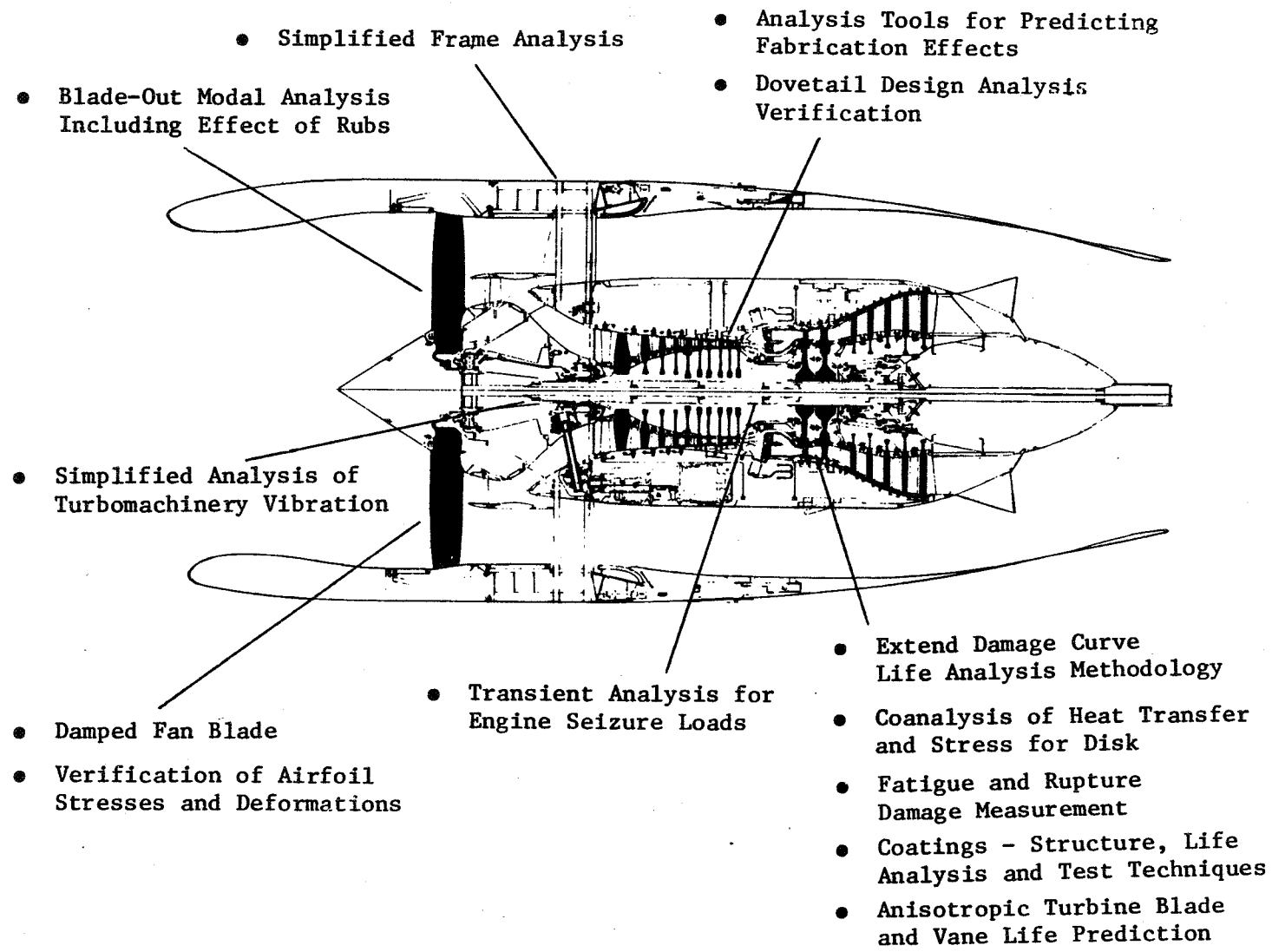
• Simplified Frame Analysis
• Analysis Tools for Predicting Fabrication Effects
• Dovetail Design Analysis Verification
• Blade-Out Modal Analysis Including Effect of Rubs
• Simplified Analysis of Turbomachinery Vibration
• Damped Fan Blade
• Verification of Airfoil Stresses and Deformations
• Transient Analysis for Engine Seizure Loads
• Extend Damage Curve Life Analysis Methodology
• Coanalysis of Heat Transfer and Stress for Disk
• Fatigue and Rupture Damage Measurement
• Coatings - Structure, Life Analysis and Test Techniques
• Anisotropic Turbine Blade and Vane Life Prediction

Figure 1-3. Structural Analysis Development Needs.

2.0 INTRODUCTION

This study addresses improved structural concepts beyond the present NASA/GE Energy Efficient Engine (E^3) technology. The E^3, whose initial technology demonstration is slated for late 1982, is used as a base to assess the Life Cycle Cost benefits of the proposed new concepts. The E^3 already incorporates many advancements beyond today's engines as shown in Figure 2-1. A comparison of the E^3 baseline with the CF6-50C engine is shown in Table 2-1.

The trend in Specific Fuel Consumption for large commercial turbofans is shown in Figure 2-2. Substantial improvements have been achieved as a result of increased propulsive efficiency from the high bypass ratios along with thermal efficiency improvement from higher cycle pressure ratios and component efficiencies. An "Ideal Cycle" sfc with the E^3 Fan Pressure Ratio, where components are 100% efficient, no pressure losses exist in the engine, burning is stoichiometric, and no turbine cooling is required, is indicated in the figure for reference.

Figure 2-3 shows the trend in some key engine performance parameters from the days of the turbojet to an extrapolation beyond the E^3 objective. The significant increase in propulsive efficiency with the advent of higher bypass ratios contributed to a large portion of the sfc increase exhibited in Figure 2-2. Examination of those parameters associated with the core stream of the engine - specifically, thermal efficiency, turbine temperatures, and metal temperatures - indicates a relatively linear improvement through the years. The trend in these variables, however, shows a decreasing rate of improvement when projected to the 1990 time period. It is in these areas that improvements can be made to continue an upward trend in the basic engine technology.

Two additional parameters which can significantly affect the amount of engine fuel burned are component efficiency and engine weight, although the latter has no effect on engine specific fuel consumption. As shown later in Section 4.1, technology advancements in metal temperature have a significant effect on engine size reduction and thus fuel burned. Also, mechanical or structural design improvements can improve the efficiency of the engine as well as providing a weight reduction.

Fuel efficiency improvements of the magnitude seen with the advent of the high-bypass-ratio engine are gone, although some room exists for higher propulsive efficiencies. Fuel-burned improvements beyond E^3 will come with an aggressive program to improve the other areas of engine technology. Although the improvement may be small, the economic payoff can be significant when considering the trend in fuel costs. Fuel costs are becoming a larger percentage of the Direct Operational Cost (DOC) of a commercial aircraft. The development items identified in this report show the economic payoffs that result when fuel costs rise to one and two dollars a gallon. With an aggressive program, an 8% Δsfc improvement beyond E^3 for the 1990 decade appears to be achievable. A post-E^3 sfc of 0.5 is a worthy goal for the commercial turbofan.

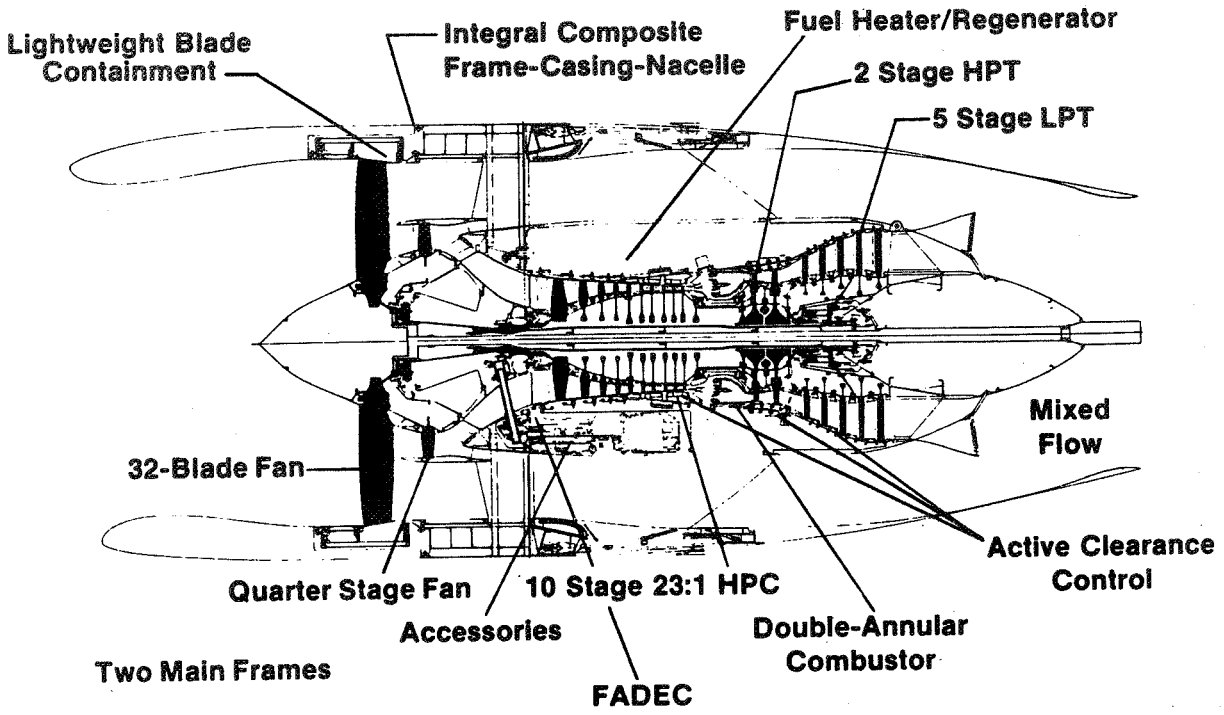

Figure 2-1. Baseline Energy Efficient Engine.

Table 2-1. Comparison of Baseline E^3 to Reference CF6-50C.

	CF6-50C	E^3
Takeoff Fn, lb	50,250	36,500
Cycle Pressure Ratio, Max Climb	32	38
Bypass Ratio, Max Climb	4.2	6.8
Fan Pressure Ratio, Max Climb	1.76	1.65
Turbine Rotor Inlet Temperature SLS/86° F Day T/O, °F	2445	2450
Sfc, 35,000/0.8M Max Cruise,%	Base	-14.2

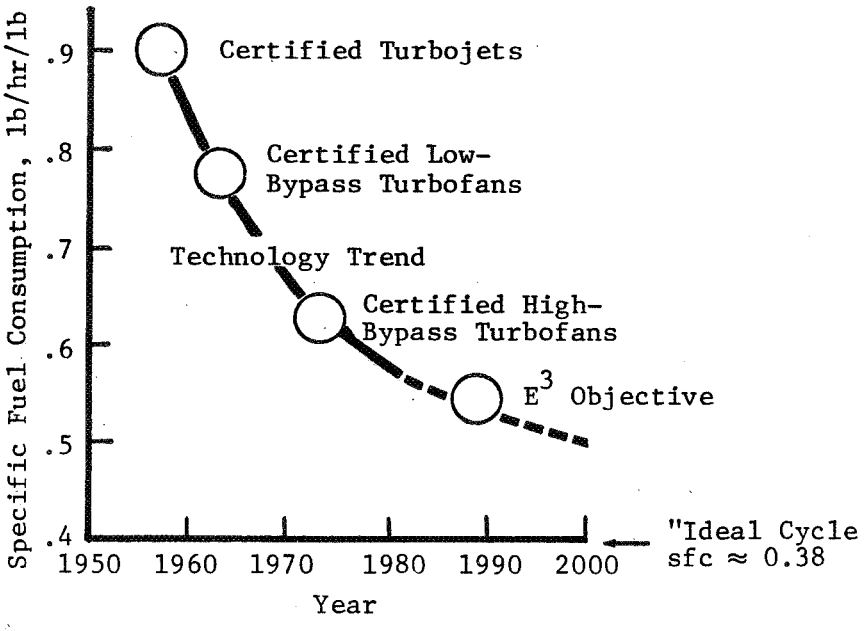

Figure 2-2. Large U.S. Commercial Transport Engines Fuel Consumption Trend.

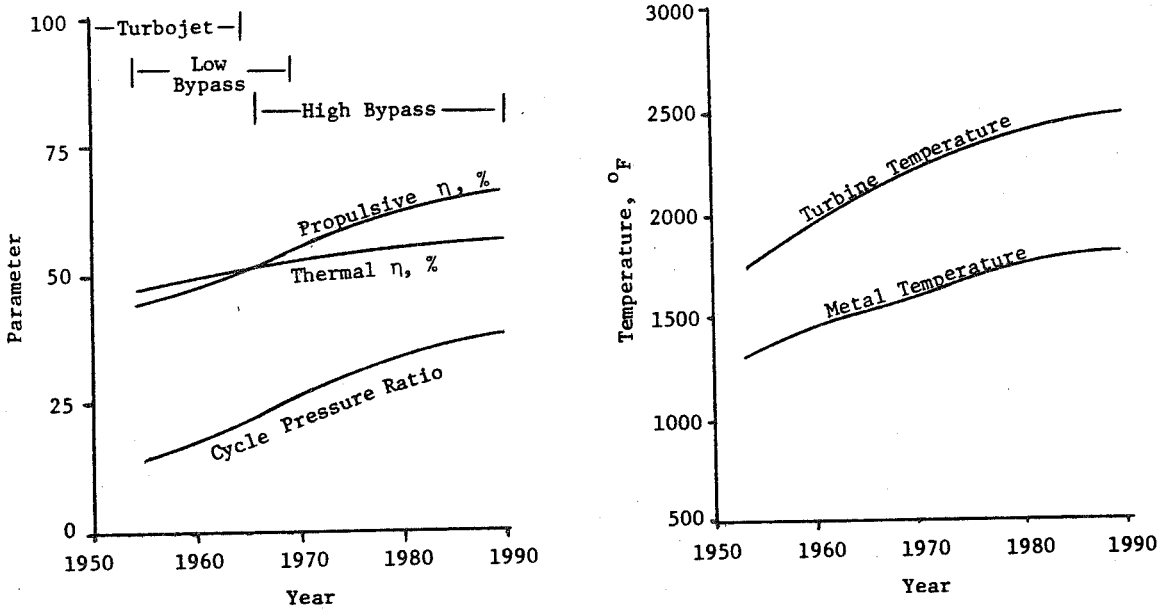

Figure 2-3. Trend in Engine Performance Parameter Technology.

3.0 METHOD OF ANALYSIS

An economic analysis of each technology concept determines the fuel savings and return on investment. These, in turn, identify which concepts are most worth pursuing. This section describes that analysis.

In general, a conceptual design was executed for each concept. This established payoffs, penalties, risks and costs. These determined the change in fuel burned and direct operating costs (DOC). The improvement in DOC determined the dollar savings which was compared to the initial investment. The ratio of dollar savings to investment identifies which concepts should be developed.

STUDY ENGINE AND AIRCRAFT

The fuel savings and economic payoff due to each technology advancement were evaluated for a typical commercial airliner. General Electric's Energy Efficient Engine (E^3) was used as the study vehicle. This engine represents the latest state-of-the-art high-bypass-ratio turbofan technology. Detailed optimization analysis had been developed for the E^3 program. This analysis provided accurate and timely assessment of the impact due to improvements in the engine, and therefore was very suitable for this program.

The analysis was performed by first determining the weight, engine cost, maintenance cost and performance differences for each study item. Performance differences due to component efficiency changes, cooling flow changes and other cycle effects established a change in specific fuel consumption.

If the changes allowed a reduction in flow while keeping the same thrust, the engine was down-sized and the weight and cost were appropriately reduced. The following relationships between weight and cost with flow were used:

$$\frac{\text{Core Weight}}{\text{Base Core Weight}} = \left(\frac{\text{Core Flow}}{\text{Base Core Flow}}\right)^{1.4}$$

$$\frac{\text{LP System Weight}}{\text{Base LP System Weight}} = \left(\frac{\text{Fan Flow}}{\text{Base Fan Flow}}\right)^{1.3}$$

$$\frac{\text{Core Cost}}{\text{Base Core Cost}} = \left(\frac{\text{Core Flow}}{\text{Base Core Flow}}\right)^{.55}$$

Base E^3 core weight was taken to be 2317 lb, LP system weight 4280 lb, and base core selling price $1.50 million. All costs in this program are in 1980 dollars.

The fuel savings and economic payoff were evaluated using an aircraft which is considered typical of what will be introduced in the 1980's to 1990's decades. This aircraft is a twin-engine passenger transport flying a domestic route.

Aircraft Design

3000 Nautical Mile Range
35,000 ft Cruise Altitude
0.8 Cruise Mach No.
225 Passengers (100% Payload)
282,670 lb takeoff Gross Weight
40,590 lb thrust per engine, SLS, Uninstalled

Aircraft Mission For Analysis

700 Nautical Mile Flight
35,000 & 39,000 ft (Stepped) Cruise Altitude
0.8 Cruise Mach No.
55% Load Factor
14,242 lb Fuel Burned Per Flight
1.895 Hours Per Flight

The aircraft is assumed to fly 3452 hours per year which gives 3,870,000 gallons of fuel used per year per aircraft.

E^3 design thrust is 36,500 lb. Therefore, weights and costs were scaled to the 40,590 lb thrust needed for the domestic twin-fan. The following scaling exponents apply:

$$\frac{\text{Item}}{\text{Base Item}} = \left(\frac{\text{Thrust}}{\text{Base Thrust}} \right)^N$$

Item	Scaling Exponents, N
Bare Engine Cost	0.55
Nacelle Cost	0.8
Bare Engine Weight	1.35
Core Engine Weight	1.4
LP System Weight	1.3
Nacelle Weight	1.1

Engine weight and specific fuel consumption changes determine the fuel savings. A "rubber airplane" was used which means that the aircraft is changed to fully realize the improvements due to a feature in the engines. For instance, an improvement in specific fuel consumption in the engine results in lower fuel weight carried by the aircraft which in turn allows reduced wing area which further reduces the engine size and fuel requirement for the same payload. If the technology advances were applied to an existing (fixed) aircraft, the compounding effects would not be realized and the benefits would be reduced. For this study, in the 40,590 lb thrust engine and using a "rubber airplane",

-1% Δ sfc saves 1.38% Fuel Burned

-863 lb saves 1.38% Fuel Burned

DIRECT OPERATING COST

The direct operating cost (DOC) incurred by an airline operator is made up of the cost of crew, fuel, airframe maintenance, engine maintenance, depreciation, and insurance. In this study, the effects of changes in engine weight, selling price, maintenance cost and fuel consumption on direct operating cost are determined.

The direct operating cost analysis used for this program was developed for the E^3 domestic twin-fan early in the E^3 program. For the present program, the analysis was inflated to 1980 dollars and was adjusted to reflect higher fuel prices. Fuel prices are currently around $1/gallon and may be expected to rise faster than the rate of inflation.

For a fuel cost of $1/gallon, in 1980 dollars, 42% of the direct operating cost is taken for fuel. If fuel cost should double, with all other costs unchanged, direct operating costs would increase by 42%. Fuel would then account for 59% of the higher direct operating cost. This effect is shown pictorially in Figure 3-1. The angle illustrates the percent ΔDOC for fuel, crew, etc. The increased area for the two-dollar-fuel pie chart illustrates the increase in total direct operating cost to the airlines caused by a one-dollar fuel increase. Fuel price projections are very important but also very uncertain. Over the next decade, industry projections of fuel price range from around $1.20/gallon to near $2/gallon, in 1980 dollars. Some projections go higher but $2/gallon could be considered the upper region of the range.

Because of the fuel price uncertainty, the economic analysis was carried out for both $1 and $2/gallon fuel. The following relationships established direct operating cost effects:

	Base Direct Operating Cost	
	For $1/Gal.	For $2/Gal.
DOC, $/Hour/Airplane	2700	3840
	% ΔDOC	
	For $1/Gal.	For $2/Gal.
423 lb ΔWeight	0.91	1.28
$245,000 ΔSelling Price	0.43	.3
$6.70/Engine Flight Hr. ΔMaintenance	0.43	.3
1% Δsfc	0.91	1.28

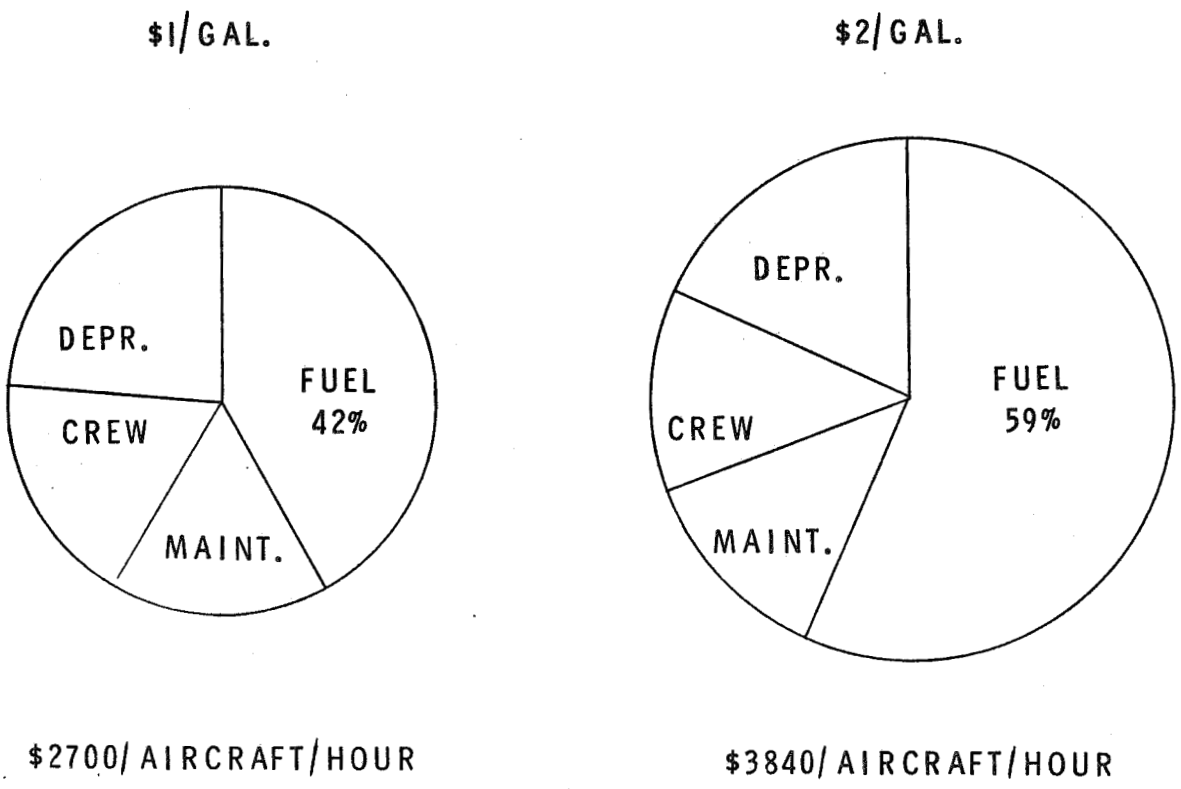

Figure 3-1. Direct Operating Cost Variation with Fuel Price.

PRESENT WORTH

Payoffs due to technical innovations have to be compared to investment costs and risks. Present worth was used to represent the payoff. Present worth is an "equivalent initial value of the discounted future savings to be accumulated over the life of a fleet of airplanes". It recognizes the value of money over time and, therefore, provides a means for comparing payoffs with initial investment. For instance, $1 ten years from now is really only worth 26¢ now if the 26¢ could be invested at, say 14.6% interest rate.

To calculate present worth, first the dollar savings due to the technology is calculated for each year, based on the number of aircraft, hours utilization and ΔDOC.

$$\text{Savings In One Year} = (\Delta\text{DOC}) \times \left(\frac{\text{No. Flt.-Hrs}}{\text{Year}}\right) \times \left(\text{No. Aircraft}\right)$$

For each year, a calculation is made of an "equivalent investment" at year zero which, if returning 14.6%, would equal the dollar savings.

$$\text{Equivalent Invest.} = \frac{\text{Savings In Nth Year}}{(1 + \text{Discount Rate})^N}$$

where Discount Rate = 14.6%

The sum of the "equivalent investments" for all N years is the present worth.

Selection of the discount rate is arbitrary. A value of 14.6% is typical and was used in the E^3 program.

For the present-worth calculation, a fleet of aircraft was assumed to enter service 8 years after investment in the technology being evaluated. Seven years later, the fleet was assumed to reach a full size of 300 aircraft. Fleet size was held steady and then was gradually retired as shown in Figure 3-2.

A sample calculation of present worth is shown in Table 3-1. A 1% saving in DOC produces $37,000,000 Present Worth if fuel costs $1/Gallon and $52,600,000 Present Worth if fuel costs $2/Gallon.

CONCEPT RANKING

Initial development costs were estimated for each technology item. These included the cost of demonstrating the technology on an engine. They do not include certification testing or tooling for production. Also, the probabilities of success for design and development, manufacturing, and user acceptance were estimated. The lowest of these was taken as the overall probability of success.

These were incorporated into the ranking parameter:

$$\frac{\text{Present Worth x Probability Of Success}}{\text{Initial Development Cost}}$$

If greater than unity, for the assumptions made, investment in the technology should be worthwhile. Comparison of the ranking parameters for competing technologies shows which offers the greater payoffs.

Because of the arbitrariness of some assumptions, care should be exercised when making comparisons with other studies. For instance, a 1200-aircraft fleet could be assumed. Or, it could be assumed that engine testing could be combined with separately funded testing, substantially reducing development costs. Sometimes life cycle costs are used rather than present worth. Life cycle cost savings are the total savings for all years and are about ten times the present worth. Comparisons should be restricted to one study where the assumptions and calculation procedure are consistent.

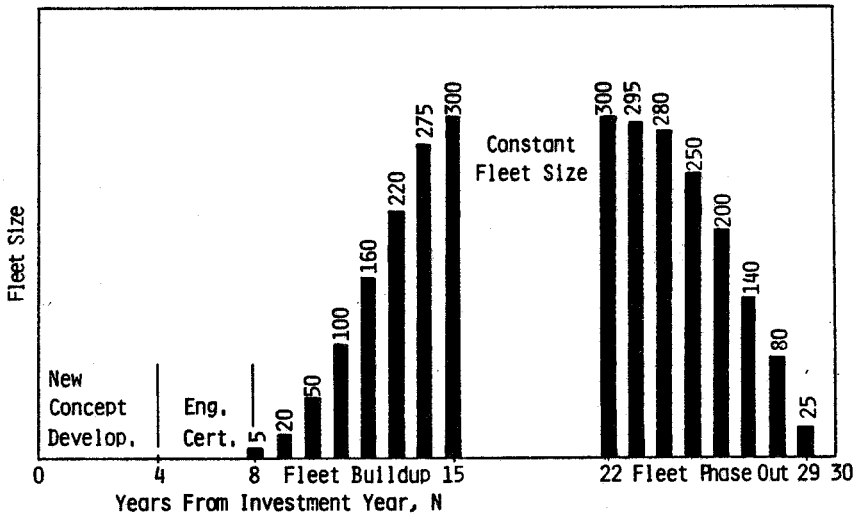

Figure 3-2. Aircraft Fleet Definition.

Table 3-1. Present-Worth Example Calculation.

FOR 1% △ DOC AND DOC=$3840/FLT.HR/AIRCRAFT ($2/GAL FUEL)

YEAR,N	NO. OF AIRCRAFT	SAVINGS IN NTH YEAR	PRESENT WORTH
0	0	0	0
7	0	0	0
8	5	$0.66M	$.22M
9	20	2.65	.78
10	50	6.62	1.70
⋮	⋮	⋮	⋮
15	300	39.75	5.15
⋮	⋮	⋮	⋮
22	300	39.75	1.98
⋮	⋮	⋮	⋮
26	200	26.50	0.77
27	140	18.55	0.47
28	80	10.60	0.23
29	25	3.31	0.06
30	0	0	0
		TOTAL	52.6M

4.0 ADVANCED CONCEPT STUDIES

New technology concepts which appear promising beyond the E^3 Flight Propulsion System (FPS) are presented in this section. The concept benefits are summarized as Table 4.0-1. The left column refers to sections in this report where the subject is covered. After the concept items, the next four columns list the direct benefits of weight, price, maintenance cost and sfc of the concepts relative to the E^3 FPS in its thrust size. The center four columns list assumed initial development costs, the probability of a concept being incorporated into the fleet, and the fuel-burned advantage both in difference in percentage and in savings per aircraft per year. The percent Δ DOC, present worth of future dollar savings, and the present worth ranking parameter are shown next for both two- and one-dollar fuel prices. The domestic twin aircraft was assumed in the last eight columns.

This section begins with the cycle performance improvement studies which were used as a guide to potential future payoffs.

Table 4.0-1. Concept Benefit Summary.

REPORT SECTION	ITEM	ΔWGT. LBS.	ΔSELLING PRICE $K	ΔMAINT. $/EFH.	ΔSFC %	INIT. DEV. COST	PROB. OF SUC.%	ΔFUEL BURNED %	ΔFUEL BURNED KG/AC/YR	FOR $2/GAL FUEL			FOR $1/GAL FUEL		
										ΔDOC %	PRES. WORTH $M	PWxPS / IDC	ΔDOC %	PRES. WORTH $M	PWxPS / IDC
4.2	HPT METAL COOL. IMPROV.	-64	4.1	.30	-.80	1.0	90	-1.2	47	-1.2	65	58	-.86	32	29
4.19	ALL ELECTRIC AIRCRAFT	103	15	-.10	-1.5	1.0	70	-1.9	73	-1.5	81	57	-1.1	40	28
4.4	HPT METAL TEMP. IMPROVE.	-722	179	.60	-1.9	4.2	70	-4.0	153	-4.7	247	41	-3.1	116	19
4.3	MODULATED COOLING FLOW	14	39	.05	-.70	1.0	95	-.94	36	-.80	42	40	-.53	20	19
4.5	METAL COATING IMPROVE.	-38	5.4	1.0	-.52	1.6	65	-.79	31	-.75	39	17	-.49	18	7.6
4.6	SHORTENED FAN FLOWPATH	-185	-19	-.25	-.13	2.5	90	-.52	20	-.85	45	16	-.63	23	8.3
4.7	HPC ACC - FAN AIR	-80	-40	-.20	0	1.0	85	-.15	5.8	-.34	18	15	-.29	11	9
4.9	SINGLE ANNULAR COMB.	-70	-69	-1.9	0	2.0	95	-.13	5.0	-.43	23	11	-.43	16	7.6
4.13	COMPONENT η IMPROVEMENT	-74	-18	0	-3.6	24.5	80	-5.1	197	-4.9	257	8.4	-3.5	129	4.2
4.14	VARIABLE A_8 NOZZLE	130	41	.50	-.5	0.8	95	-.46	18	-.12	6.4	7.6	-.03	1.1	1.3
4.15	3-D AERO ANALYSIS	0	0	0	-.20	1.0	50	-.28	11	-.26	14	6.9	-.18	6.7	3.4
4.8	ADV. FAN BLADE FIB. REIN. Ti, 1.5"	-176	-14	.30	-.21	4.0	50	-.61	24	-.88	47	5.8	-.63	23	2.9
4.16	LPT - FLARED FLOWPATH	74	2.6	0	-.36	1.5	95	-.34	13	-.17	8.8	5.6	-.12	4.3	2.7
4.11	COMPOSITE VANES	-75	-17	0	0	2.5	85	-.14	5.4	-.28	15	5.1	-.22	8.1	2.7
4.12	COMPOSITE SPINNER	-7.0	-4.1	0	0	.35	90	-.01	0.5	-.03	1.5	3.9	-.02	.92	2.4
4.10	HPC BLISK, BONDED	-26	-4.3	1.0	-.40	6.5	70	-.60	23	-.56	30	3.2	-.37	14	1.5
4.17	LPT ORTHOGONAL BLADING	0	0	0	-.1	2.5	80	-.14	5.3	-.13	6.7	2.2	-.09	3.4	1.1
4.18	ADVANCED FUEL SYSTEM	-28	-6.2	0	0	5.0	95	-.05	2.0	-.11	5.5	1.1	-.08	3.0	.57

4.1 CYCLE PERFORMANCE IMPROVEMENT STUDIES

4.1.1 Objective

Cycle and performance studies were conducted to investigate performance improvement potential beyond the E^3 engine technology. These studies were grouped into two categories. The first, parametric cycle studies, evaluated the impact of technology advances on the selection of cycle design parameters for new engines. The second group included specific modifications to the current E^3 Flight Propulsion System (FPS) as defined in Table 4.1-1.

4.1.2 Cycle Parameter Study

A parametric study of turbine rotor inlet temperature, cycle pressure ratio and fan pressure ratio was completed to evaluate assumed improvements in component efficiency and turbine metal temperature capability (cooling air reduction) and their effects on the cycle design. The selected matrix of turbine rotor inlet temperatures (T41), cycle pressure ratios (CPR) and fan pressure ratios (FPR) is shown in Table 4.1-2. Improvements of one percent in rotating component efficiencies, +100°F in metal temperature capability and 5 percent in mixer effectiveness were assumed. Cooling flows were adjusted to account for the increase in metal temperature and for the variations in turbine inlet temperature and compressor exit temperature. Cycle pressure ratio variations were achieved by variations in the core boosting while the compressor pressure ratio was maintained at the same level as the FPS. All cycles were sized at the same Max Climb uninstalled net thrust at flight conditions of 35,000 ft/0.8 Mach/Std. Day +18°F T_{amb}. All performance comparisons are made at these flight conditions. All installed performance comparisons include the effects of customer bleed, power extraction, ram recovery and isolated nacelle drag. The assumed improvements are summarized in Table 4.1-3.

4.1.2.1 Cycle Pressure Ratio and Turbine Inlet Temperature Variations

The component efficiency improvements and the metal temperature increase were evaluated both separately and combined for the matrix of T41's and CPR's at a fan pressure ratio of 1.65. Figure 4.1-1 shows the resulting uninstalled specific fuel consumption at Max Climb thrust with only the efficiency improvements. It can be seen that the cycle pressure ratio and turbine rotor inlet temperature at which the best sfc occurs did not shift from the FPS levels with improvements in component efficiency levels.

When only the metal temperature increase was assumed, the sfc vs. CPR and T41 was as shown on Figure 4.1-2. The point at which the best sfc occurs is now at a CPR between 45 and 50 and at a T41 200 to 300°F higher than the FPS.

Combining the efficiency improvements with the metal temperature increase reduces the sfc's to the levels shown in Figure 4.1-3. The best sfc again occurs between 45 and 50 CPR and between +200°F to +300°F T41.

The component efficiency increases are seen to produce a best uninstalled sfc that is 3.6% lower than the FPS level. The best uninstalled sfc with only

Table 4.1-1. E^3 FPS Cycle Definition.

35000 ft/0.8 Mach/Std. Day +18°F

Parameter	Max Climb
Uninstalled Net Thrust, lb	9040
Uninstalled sfc (Std. +18°F Day)	.561
Overall Pressure Ratio	37.7
Bypass Ratio	6.8
Fan Bypass Pressure Ratio	1.65
Fan Hub Pressure Ratio	1.67
Compressor Pressure Ratio	23.0
Corrected Compressor Flow, lbm/sec	120.0
HPT Rotor Inlet Temp. °F	2340

Table 4.1-2. Design Variable Matrix.

Cycle Pressure Ratio (CPR)	Increase in Turbine Rotor Inlet Temperature Above FPS-ΔT41 (°F)			Fan Pressure Ratio (FPR)
	200	300	400	
38	↓	↓	↓	1.55
45	↓	↓	↓	1.55
50	↓	↓	↓	1.55
55	↓	↓	↓	1.55
60	↓	↓	↓	1.55
38	↓	↓	↓	1.65
45	↓	↓	↓	1.65
50	↓	↓	↓	1.65
55	↓	↓	↓	1.65
60	↓	↓	↓	1.65
38	↓	↓	↓	1.75
45	↓	↓	↓	1.75
50	↓	↓	↓	1.75
55	↓	↓	↓	1.75
60	↓	↓	↓	1.75

Table 4.1-3. Parametric Study Assumptions.

Mixed Flow Engine - Mixing Effectiveness Improved (80% vs. 75%)	+5%
Fan Pressure Ratio Range	1.55 to 1.75
Each Rotating Component Efficiency is Improved Above the E^3 Objective	+1%
Improved Metal Temperature Capability	+100° F
Cycle Pressure Ratio Range (Varied by Boosting the Core)	38 to 60
Core Compressor Pressure Ratio is the Same as the E^3 FPS	23:1
Range of T41 Increase Above E^3 FPS	+200° F to +400° F
Cooling for HP and LP Turbines Adjusted for T3 Levels and Increased Metal Temperature Capability	
All Engines Sized at Constant Uninstalled Net Thrust	

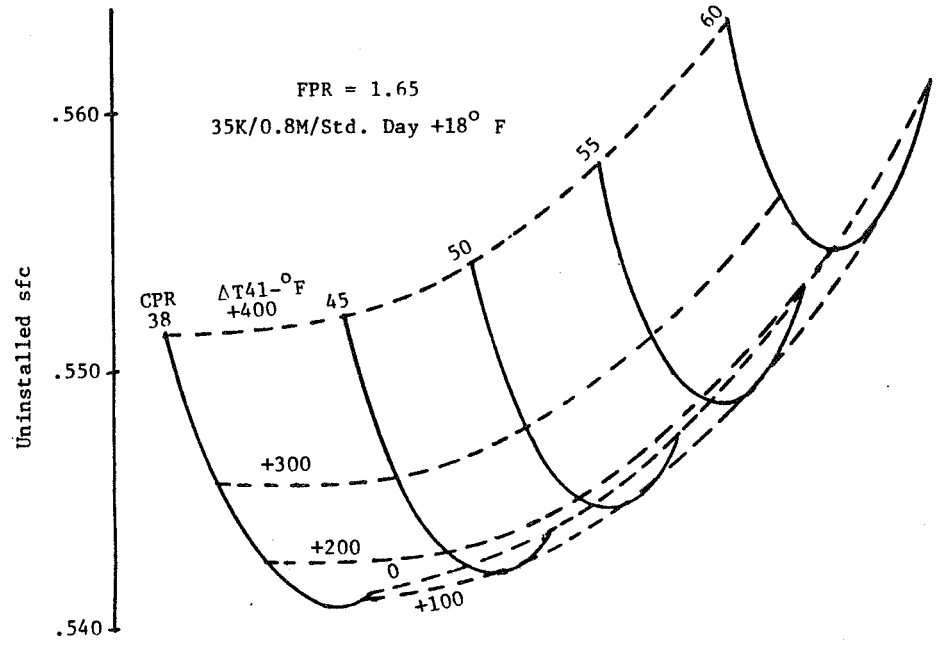

Figure 4.1-1. Uninstalled sfc at Max Climb vs. CPR and ΔT41 with Assumed Component Efficiency Improvements.

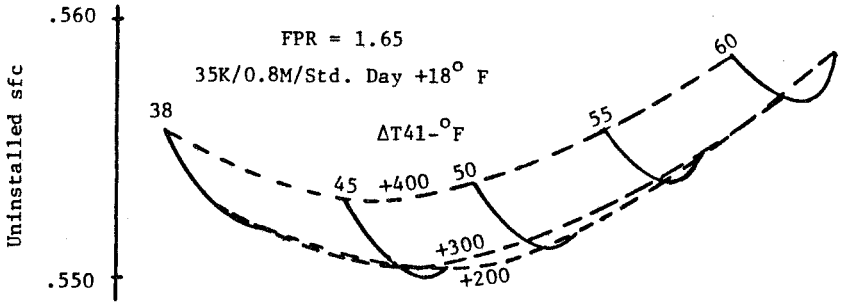

Figure 4.1-2. Uninstalled sfc at Max Climb vs. CPR and ΔT41 with Assumed Metal Temperature Improvement.

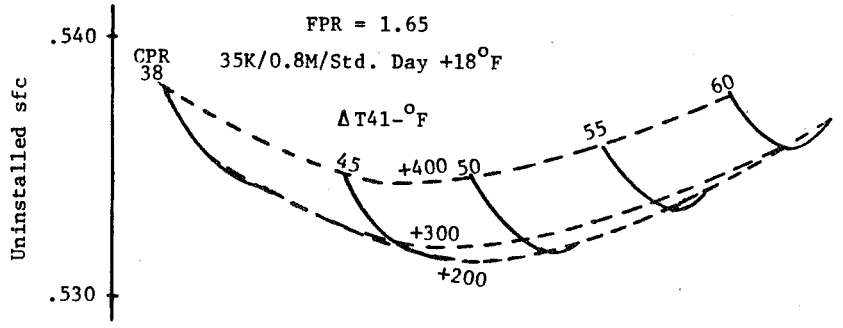

Figure 4.1-3. Uninstalled sfc at Max Climb vs. CPR and ΔT41 with Combined Component Efficiency and Metal Temperature Improvements.

the metal temperature increase is 1.9% lower than the FPS and the combination of efficiency and metal temperature improvements results in a 5.3% uninstalled sfc improvement at Max Climb.

It should be noted that the additional improvements in sfc can be achieved with improved cooling circuit design. The net effect is the same as shown for metal temperature improvements since both result from reduced cooling flow requirements. An additional 1.9% improvement could be realized if the gas temperature could be increased by 200°F at constant blade life.

Installed sfc was evaluated for the 1.65-fan-pressure-ratio cycles with the combined efficiency and metal temperature increases. Equal levels of customer bleed, power extraction and inlet ram recovery were applied to each cycle. Nacelle dimensions were scaled in proportion to the fan diameters in order to evaluate nacelle drag. Figure 4.1-4 is a plot of the resulting installed sfc's at Max Climb thrust. Relative to the uninstalled sfc results, the region of best sfc has shifted toward a higher CPR and to the lower T41 of 200°F above FPS. The best installed sfc is 5.0% lower than an FPS engine with the same installation effects.

Engine size is affected significantly by the changes in cycle pressure ratio and turbine inlet temperature. Figure 4.1-5 shows the fan corrected flow change as a function of CPR. As indicated, the T41 level has little effect on the fan size. The core size change with CPR and T41 variations is shown in Figure 4.1-6. The resulting bypass ratios are shown in Figure 4.1-7.

Table 4.1-4 provides a summary of the significant cycle design parameters for the cycles that produce minimum sfc. This illustrates how metal temperature technology improvements have a significant payoff when considering the effects on engine size and weight. Table 4.1-5 shows how this impact on component size can be viewed in terms of engine thrust capability. Two engines with the +100°F metal temperature improvement are compared with the E^3 baseline engine. The first engine has the -1.9% sfc improvement at the same fan size, but only a 92.5 lb/sec corrected flow core size and a 45:1 cycle pressure ratio. The takeoff thrust would increase about 0.5% to 37,000 lb. The second engine would keep the baseline core size of 120 lb/sec, but would be configured with a 92-inch fan for a 20% thrust increase to 44,600 lb at takeoff. As shown in Figure 4.1-7, both engines have higher bypass ratios than the E^3 baseline. This illustrates how technology advancements are fully utilized by changing the configuration of the engine.

4.1.2.2 Fan Pressure Ratio Variations

Following the evaluation of the CPR and T41 matrix the study was expanded to include the variations in fan pressure ratio. The fan performance characteristics assumed for the three levels of fan pressure ratio are provided in Table 4.1-6. The LP turbine efficiency and the interturbine transition duct losses were initially assumed constant.

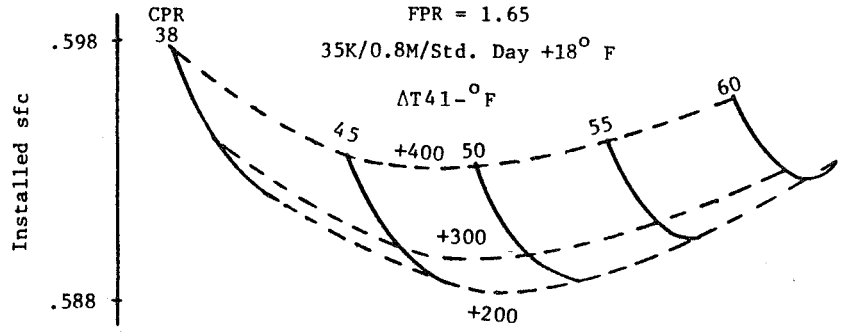

Figure 4.1-4. Installed sfc at Max Climb vs. CPR and ΔT41 with Combined Component Efficiency and Metal Temperature Improvements.

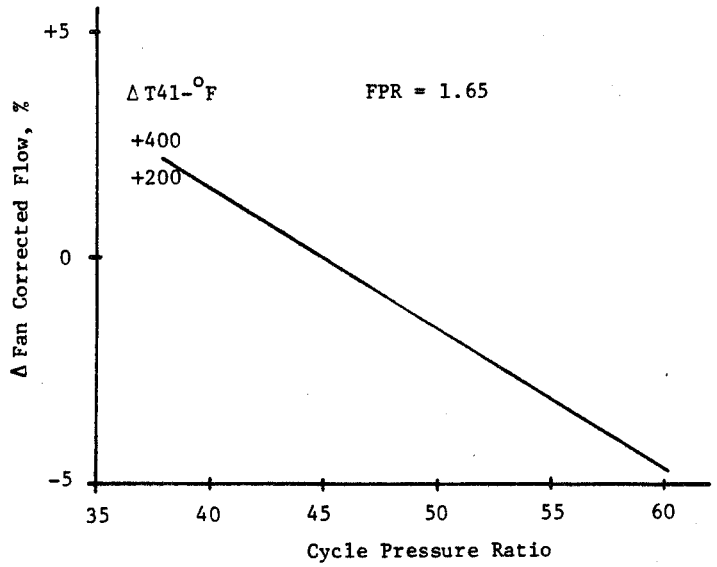

Figure 4.1-5. Fan Corrected Flow Variation vs. CPR and ΔT41.

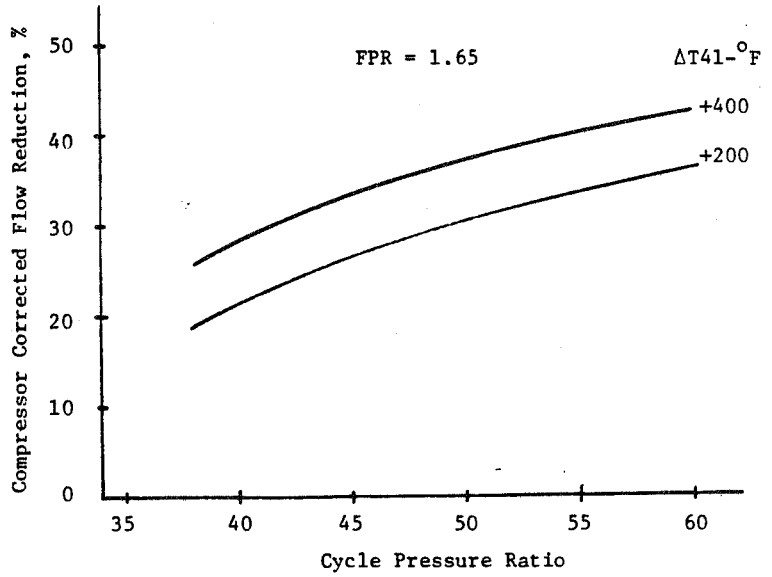

Figure 4.1-6. Compressor Corrected Flow Reduction vs. CPR and ΔT41.

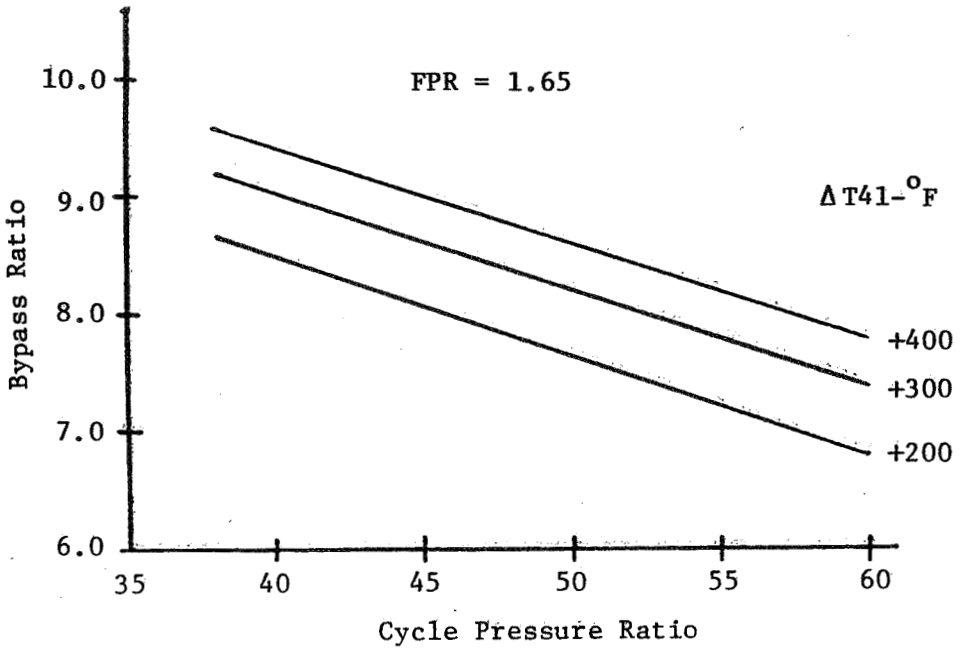

Figure 4.1-7. Bypass Ratio vs. CPR and Δ T41.

Table 4.1-4. Improved Efficiencies and Metal Temperature Capability - Cycle Selection Results at Minimum sfc.

35000 FT./0.8MACH/CYCLE DESIGN POINT

	E^3 - FPS	EFFICIENCY IMPROVEMENTS	METAL IMPROVEMENTS	COMBINED IMPROVEMENTS
FAN FLOW	BASE	+1.3%	- 1.4%	UNCHANGED
CORE FLOW	BASE	-4.2%	-23.5%	-26.5%
CYCLE PRESSURE RATIO	38	38	45	45
HP TURBINE INLET TEMPERATURE	BASE	UNCHANGED	+200°F	+200°F
UNINSTALLED SFC IMPROVEMENT	BASE	-3.6%	-1.9%	-5.3%

Table 4.1-5. Engine Sizing Benefits Resulting from Improved Metal Temperature Capability.

Parameter	E^3	Same Fan Size	Same Core Size
Fan Diameter, in.	83	83	92
Corrected Core Flow, lb/sec	120	92.5	120
Thrust Rating, lb	36,500	37,000	44,600
Cycle Pressure Ratio	38	45	45
HPT Temperature Increase, °F	Base	+200	+200
Sfc Improvement, %	Base	-1.9	-1.9

Table 4.1-6. Fan Design Assumptions.

Pressure Ratio	1.55	1.65	1.75
Efficiency	.910	.891	.873
Corrected Tip Speed, (ft/sec)	1200	1350	1500
Specific Flow	41.8	42.8	43.8

Design points were generated for each CPR/T41/FPR combination with the efficiency and metal temperature improvements applied. The uninstalled sfc's at the Max Climb design point, plotted in Figure 4.1-8, show that the region of best uninstalled sfc remains in the 45 to 50 CPR range and the +200°F to +300°F ΔT41 range as fan pressure ratio varies. Fan and compressor corrected flow variations with CPR and FPR are shown in Figure 4.1-9 for a ΔT41 of +200°F. In order to evaluate installed sfc, data were generated for each FPR/CPR combination with the design T41 that produced the best uninstalled sfc. Installed sfc's for these cycles are plotted in Figure 4.1-10. The 1.55 fan pressure ratio cycle with the lowest sfc has a 1.7 percent installed sfc advantage over the best 1.65 FPR cycle; however, this assumes a constant level of LP turbine efficiency and interturbine transition duct pressure loss. The lower fan pressure ratio would require either increased turbine loading or a larger transition duct (or some combination of the two) which would offset some of the benefit of the lower fan pressure ratio cycle.

An evaluation of LP turbine loading was made for the 45:1 CPR/+200°F T41 cycles with the three different fan pressure ratios. LP turbine diameters were changed to maintain the same pitchline speeds as the FPS and stages were added to bring the loading down to the FPS level. The resulting changes in turbine design are shown in Table 4.1-7. For each FPR the turbine diameter changes by about the same amount as the fan diameter to maintain pitchline speeds and an additional stage is needed to reduce the average loading to the FPS level.

Since the HP turbine diameter decreases and the LP turbine diameter increases with decreasing fan pressure ratio, the transition duct pressure losses will be higher with the lower fan pressure ratio. Assuming the constant level of LP turbine loading and efficiency and a 1 percent increase in transition duct pressure loss between the 1.65 and 1.55 FPR cycles, the installed sfc of the 1.55 FPR cycle will be about 1.2% lower than the 1.65 FPR cycle.

4.1.3 E^3 Design Modification Studies

Specific modifications that were evaluated include a lower-pressure-ratio fan, a cooling flow modulation system, a variable exhaust nozzle and a Rankine bottoming cycle for aircraft power supply. Performance sensitivity coefficients were determined for changes in component efficiencies, cooling flows and power extraction. Detailed cycle calculations were made to evaluate modifications where necessary. For some evaluations, use of sensitivity coefficients was adequate.

4.1.3.1 Component Efficiency Sensitivity Coefficients

The effects of component efficiencies on specific fuel consumption are shown in Table 4.1-8. As shown, efficiency improvements have less of an impact on a fixed engine size than they would have on an all-new engine. As seen in Table 4.1-5, the component efficiency levels have an impact on the core and fan flow sizes for a given thrust level. Higher component efficiencies result in

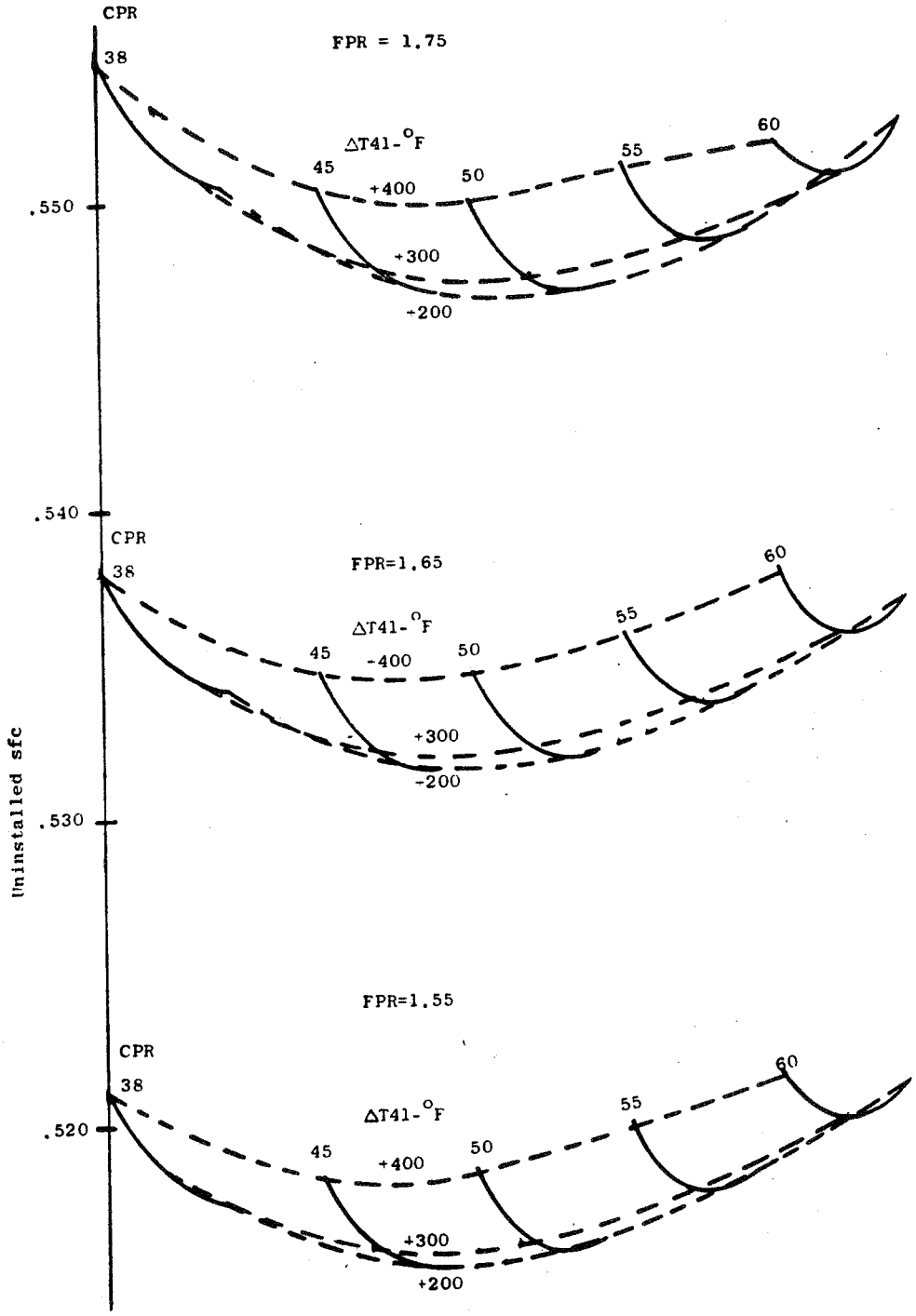

Figure 4.1-8. Uninstalled sfc at Max Climb Thrust vs. CPR, ΔT41, and FPR - 35K/0.8M/Std. Day +18° F.

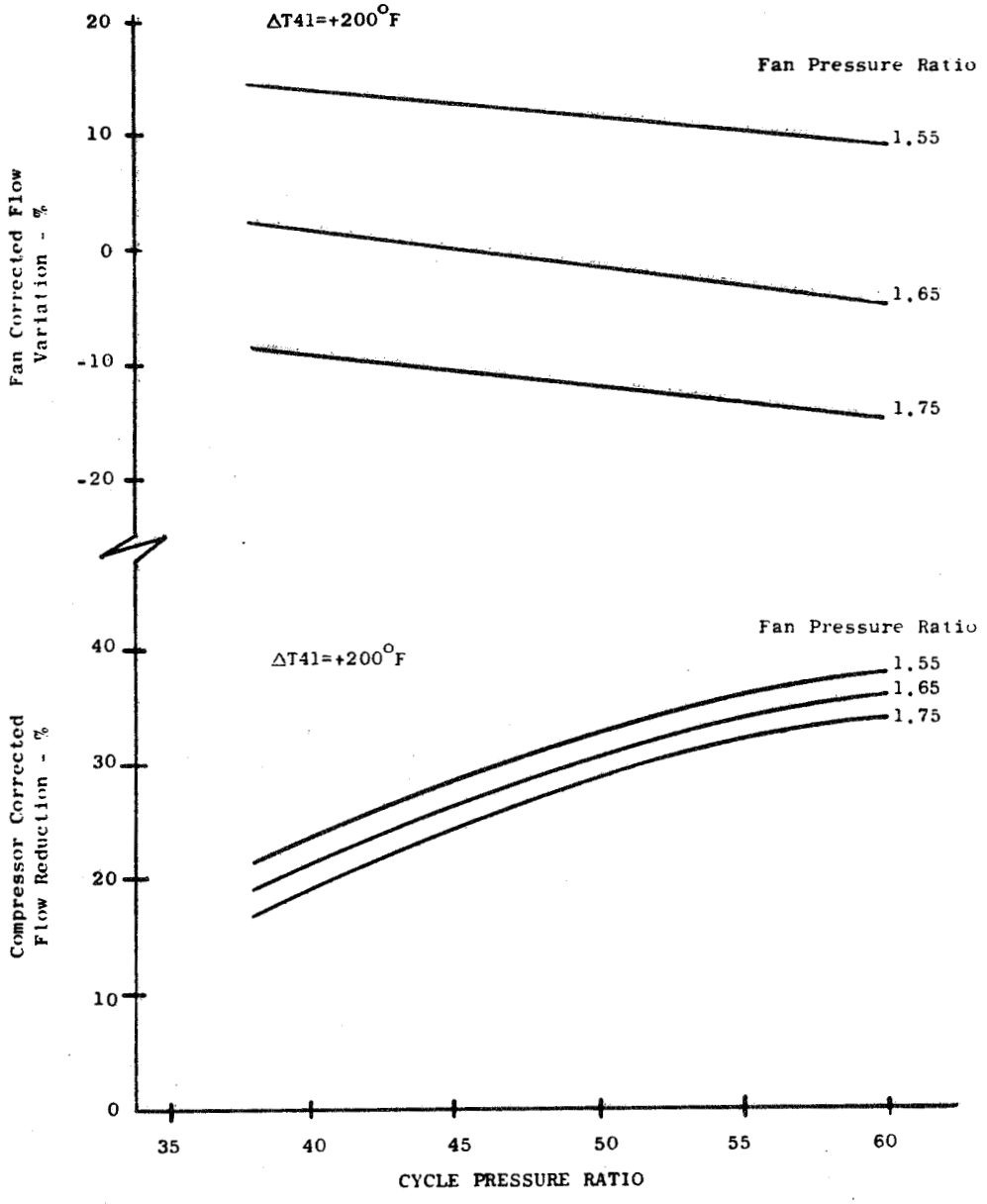

Figure 4.1-9. Fan and Compressor Corrected Flow Variation vs. CPR and FPR.

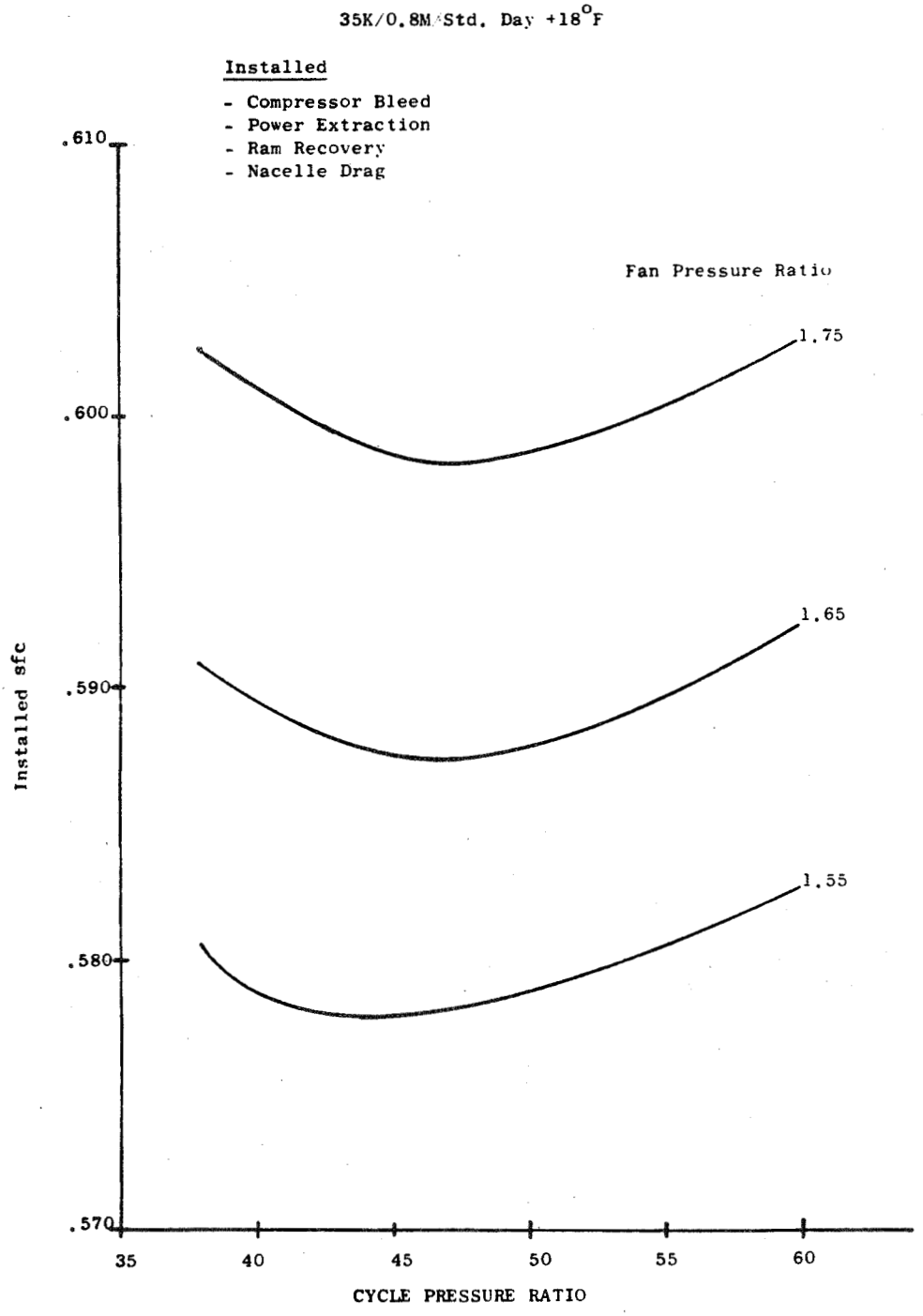

Figure 4.1-10. Installed sfc at Max Climb vs. CPR and FPR with Improvements in Component Efficiencies and Metal Temperatures.

Table 4.1-7. LP Turbine Design Variation with Fan Pressure Ratio.

	E^3 FPS	Post-E^3 Cycles		
Fan Pressure Ratio	1.65	1.55	1.65	1.75
Δ Fan Diameter (in.)	Base	+6.8	0	-5.4
LP Turbine Average Stage Loading	1.29	1.29	1.29	1.29
Number of LPT Stages	5	6	6	6
Δ Diameter LPT Rotor 1 Diameter (in.)	Base	+6.8	0	-4.8

Table 4.1-8. Sfc Sensitivity to Component Efficiency - E^3 FPS Cycle Design Point. 35000 ft/0.8M/Std. Day

Efficiency Improvement	New Engine Size	Fixed Engine Size
+1% Rotating Components		
Fan Bypass	.75	.50
Fan Hub	.20	.15
Compressor	.75	.40
HP Turbine	.80	.55
LP Turbine	.80	.60
Mixer Effectiveness +5%	.30	.25

higher bypass ratios for constant fan pressure ratio. Once the engine geometry is fixed, however, the effect of efficiency improvements is reduced. Knowing the component performance levels attainable is essential to proper sizing of a new engine.

4.1.3.2 Cooling Flow Effects

The effects of cooling flows on specific fuel consumption were examined for the high-pressure turbine first and second rotors, second vane, and first-stage shroud. Elimination of the cooling flow going to all of these parts would improve the specific fuel consumption by 2 percent at max cruise thrust, the first rotor providing over half the improvement. The first-stage-shroud cooling flow has the least impact on sfc.

4.1.3.3 Power Extraction Effects

The sensitivity of sfc to power extraction for aircraft use was determined for extraction from the high-pressure shaft and from the low-pressure shaft. At the E^3 FPS cycle design point of 35,000 ft/0.8 Mach, extraction of 100 horsepower from the high-pressure shaft increases sfc by 0.45 percent and extraction of 100 horsepower from the low-pressure shaft increase sfc by 0.52%.

4.1.3.4 Lower Fan-Pressure-Ratio Studies

Since the parametric studies on fan pressure ratio variations indicated that a 1.2 percent installed sfc benefit was possible using a 1.55 fan pressure ratio instead of the 1.65 in the E^3 FPS cycle, the lower fan pressure ratio was also examined for a cycle with FPS technology. Studies to identify the weight versus sfc tradeoffs of the 1.55 FPR were conducted. The study showed that the same 1.2 percent installed sfc reduction would occur. Weight estimates were defined for both five-stage and six-stage LP turbine configurations. Both flowpath and weight results indicated that a six-stage LP turbine would be more desirable than a five-stage turbine. A five-stage turbine would weigh 400 lb more than the current FPS turbine while a six-stage turbine would be only 333 lb heavier. The five-stage turbine would have a larger exit diameter and a longer interturbine transition duct than the six-stage turbine.

The total weight of the fan, inlet, necelle, thrust reverser, and fan duct was estimated to be 395 lb greater than the weight of the present FPS configuration. The total engine weight increase, then, is 728 lb for the 1.55 fan pressure with a six-stage LP turbine. This configuration, which is larger in diameter, is shown in Figure 4.1-11 in comparison with the current FPS engine flowpath. Weight differences in the various areas are also shown. Tables 4.1-9 and 4.1-10 compare the performance and mechanical design of this configuration with the baseline E^3 engine.

For a domestic aircraft, an increase in engine weight of 728 lb would increase fuel burned by 1.28 percent. An sfc improvement of 1.2 percent would reduce fuel burned by 1.57 percent. The net effect of the lower fan pressure ratio would, therefore, be a 0.3% reduction in fuel burned.

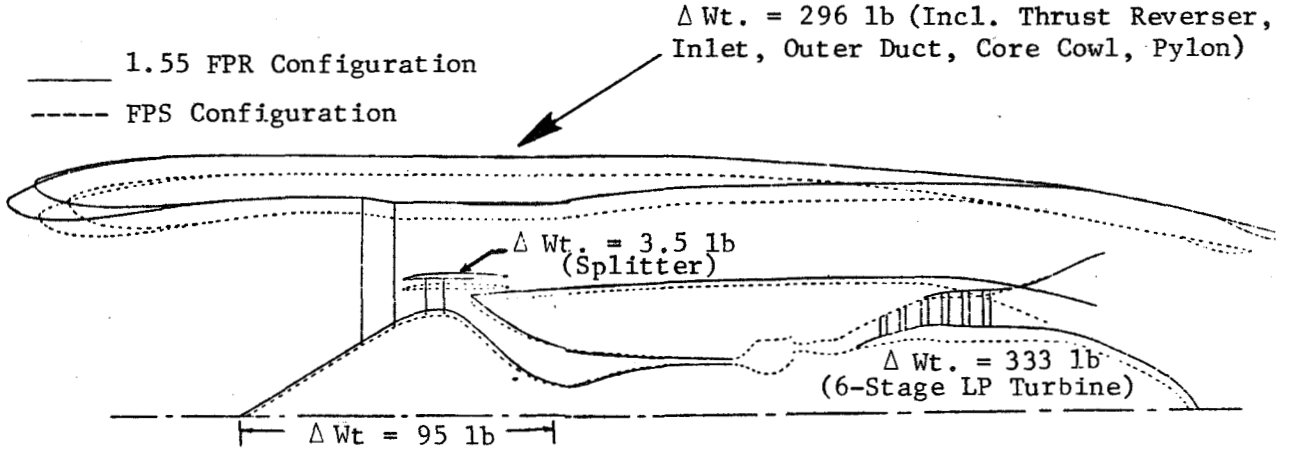
Δ Wt. = 296 lb (Incl. Thrust Reverser, Inlet, Outer Duct, Core Cowl, Pylon)
1.55 FPR Configuration
FPS Configuration
Δ Wt. = 3.5 lb (Splitter)
Δ Wt. = 333 lb (6-Stage LP Turbine)
Δ Wt = 95 lb

Δ Wt = 42.5 lb (Includes Fan & Booster Rotor)

Δ Wt = 52.5 lb (Includes Fan & Booster Frame/Stator)

Figure 4.1-11. Weight Comparison Between Lower-Fan-Pressure-Ratio Flowpath Configuration and Current FPS E^3 Configuration.

Table 4.1-9.

Reduced Fan Pressure Ratio - E^3 FPS Technology Performance Comparison

35000 ft/0.8M/Std. Day + 18° F

	E^3 FPS	Alternate Fan
Assumptions		
Fan Pressure Ratio	1.65	1.55
Uninstalled Net Thrust	9040	9040
HP Turbine Rotor Inlet Temperature	Base	Base
LP Turbine Average Stage Loading	Base	Base
Results		
Uninstalled sfc	Base	-2.6%
*Installed sfc	Base	-1.2%
Bypass Ratio	6.8	8.1

*Isolated nacelle with customer bleed and power extraction

Table 4.1-10.

Size Comparison Between E^3 FPS and Reduced Fan-Pressure-Ratio Technologies.

	E^3 FPS	Alternate Fan
Fan Pressure Ratio	1.65	1.55
Fan Diameter	83 in.	+ 6.8 in.
Number of LP Turbine Stages	5	6
LPT 1st Rotor Tip Diameter	Base	+ 3.4 in.
LPT Last Rotor Tip Diameter	Base	+ 2.9 in.
Engine and Nacelle Weight	Base	+ 728 lb
Engine Length	Base	+ 14 in.
CG Location Relative to Nozzle Exit Plane	Base	7 in. Forward

The increased length of this engine could result in an additional fuel-burned penalty. Since the nozzle exit plane for a mixed-flow nacelle would be expected to remain at about the same location relative to the wing, the engine center of gravity would move forward. The additional amount of aircraft structure needed to accommodate this forward CG shift could produce an increase in fuel burned as high as 0.3%, resulting in a zero net change in total mission fuel burned.

4.1.3.5 Cooling Flow Modulation

The performance benefits of an advanced-technology cooling-flow modulation system that would control seventh-stage and compressor discharge air were examined. The system could be utilized in several ways to provide additional flexibility in the tradeoff of thrust ratings, fuel consumption, and hot section life. The system could be designed to reduce flow when it is not needed so that fuel consumption is improved, or it could be used to increase flow at critical thrust conditions, allowing thrust growth or improved life without sacrificing cruise fuel consumption.

If the full modulation capability that could be expected for the FPS engine were used to reduce flow below the current FPS levels, the 35,000 ft/0.8 Mach cruise specific fuel consumption would be improved by 0.7%. If the modulation system only increased the cooling flow above current FPS levels the takeoff thrust at sea level static/standard day +27°F could be increased by more than 15 percent without increasing the metal temperature of cooled parts. However, other factors, such as the higher stresses as rotational speeds increase and the higher temperatures in uncooled parts, could limit the thrust growth to a level below this 15 percent. These factors would have to be examined in detail to determine the actual level of thrust growth that could be achieved for a specific application.

4.1.3.6 Variable Primary Nozzle

The use of a variable primary nozzle was evaluated to determine the potential sfc improvements. For the E^3 FPS at 35,000 ft/0.8 Mach/standard-day cruise conditions, a reduction in nozzle area will improve sfc at thrusts below 75 percent of the max-cruise thrust as shown on Figure 4.1-12. At 60 percent of max-cruise thrust the sfc is reduced by 1.7 percent when the nozzle area is closed 5 percent. At typical loiter thrust levels for 15,000 ft/0.5 Mach conditions, the sfc is reduced by anywhere from 3 to 4 percent with a 5 percent nozzle area reduction. A typical short-range commercial mission analysis indicated that these improvements would reduce mission fuel consumption by about 0.5%. However, the weight increase for the variable nozzle of about 130 lb would reduce the improvement to about 0.3%. Table 4.1-11 shows the effect of a 5 percent nozzle area reduction on engine fuel for various segments of a typical mission profile and the net mission fuel benefit.

It should be emphasized that the typical reference commercial mission profile does not have a long loiter time block. In this respect, the improvement projection can be considered conservative. When considering military

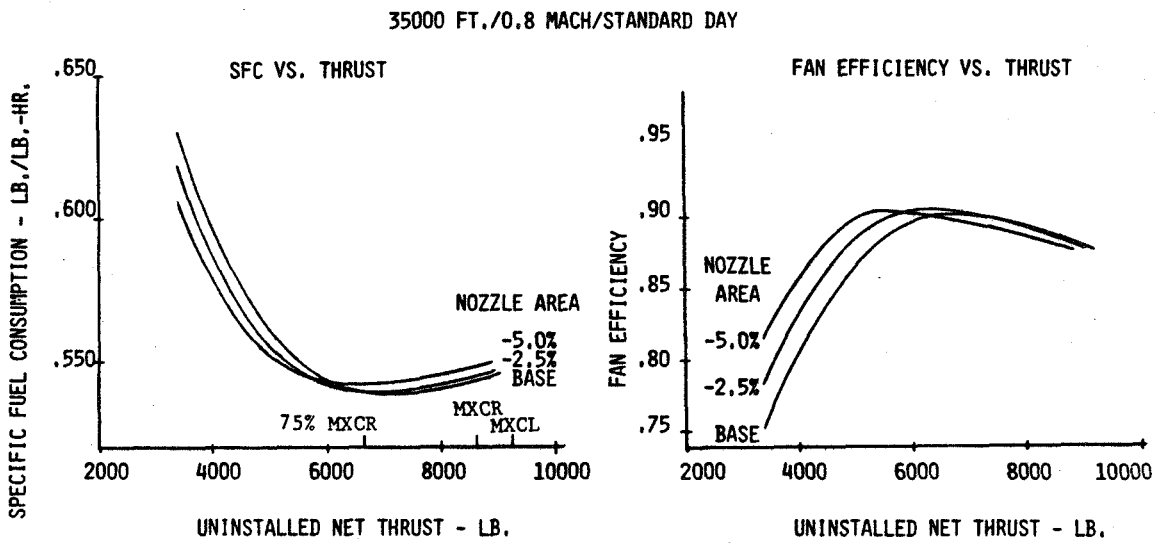

Figure 4.1-12. Effects of Variable Exhaust Nozzle Area for E^3 FPS.

Table 4.1-11. Mission Profile sfc Benefits of a 5% Variable Area Nozzle.
30,000 ft - Short-Range Mission

Mission Segment	% Engine Fuel
Idle and Takeoff	+.1
Climb	+.1
Cruise	-.65
Descent	0
Loiter	-3.3
Approach	-1.1
Engine Mission Fuel-Burned Benefit	-0.5%
130 lb Weight Penalty	+0.2%
Net Mission Fuel Benefit	-0.3%

applications where endurance or station keeping missions are involved, the fuel savings can be substantial as indicated by the 3 to 4 percent improvement at loiter power. Such missions could include airborne early warning or command-post aircraft.

4.1.3.7 Rankine Bottoming Cycle

A concept for a Rankine bottoming cycle for use in customer energy extraction was examined and was found to be unfeasible since the system would cause high pressure losses in the engine flowpaths, resulting in significant thrust loss and thus a significant penalty in specific fuel consumption. As a consequence of the thrust loss, the engine size (and weight) would increase to meet the required thrust rating. The increased engine weight would then be reflected in an increase in fuel burned.

4.1.4 Cycle & Performance Studies Summary

These studies addressed engine design technology in three areas: component efficiencies, metal temperature, and cooling air requirements. The results show that substantial savings could be achieved with advances in these areas along with proper reoptimizing of the engine cycle and component sizes. The technology improvement assumptions used in this study represent a substantial challenge and would require an aggressive effort in order to achieve these levels. The economic payoffs in terms of fuel burned and DOC savings, however, are significant.

Component efficiency (η) improvements of one percent beyond the E^3 FPS level are a challenge. An increase from 90% to 91% on the surface may not seem difficult; however, if the perspective is taken relative to the "loss factor" $(1 - \eta)$, a 1% improvement represents a 10% reduction in the loss factor. A series of development tests for each component would be necessary to achieve such an improvement.

Component efficiency improvements are a result of advances in both aero and mechanical design. Blade loading distribution, cambering, and tip losses are some of the factors in the aero design area. In the mechanical design area, factors of concern are clearances, shroud roundness control, blade row gaps, dovetail leakages, and bearing locations.

Advances in metal temperature technology are very important in that they not only improve sfc but result in a substantially smaller core-flow size for a given thrust-size engine. The +100° F example used in this study reduced the sfc by -1.9%, but also important was a 23% reduction in core-flow size requirement. This results in an additional fuel-burned benefit for an E^3 size through a 720-pound weight reduction, or permits a 20% thrust growth for the same-size core with a slightly larger fan.

Cooling air circuit technology advances offer an additional sfc improvement to metal temperature benefits by permitting operation at higher turbine temperatures. The additional reduction in core size, however, is not as significant, and current limitations on compressor discharge temperature are

not improved. This could provide a constraint on the increase in cycle pressure ratio which would be desired with the increased turbine inlet temperature capability. Examination of the technology trend curves in Section 2.0 for metal temperature and turbine temperatures shows a continuing divergence of the two curves as a result of cooling technology advances. Cooling-air reductions from heat transfer improvements, thermal barrier coatings, and modulated turbine cooling air provide additional payoffs to that achieved with the metal temperature improvement and should be continued.

4.2 HPT METAL COOLING IMPROVEMENTS

Selection of a turbine cooling design balances the substantial cycle benefits of high turbine inlet temperatures against the substantial penalties of reduced turbine efficiency and bleeding of high-pressure air. A moderate improvement in cooling effectiveness can produce very significant fuel savings.

More efficient cooling methods have been explored in military engine demonstrator programs. These involve the use of more impingement inserts, multiple cooling passages, shaped film holes, and smaller holes. They will not be incorporated into near-term commercial engines because of manufacturing impracticability, life concerns, and possible hole plugging. They will be realizable for commercial use when the design, analysis, and manufacturing technologies are developed.

Elimination of all cooling flow to the Stage 1 and 2 blades, Stage 2 vanes, and Stage 1 shroud will improve specific fuel consumption by 2%. A realizable improvement in cooling technology has been assessed at giving a 0.8% improvement in sfc.

Cooling flow reductions allow the core to be down-sized for the same total thrust. Down-sizing the core reduces weight by 64 lb and reduces engine cost, partially balancing the higher cost of the cooling design.

Figure 4.2-1 and Table 4.2-1 summarize the benefits of this concept.

Included in the technology needed to improve turbine cooling are:

- Prediction of insert life
- Prediction of blade LCF and rupture life
- Blade tip durability
- Analysis of platform cooling
- Prediction of blade gas-side heat transfer coefficient in a rotating environment
- Prediction of radial gas temperature profiles considering energy extraction, dilution, and mixing
- Prediction of rotating cavity flow (windage, pumping, and recirculation)
- Prediction of internal cooling in high "g" field (high buoyancy and Coriolis forces)
- Improved rotor seals (windage and leakage considerations)
- Improvement of flowpath seals (spline seals, hourglass seals)

The technology is applicable to all gas turbines.

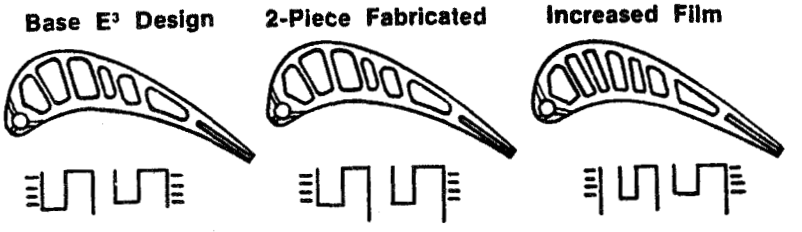

BENEFITS

- Reduced Cooling Flow In HPT

BARRIER PROBLEMS

- Cost

PROBABILITY OF SUCCESS

- DESIGN AND DEV. - 90%
- MANUFACTURING - 90%
- ACCEPTANCE - 90%

Figure 4.2-1. HPT Metal Cooling Improvements.

Table 4.2-1. HPT Metal Cooling Improvements.

DESIGN IMPACTS	DIRECT	SECONDARY (RESIZING)	TOTAL
△ WT., LBS.	0	-64	-64
△ COST, $K	+21	-17	+4
△ MAINT., $/FLT.-HR.	+.30	N.A.	+.30
△ SFC, %	-.8	N.A.	-.8

MERIT FACTORS -1.2 $\triangle W_f$-% -1.2 $\triangle$DOC-% 65 PW - $M

RANKING 58 $\frac{P.W. \cdot Ps}{IDC}$

4.3 HPT MODULATED COOLING FLOW

Cooling flow rates are set by takeoff and climb, the high-temperature segments of the flight. Flows established at those conditions are somewhat wasted at the lower-temperature segments of cruise, loiter, and descent.

	Combustor Discharge Temperature, °F
High-Altitude Hot-Day Takeoff (Special Rating For Denver Bump)	2630
Hot-Day Takeoff	2590
Standard-Day Takeoff	2450
Warm-Day Max Climb	2480
Standard-Day Max Cruise	2300
Standard-Day 80% Cruise	2120
Loiter	1770
Descent	1120

The performance benefits of an advanced-technology cooling-flow modulation system that would control seventh-stage and compressor discharge air were examined. The system could be utilized in several ways to provide additional flexibility in the tradeoff of thrust ratings, fuel consumption, and hot section life. The system could be designed to reduce flow when it is not needed so that fuel consumption is improved, or it could be used to increase flow at critical thrust conditions, allowing thrust growth or improved life without sacrificing cruise fuel consumption.

If the full modulation capability that could be expected for the FPS (Flight Propulsion System) engine were used to reduce flow below the current FPS levels, the mission specific fuel consumption would be improved by 0.7%. If the modulation system only increased the cooling flow above current FPS levels, the takeoff thrust at sea level static/standard-day +27° F could be increased by more than 15% without increasing the metal temperature of cooled parts. However, other factors, such as the higher stresses as rotational speeds increase and the higher temperatures in uncooled parts, could limit the thrust growth to a level below this 15%. These factors would have to be examined in detail to determine the actual level of thrust growth that could be achieved.

This concept applies to gas turbines in general and does not require new analysis or structural advancements. Its control could be handled by Full Authority Digital Electronic Controls (FADEC's) now under development. Figure 4.3-1 and Table 4.3-1 summarize the benefits of the HPT modulated-cooling-flow concept.

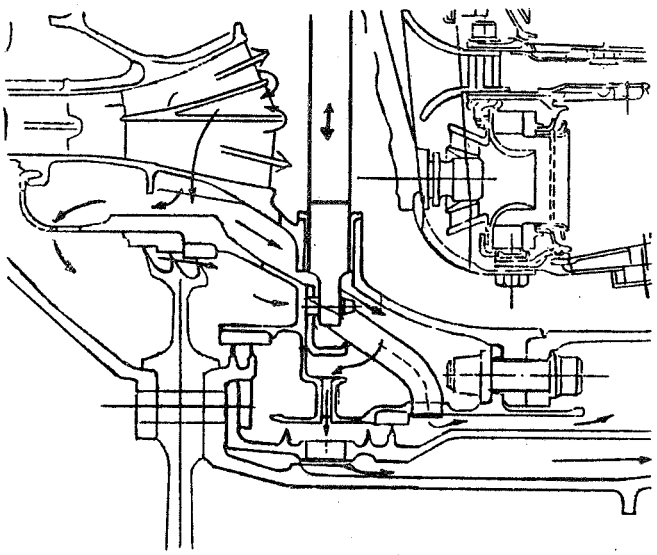

BENEFITS

- Reduce HPT Cooling At Cruise
- Increase HPT Cooling At Hot Day Takeoff

BARRIER PROBLEMS

- None

PROBABILITY OF SUCCESS

- DESIGN AND DEV. - 95%
- MANUFACTURING - 95%
- ACCEPTANCE - 95%

Figure 4.3-1. Modulated Cooling Flow.

Table 4.3-1. Modulated Cooling Flow.

DESIGN IMPACTS	DIRECT	SECONDARY (RESIZING)	TOTAL
△ WT., LBS.	+14	0	+14
△ COST, $K	+39	0	+39
△ MAINT., $/FLT.-HR.	+.05	0	+.05
△ SFC, %	-.7	0	-.7

MERIT FACTORS -.9 $\triangle W_f$-% -.8 △DOC-% 42. PW - $M

RANKING FACTOR 40. $\frac{PW \cdot Ps}{IDC}$

4.4 HPT METAL TEMPERATURE IMPROVEMENT

Increasing the temperature capability of turbine materials is important because it extends life, allows increased cycle temperatures, and/or reduces the amount of cooling air needed. If materials in the turbine of an existing engine were improved by 100° F, cooling air could be substantially reduced which would very significantly improve fuel consumption.

If, instead, a new E^3 engine were designed that used materials having 100° F higher temperature capability, the engine would be quite different and the benefit due to the materials would be very substantially increased. This is the approach used here.

A 100° F increase in turbine metal temperature allows a 200° F increase in turbine inlet gas temperature. The pressure ratio of the resulting optimized engine cycle increased from 38 to 45. This increased the temperature levels in other parts of the engine. There was a major reduction in core size, with a 23.5% lower core flow, and a smaller reduction in fan size, with a 1.4% lower fan flow. The weight reduction for the smaller-size core more than offsets the weight increase due to the higher pressure ratio. And, except for the costs of higher-temperature materials, the smaller core reduces engine cost. The sfc improves 1.9%.

The engine weight and cost savings in the reoptimized engine are better than ten times the savings that would be realized by using higher-temperature materials to reduce cooling air in an existing engine.

Achievement of a 100° F higher temperature capability is a major metallurgical advancement. It is associated with directionally solidified eutectic alloys, which require coatings. While current coatings may have the temperature capability, a higher-temperature bond coat would have to be developed. Hollow airfoils may have to be fabricated in order to expose inner surfaces so the surface grains can be treated. Fabrication technology would permit more intricate cooling designs. The resulting development cost is high and there is a significant risk. Figure 4.4-1 and Table 4.4-1 summarize the benefits of this concept.

Technologies which need to be developed are in the materials and processes fields. These technologies are applicable to any gas turbine.

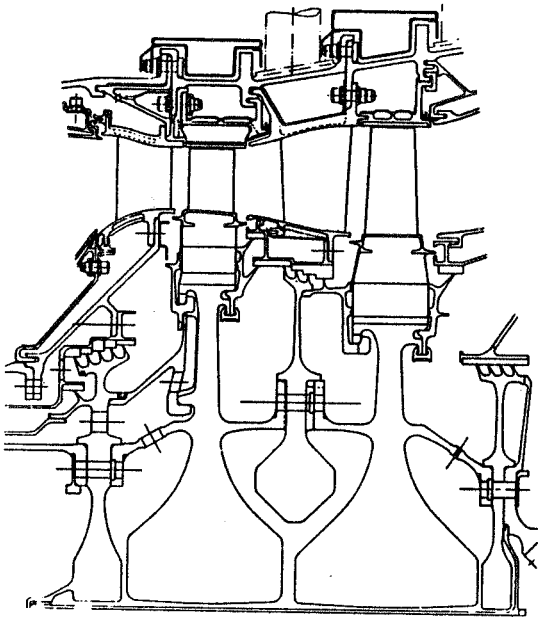

BENEFITS

- Lower Cooling Flow, Better SFC

BARRIER PROBLEMS

- Low Casting Rate
- Coating Temp. Capability
- Repairability

PROBABILITY OF SUCCESS

- DESIGN AND DEV. - 70%
- MANUFACTURING - 80%
- ACCEPTANCE - 90%

Figure 4.4-1. Metal Temperature Improvement - 100° F HPT Materials.

Table 4.4-1. Metal Temperature Improvement - 100° F HPT Materials.

DESIGN IMPACTS	DIRECT	SECONDARY (RESIZING)	TOTAL
△ WT.; LBS.	0	-722	-722
△ COST; $K	360	-180	+180
△ MAINT.; $/FLT.-HR.	+.6	N.A.	+.6
△ SFC, %	-1.9	N.A.	-1.9

MERIT FACTORS -4.0 $\triangle W_f$-% -4.7 △DOC-% 247 PW - $M

RANKING FACTOR 41 $\frac{P.W \cdot Ps}{IDC}$

4.5 METAL COATINGS IMPROVEMENT

Like higher-temperature materials, thermal barrier coatings can extend life, allow increased cycle temperatures, and/or reduce cooling air. Coatings are currently in use, but they are not relied upon to last the entire life of the blade. Cooling levels are selected so that a blade can last until an overhaul, even if the coating should fail. A significant improvement in performance can be realized if coating reliability can be improved to the level where cooling flows can be reduced to take full advantage of the insulating qualities of the coatings. That is the subject of this study: coatings with life increased to the level of the turbine blades. This approach is different from what was used for the +100° F material, where turbine inlet gas temperature was increased and the cycle was reoptimized. The approach here is a less bold step and does not require that coatings operate in a different environment from what is currently in use.

Coatings are being considered for use on the blades of the present E^3 turbine. These blades are DS Rene' 150 which requires a 1900° F bond coat. The coating life is required to be 9000 hours and 9000 cycles.

Coatings are applied to the combustor and all four blade-rows and bands in the HP turbine. Applying coatings to the combustor allows a reduction in liner cooling. This flattens the profile of temperatures going into the turbine, which reduces turbine cooling requirements.

Coatings are projected to have moderate development cost, moderate application cost, and promise of substantial fuel savings. This type of technology yields a good return on investment over a broad range of fuel prices.

Figure 4.5-1 and Table 4.5-1 summarize the benefits of this concept. The technology development is metallurgical and applies to all cooled turbine engines.

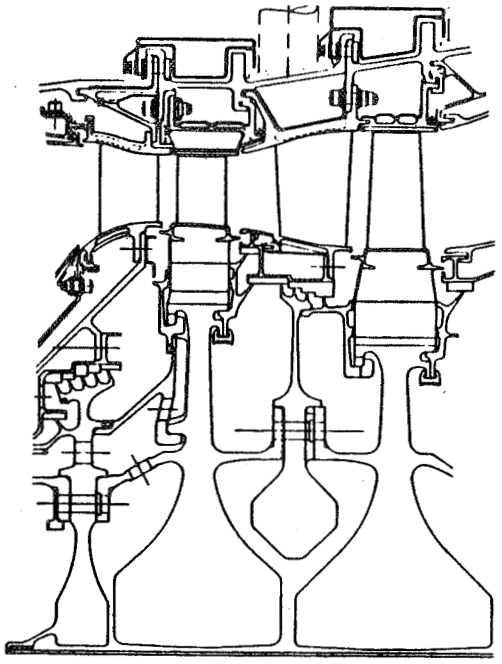

BENEFITS

- Lower Cooling Flow, Better SFC

BARRIER PROBLEMS

- Coating and Bond-Coat Temperature Capability

PROBABILITY OF SUCCESS

- DESIGN AND DEV. - 65%
- MANUFACTURING - 80%
- ACCEPTANCE - 90%

Figure 4.5-1. Metal Coating Improvement - Thermal Barrier Coatings in Combustor and HP Turbine.

Table 4.5-1. Metal Coating Improvement - Thermal Barrier Coatings in Combustor and HP Turbine.

DESIGN IMPACTS	DIRECT	SECONDARY (RESIZING)	TOTAL
△ WT., LBS.	+27	-65	-38
△ COST, $K	+22	-17	+5
△ MAINT., $/FLT.-HR.	+1.	N.A.	+1.00
△ SFC, %	-.52	N.A.	-.52

MERIT FACTORS: -.79 $\triangle W_f$-% ; -.74 △DOC-% ; 39 PW - $M

RANKING: 17 $\frac{P W \cdot Ps}{IDC}$

4.6 SHORTENED FAN CONFIGURATION

This effort was directed toward evaluating the positive and negative aspects of shortening the fan flowpath both from an aerodynamic and structural assessment. The objectives of the studies were to assess the effects on performance, noise, weight, engine growth capability, mechanical design, and system dynamics, based on an 8-inch-shorter fan flowpath. The E^3 FPS configuration was used as a baseline for comparison.

The objectives of the aerodynamic study were to assess the feasibility of a shorter booster stage, fan frame and core transition duct and to define a flowpath which would produce the same flow and pressure ratio as the current E^3 fan configuration. The resultant configuration was analyzed to determine the effects on fan hub efficiency and transition duct losses.

The technical approach relative to the current E^3 design was to maintain the same fan rotor tip speed, inlet radius ratio, number of blades, chord length, and part-span shroud location. The overall bypass ratio was unchanged as well as the fan hub supercharging. In order to decrease the axial length from the fan rotor exit to the core compressor inlet, the hub flowpath was dropped to a lower radius beginning at the fan rotor exit and continuing through the transition duct. The fan frame trailing edge was moved forward approximately eight inches, the core splitter nose was moved closer to the booster, and the quarter-stage island was shortened and lowered slightly. The resulting flowpath configuration is compared with the baseline E^3 configuration in Figure 4.6-1. The primary flowpath dimensional changes are as follows:

- The fan hub exit radius was reduced by 1 inch.
- The hub flowpath radius was reduced by 1-6 inches.
- The booster island lower surface radius was reduced by 1 inch.
- The island was shortened and thickened.
- A longer booster blade/vane was used.

The preliminary aero design resulted in essentially no changes to the fan rotor. The only change in the booster stator was an increase in vane aspect ratio from 1.91 to 2.17. The booster rotor blade requires significant modification, however, to maintain the overall fan pressure ratio in the shortened fan configuration. This includes the addition of two more vanes and changes in camber, stagger, and solidity. These changes reflect a design characterized by higher aerodynamic loading.

A mechanical design layout showing the shortened fan configuration is presented in Figure 4.6.2. The basic design construction of the fan/booster is unchanged with the exception of small changes in booster height and airfoil contour.

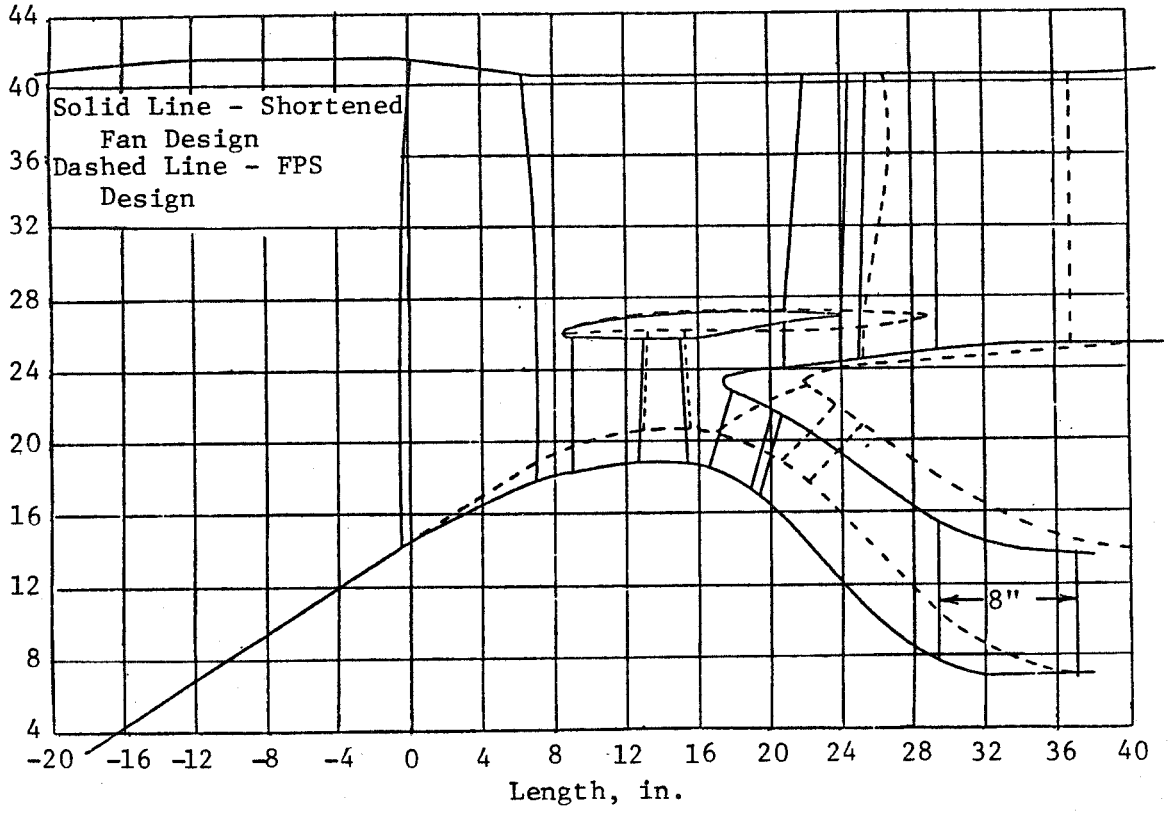

Figure 4.6-1. Flowpath Configuration Comparison Between Shortened Fan and E^3 FPS.

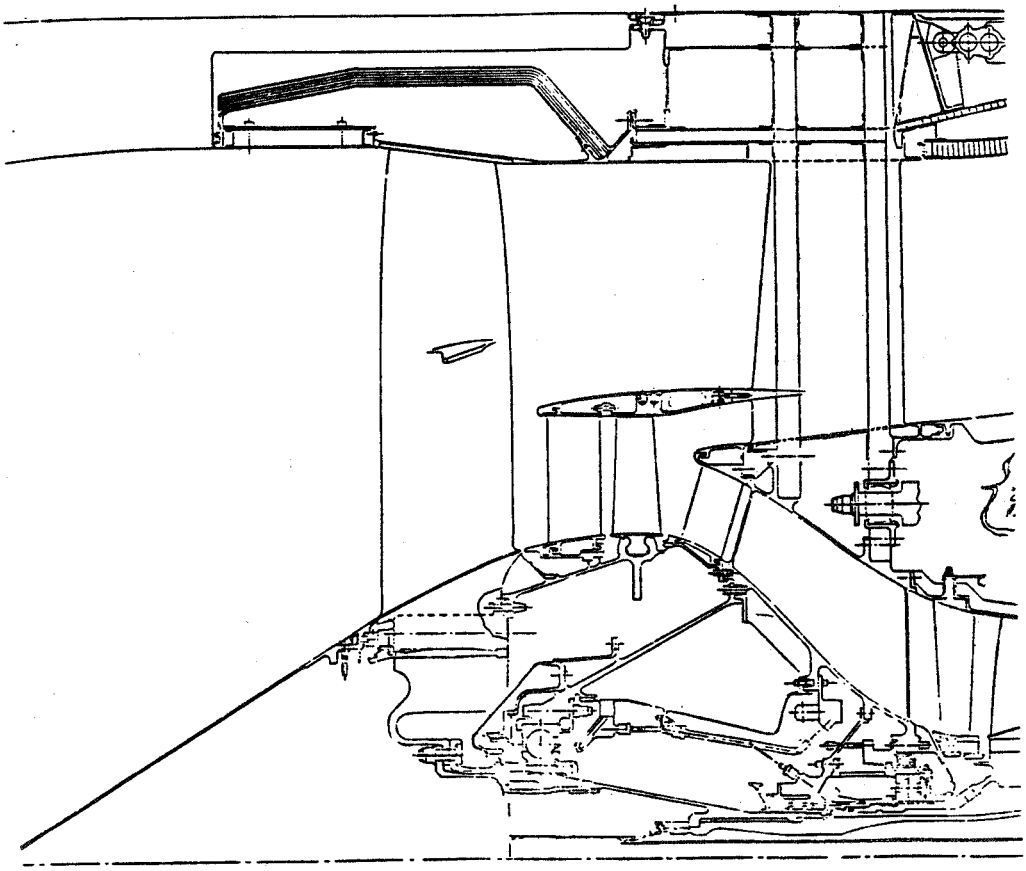

Figure 4.6-2. Shortened Fan Configuration.

In an attempt to determine the noise penalties associated with an eight-inch-shorter fan flowpath, an evaluation of noise levels was carried out as a function of E^3 rotor-to-stator spacings. In Figure 4.6-3 the component noise levels which combine to produce the total system EPNL are shown for both takeoff and approach power settings. The Boeing twinjet is used as the baseline aircraft. At takeoff the major noise component is the mixed-flow jet, with the fan inlet also contributing. The latter component will change with rotor-stator spacing, but since the jet noise remains constant the resulting change in takeoff system noise is therefore small.

At approach, however, the fan inlet is the major noise component, and the fan exhaust makes a contribution. Since both of these components are affected by rotor-stator spacing, the approach condition should show the greatest impact.

The variation in fan component and total system noise as a function of spacing was estimated for the current vane-frame design. Figure 4.6-4 shows the fan inlet and exhaust component EPNL as functions of spacing. The increase in forward-radiated fan noise for the vane frame design is due to the cut-on fan fundamental tone level increasing with decreasing spacing. This trend is substantiated by the scale-model fan vane frame test conducted as part of the E^3 acoustics program. Figure 4.6-5 shows the change in total system noise at approach as a function of rotor-OGV spacing. The slow rate of increase in system EPNL with decreasing spacing is attributable to the relatively low levels of the fan exhaust noise for the baseline case at S/C = 1.91. This is illustrated in Figure 4.6-3, which shows the fan exhaust component to be 5 EPNdB below the fan inlet component. The relative importance of the fan inlet component also explains the more rapid increase in total system noise for the vane frame spacing change, since it incurs a penalty on the forward-radiated cut-on fan tones with decreasing spacing. In summary, this shows that the shortened fan configuration results in a penalty of only 0.45 EPNdB for total system approach levels.

In order to assess the structural feasibility of a shortened fan frame configuration in terms of stiffness capability and systems vibration characteristics, further analysis was conducted. The baseline FPS frame model shown in Figure 4.6-6 was modified to reflect the shortened frame configuration. Frame stiffeners were determined for overturning moment and radial shear load. The results indicate that both bypass vane and core strut overturning moment stiffnesses are considerably lower than those of the FPS configuration. The shear load radial stiffness is equal to or greater than FPS for the shortened frame configuration.

Detailed analytical studies were also completed which investigated how fan frame flexibility and a shorter fan flowpath design affected the engine system dynamic and static response characteristics. Table 4.6-1 indicates the spring flexibilities used to represent the fan frame in the engine system planar finite-element model.

Static load response characteristics due to flight condition maneuver loads were found to be dependent on the fan frame definition. Takeoff rotation nacelle

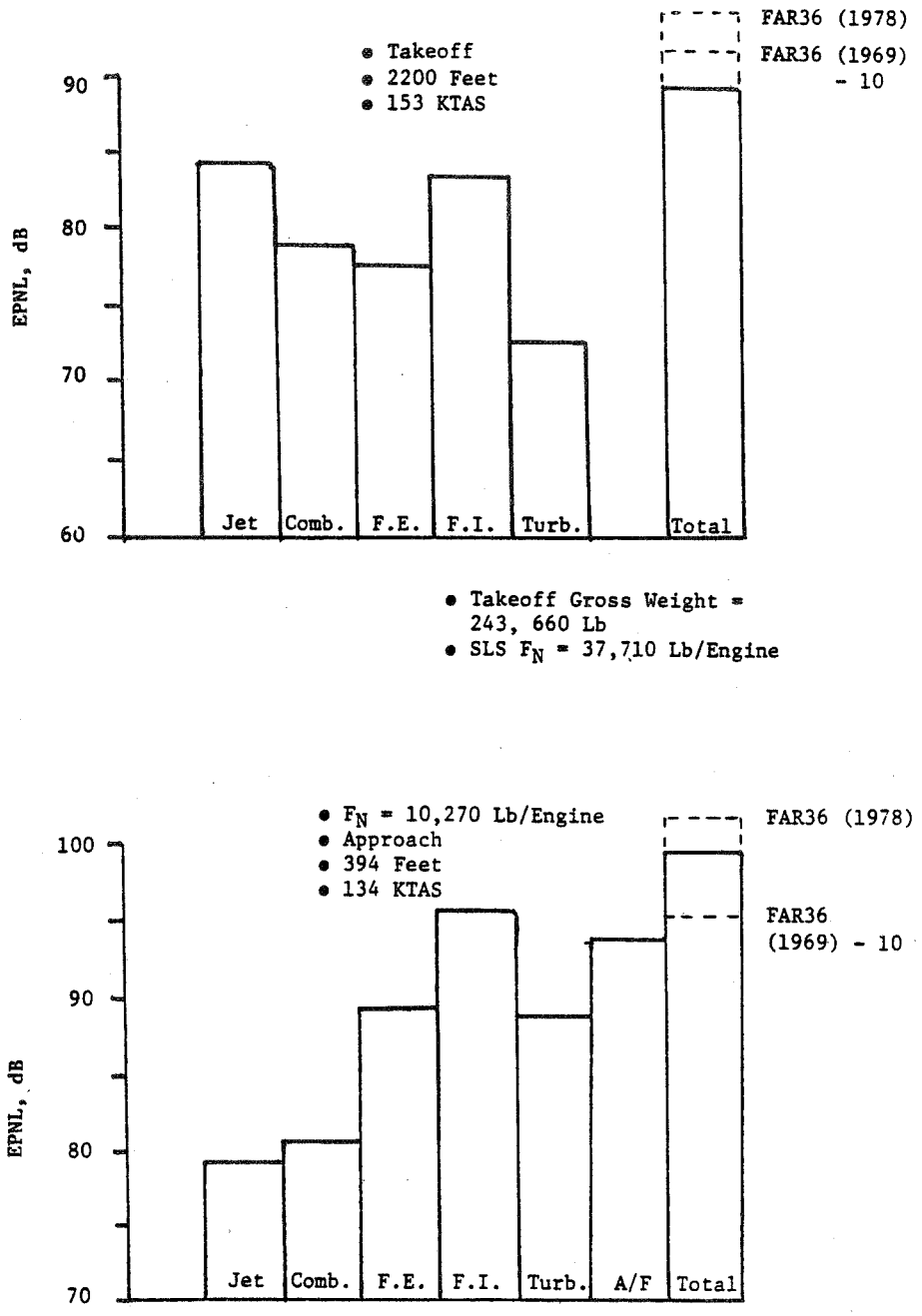

Figure 4.6-3. E^3 Engine Component Noise Summary for Takeoff and Approach Conditions Using Boeing Twinjet Aircraft.

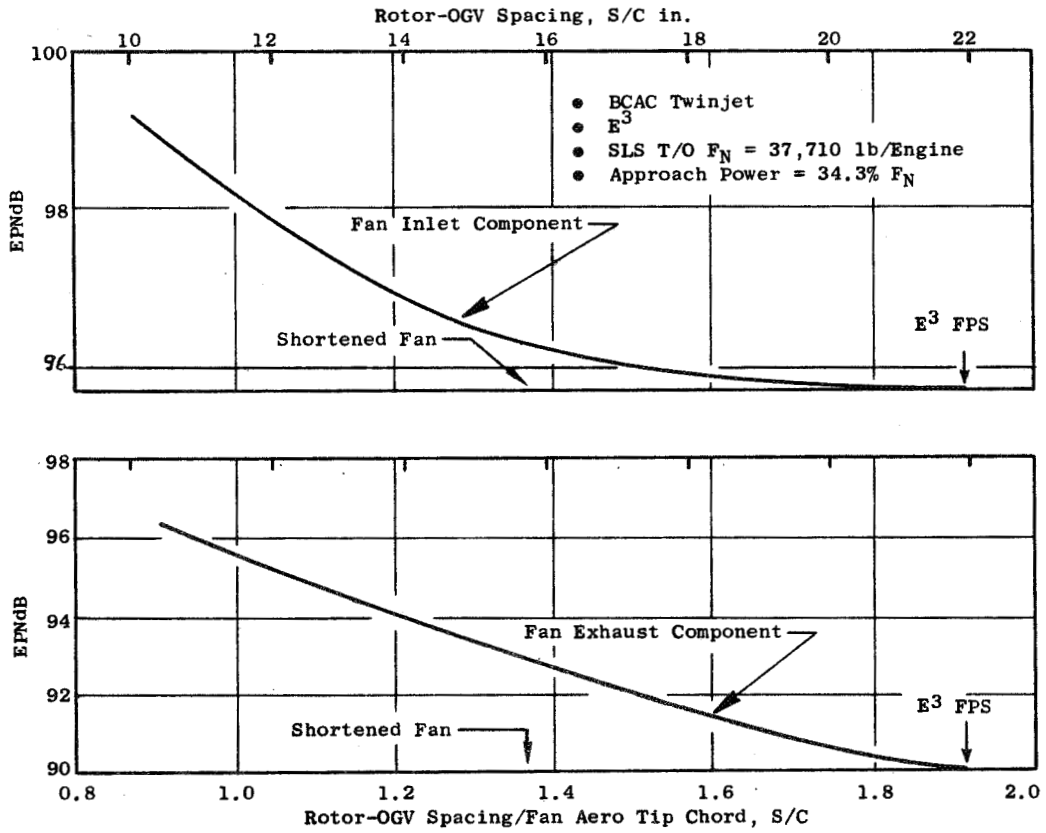

Figure 4.6-4. Change in Fan Component Noise with Rotor-OGV Spacing.

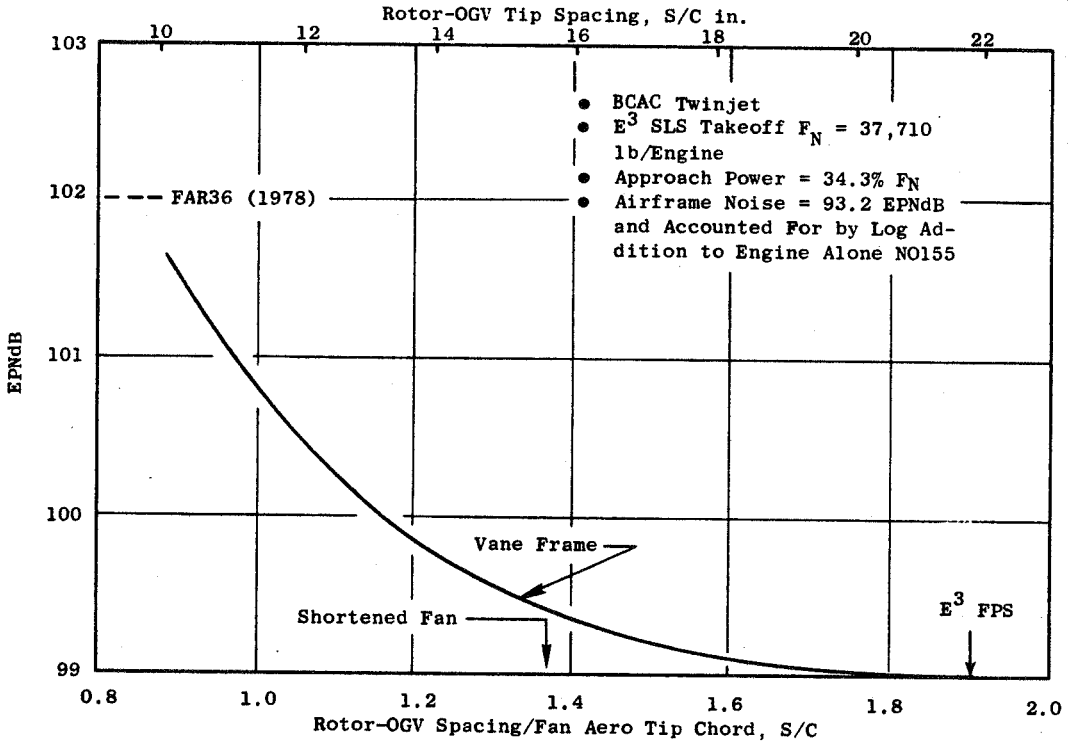

Figure 4.6-5. Variation in Total System Approach EPNL with Rotor-Stator Spacing.

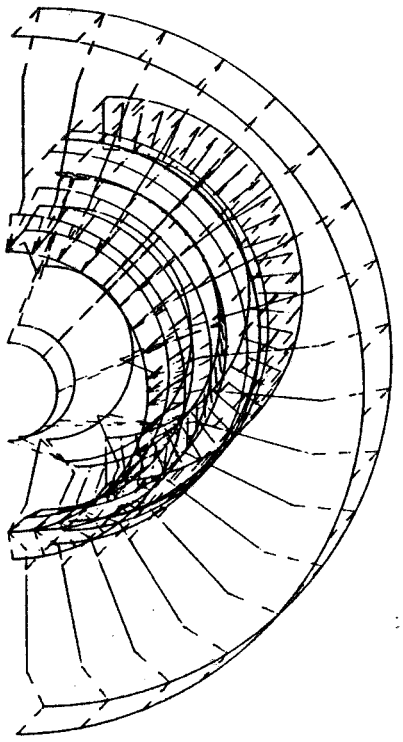

Figure 4.6-6. Nonmodified MASS Model of FPS Fan Frame.

Table 4.6-1. E^3 FPS and ICLS Frame Flexibilities.

	Flexibilities	
Configuration	Core Frame	Bypass Frame
FPS/Baseline	$\phi_M = 4.48 \times 10^{-10}$	$\phi_M = 1.07 \times 10^{-9}$
Flight Fan Frame	$\eta_V = 1.15 \times 10^{-7}$	$\eta_V = 1.91 \times 10^{-7}$
FPS/Soft	$\phi_M = 8.96 \times 10^{-10}$	$\phi_M = 2.14 \times 10^{-9}$
Flight Fan Frame	$\eta_V = 2.30 \times 10^{-7}$	$\eta_V = 3.82 \times 10^{-7}$

ϕ_M, Overturning Moment Flexibility, RAD/IN-LB

η_V, Radial Flexibility, IN/LB

airloads increased stator-rotor relative deflections by 100 percent at the fan and 40 percent at the HP turbine first stage, for a 50 percent reduction in fan frame stiffness. This decrease in stiffness resulted from the soft overturning moment-carrying capability of the core and bypass fan frames. Static response characteristics in the core were basically independent of the fan frame definition for gravity, gyro, and thrust loadings. Table 4.6-2 compares the stator-rotor relative deflections for both configurations.

Core synchronous response characteristics were found to be independent of the fan frame definition. This was expected, since the core rotor was not changed or modified and it retained the soft mounts and multifilm no-end-flow squeeze film damper. Fan synchronous response characteristics were found to be sensitive to the fan frame definition due to the sensitivity of the responsive mode to strain energy in the fan frame No. 1 bearing and support. The fan rotor-stator relative deflections and No. 1 bearing load peak responses due to fan unbalance were computed to be lower in magnitude and at lower fan speeds for the softer fan frame configurations. The peak response was found to occur above maximum fan speed for both configurations. A comparison of the two configurations was made for the No. 1 bearing load, and for relative deflections at the fan, compressor first stage, HP turbine first stage, and LP turbine first and fifth stages. The frequency response characteristics for 500 gm-in of fan unbalance are illustrated in Figures 4.6-7 through 4.6-12. The data show that while lower frame stiffnesses mean lower modal response, no new criticals appear in the fan operating speed range and in general the amplitudes are lower.

In addition to the reduced frame stiffness study previously discussed a shortened fan configuration model was constructed and analyzed for system vibration characteristics using the FPS frame stiffnesses to assess cause and effect of a shortened engine over the FPS engine.

The fan shaft was shortened between the No. 1 and No. 2 bearings by 8 inches to analyze the short-fan flowpath derivative configuration. The No. 1 bearing support remained basically the same, but the outer inlet nacelle and booster island were shortened to match the new flowpath.

Table 4.6-3 summarizes the static response characteristics due to maneuver loads. The stator-rotor relative deflections were found to be similar to those of the baseline configuration. The only significant change in static response was a 40 percent increase in the No. 1 and No. 2 bearing loads due to gyro loads and the shortened wheelbase. Static response bearing loads are listed in Table 4.6-4. In general the static-response data indicate that there are no adverse deflections and/or bearing load conditions for the shortened fan configuration.

The core synchronous response characteristics were found to be independent of the wheelbase between the No. 1 and No. 2 bearings. The peak fan synchronous response remained above the maximum fan speed; this was expected since the fan frame and bearing support were the same as on the baseline configuration. The critical speeds and mode shapes changed, and two secondary low-amplitude modes were found within the speed range which were responsive to fan unbalance. Figures 4.6-13 through 4.6-16 compare the frequency response characteristics of the short fan flowpath with the baseline configuration.

Table 4.6-2. E^3 FPS Beam Bending Clearance Comparison for Static Loads.

	Stator-Rotor Relative Deflections, Mils										
	Fan	Booster	HPC 1	HPC 5	HPC 9	CDP Seal	HPT 1	HPT 2	LPT 1	LPT 3	LPT 5
1-G Down Gravity Load											
FPS/Baseline	+ 1.70	+ .72	+ 3.17	+ 4.60	+ 5.56	+ 5.86	+ 6.22	+ 6.31	+ 3.67	+ 2.67	+ 1.63
FPS/Soft	+ 2.11	+ 1.51	+ 3.12	+ 4.24	+ 4.86	+ 5.13	+ 5.86	+ 6.03	+ 3.53	+ 2.67	+ 1.73
Thrust, 27,000 lbs.											
FPS/Baseline	+ .16	- .10	- .81	- 1.88	- 2.39	- 2.40	- 2.20	- 2.02	- 1.32	- .71	+ .21
FPS/Soft	+ .75	- .88	- 1.00	- 2.44	- 2.68	- 2.76	- 2.73	- 2.48	- 1.56	- .66	+ .27
Gyro Load, 0.3 Rad/Sec											
FPS/Baseline	+13.71	- 8.05	+ 6.29	+ 6.13	+ 5.37	+ 5.20	+ 4.56	+ 4.07	+12.57	- 5.33	-24.41
FPS/Soft	+14.84	- 6.14	+ 6.41	+ 6.86	+ 6.14	+ 6.13	+ 5.19	+ 4.45	+12.59	- 5.39	-24.67
T/O Rotation Airloads, M = 500,000 M-lb, F = 10,000 lbs											
FPS/Baseline	+28.48	- .30	- 2.39	- 4.87	- 5.38	- 5.11	- 5.73	- 5.68	- 3.97	- 2.21	+ .75
FPS/Soft	+58.33	- 2.72	- 3.08	- 7.51	- 8.24	- 8.49	- 8.38	- 7.63	- 4.81	- 2.03	+ .84

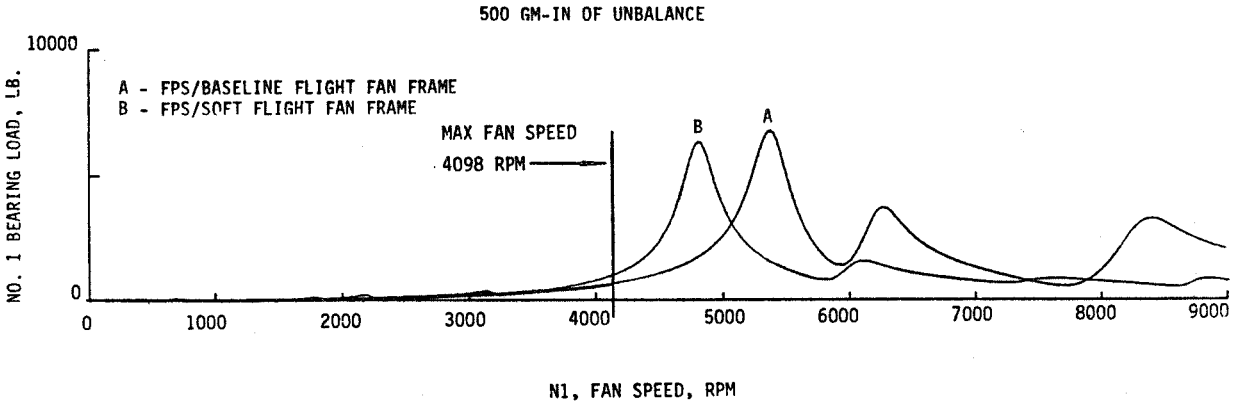

Figure 4.6-7. E^3 FPS Fan Synchronous Combined-Modes Frequency Response - No. 1 Bearing Load.

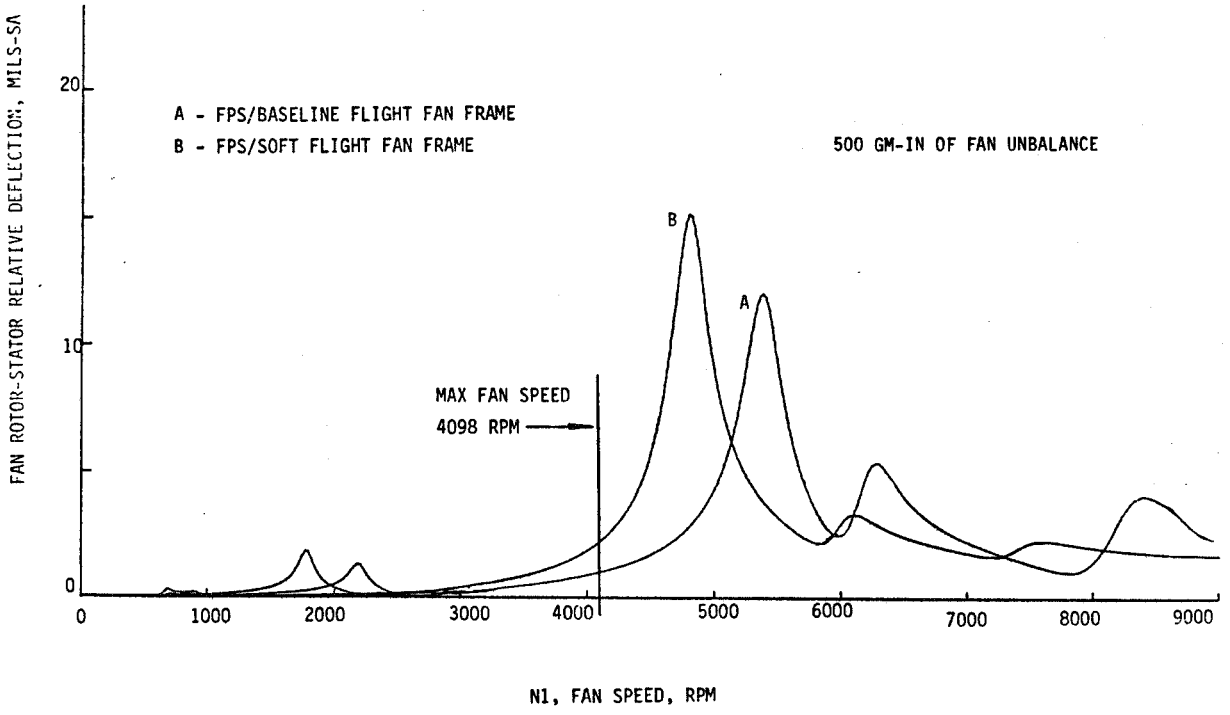

Figure 4.6-8. E^3 FPS Fan Synchronous Combined-Modes Frequency Response - Fan Relative Deflection.

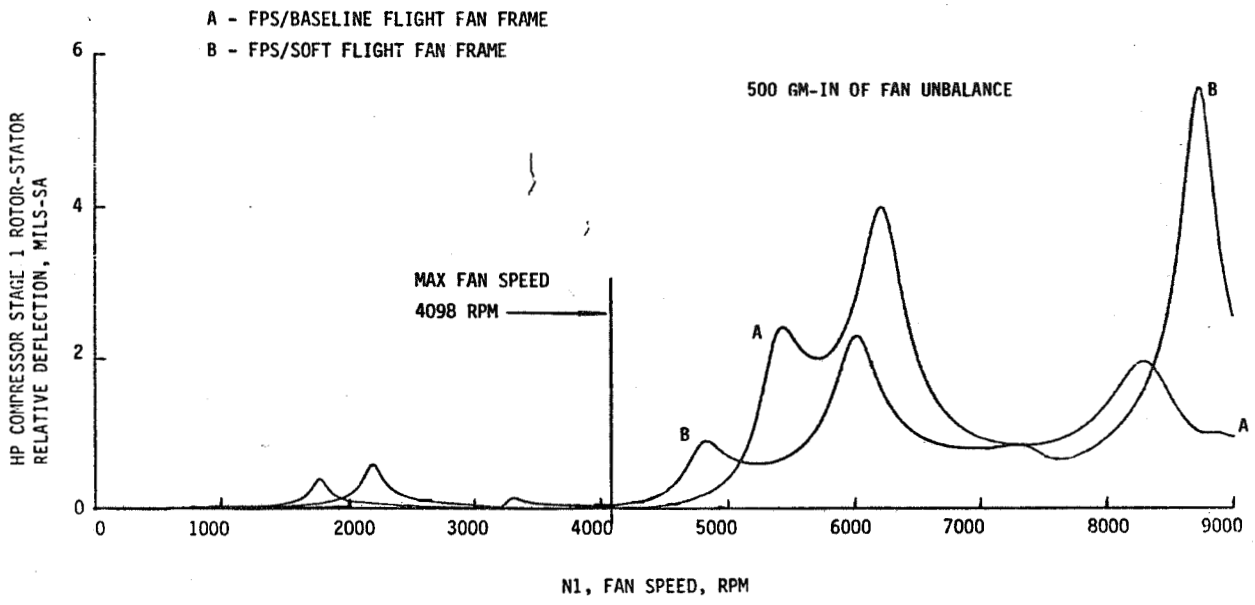

Figure 4.6-9. E^3 FPS Fan Synchronous Combined-Modes Frequency Response - HP Compressor Stage 1 Relative Deflection.

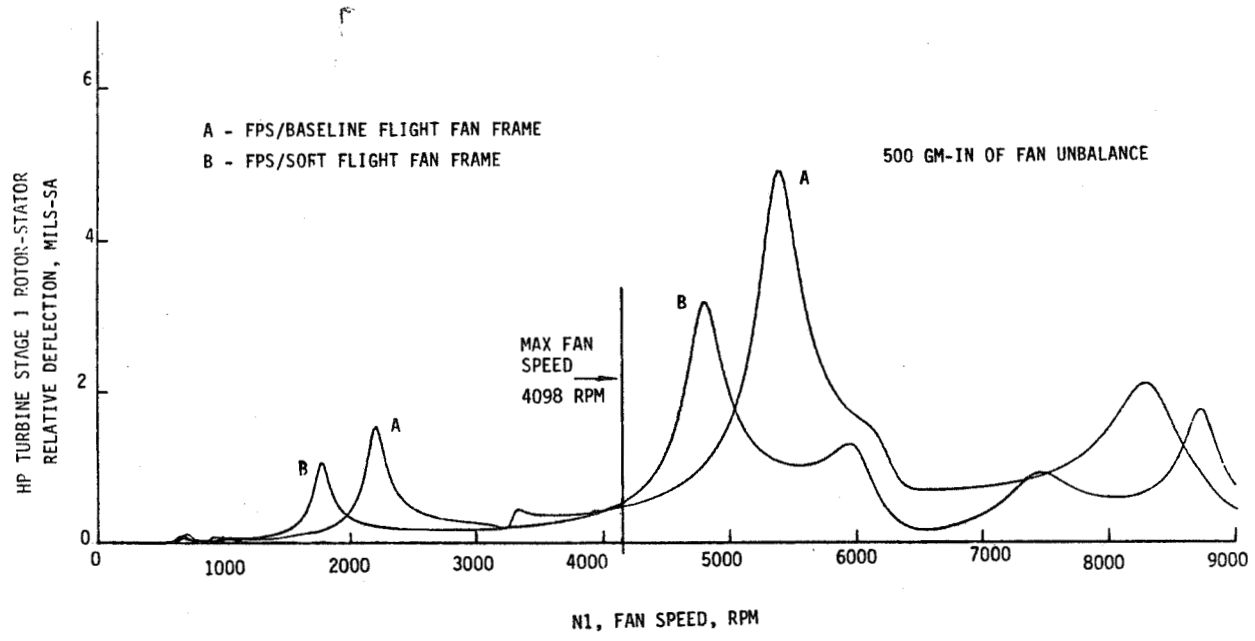

Figure 4.6-10. E^3 FPS Fan Synchronous Combined-Modes Frequency Response - HP Turbine Stage 1 Relative Deflection.

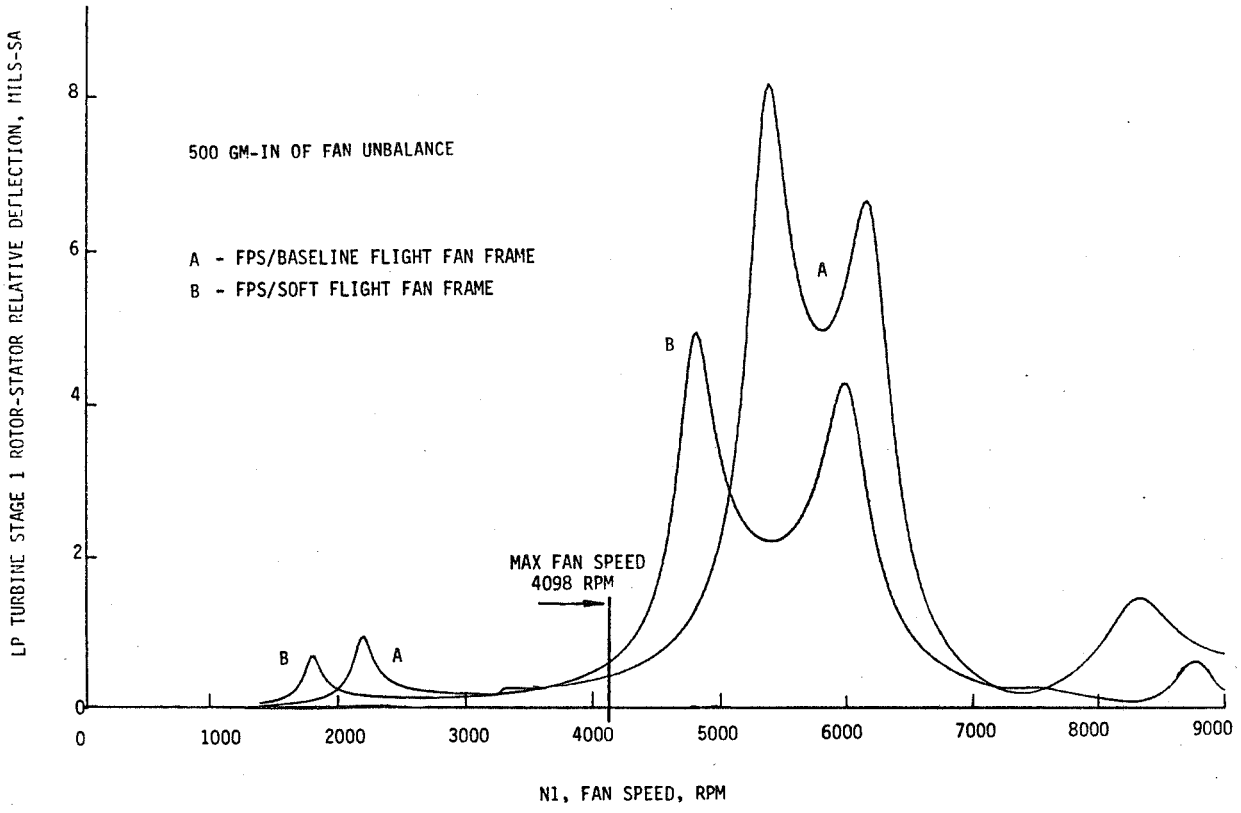
LP TURBINE STAGE 1 ROTOR-STATOR RELATIVE DEFLECTION, MILS-SA
500 GM-IN OF FAN UNBALANCE
A - FPS/BASELINE FLIGHT FAN FRAME
B - FPS/SOFT FLIGHT FAN FRAME
MAX FAN SPEED
4098 RPM
N1, FAN SPEED, RPM

Figure 4.6-11. E^3 FPS Fan Synchronous Combined-Modes Frequency Response - LP Turbine Stage 1 Relative Deflection.

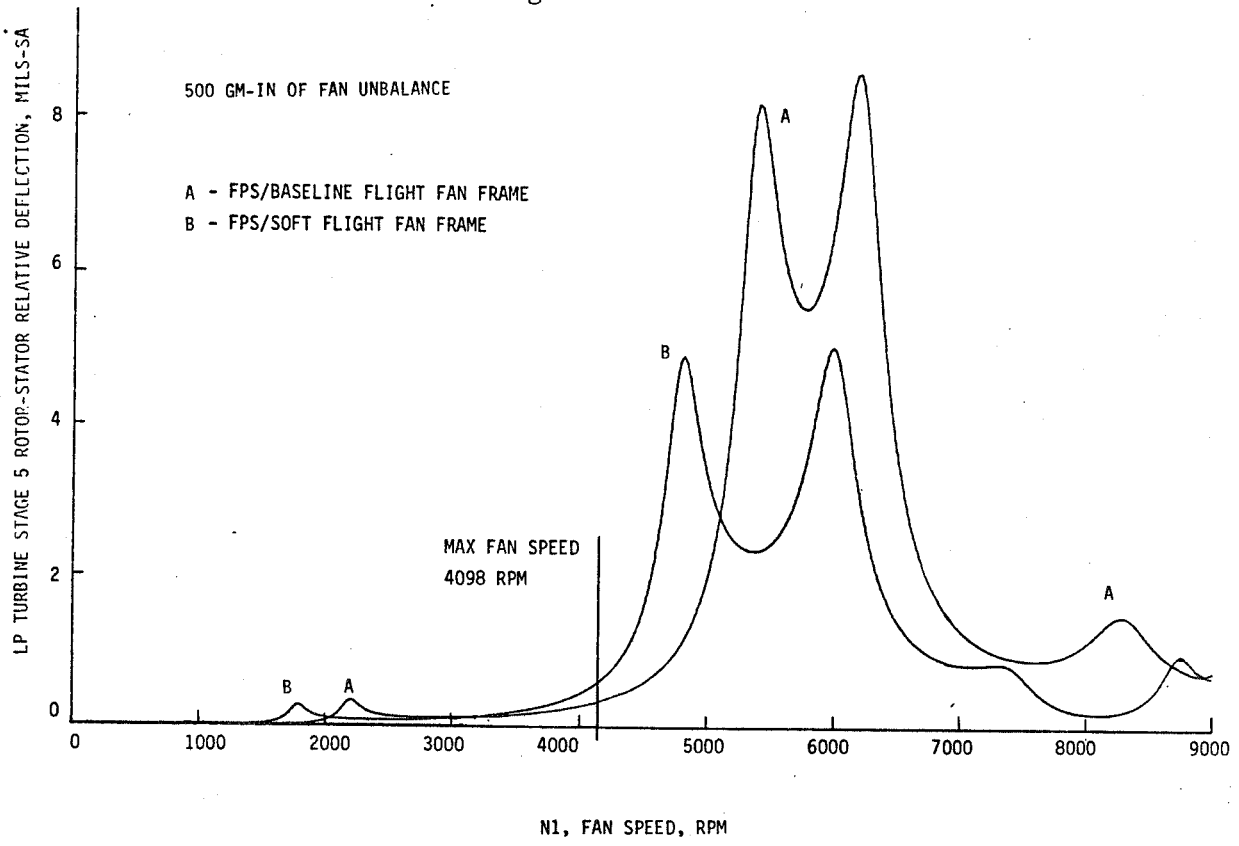
LP TURBINE STAGE 5 ROTOR-STATOR RELATIVE DEFLECTION, MILS-SA
500 GM-IN OF FAN UNBALANCE
A - FPS/BASELINE FLIGHT FAN FRAME
B - FPS/SOFT FLIGHT FAN FRAME
MAX FAN SPEED
4098 RPM
N1, FAN SPEED, RPM

Figure 4.6-12. E^3 FPS Fan Synchronous Combined-Modes Frequency Response - LP Turbine Stage 5 Relative Deflection.

Table 4.6-3. E^3 FPS Baseline and Short Fan Flowpath - Beam Bending Comparison for Static Loads.

	STATOR-ROTOR RELATIVE DEFLECTIONS, MILS										
	FAN	BOOSTER	HPC 1	HPC 5	HPC 9	CDP SEAL	HPT 1	HPT 2	LPT 1	LPT 3	LPT 5
1-G Down Gravity Load											
FPS/Baseline	+ 1.70	+ .72	+ 3.17	+ 4.60	+ 5.56	+ 5.86	+ 6.22	+ 6.31	+ 3.67	+ 2.67	+ 1.63
Short Fan Flowpath	+ 1.36	+ .97	+ 2.92	+ 3.97	+ 4.60	+ 4.86	+ 5.61	+ 5.79	+ 3.35	+ 2.63	+ 1.83
Thrust, 27000 Lbs.											
FPS/Baseline	+ .16	- .10	- .81	- 1.88	- 2.39	- 2.40	- 2.20	- 2.02	- 1.32	- .71	+ .21
Short Fan Flowpath	+ .80	- 1.00	- 1.00	- 2.44	- 2.68	- 2.76	- 2.73	- 2.49	- 1.58	- .66	+ .28
Gyro Load, 0.3 Rad/Sec											
FPS/Baseline	+13.71	- 8.05	+ 6.29	+ 6.13	+ 5.37	+ 5.20	+ 4.56	+ 4.07	+12.57	- 5.33	-24.41
Short Fan Flowpath	+13.86	- 3.61	+ 6.25	+ 6.12	+ 4.97	+ 4.84	+ 3.49	+ 2.60	+10.16	+ 5.48	-22.26
T/O Rotation Airloads, M = 500,000 in-lb, F = 10,000 lbs.											
*FPS/Baseline	+28.48	- .30	- 2.39	- 4.87	- 5.38	- 5.11	- 5.73	- 5.68	- 3.97	- 2.21	+ .75
**Short Fan Flowpath	+20.98	- .05	- 2.78	- 6.81	- 8.46	- 7.71	- 7.62	- 6.94	- 4.39	- 1.85	+ .79

* M&F act on the Nacelle 30 inches forward of Fan Frame Bypass Strut Centerline

** M&F act on the Nacelle 22 inches forward of Fan Frame Bypass Strut Centerline

Table 4.6-4. E^3 Baseline and Short Fan Flowpath - Bearing Load Comparison for Static Loads.

	Bearing Load, lb				
	No. 1	No. 2	No. 3	No. 4	No. 5
1-G Gravity Load					
FPS/Baseline	+1160	+ 175	+ 487	+ 764	+1550
Short Fan Flowpath	+1180	+ 127	+ 487	+ 764	+1550
Gyro Load, 0.3 rad/sec					
FPS/Baseline	+5670	-4950	+1380	-1380	-2110
Short Fan Flowpath	+7870	-7010	+1380	-1380	-2240

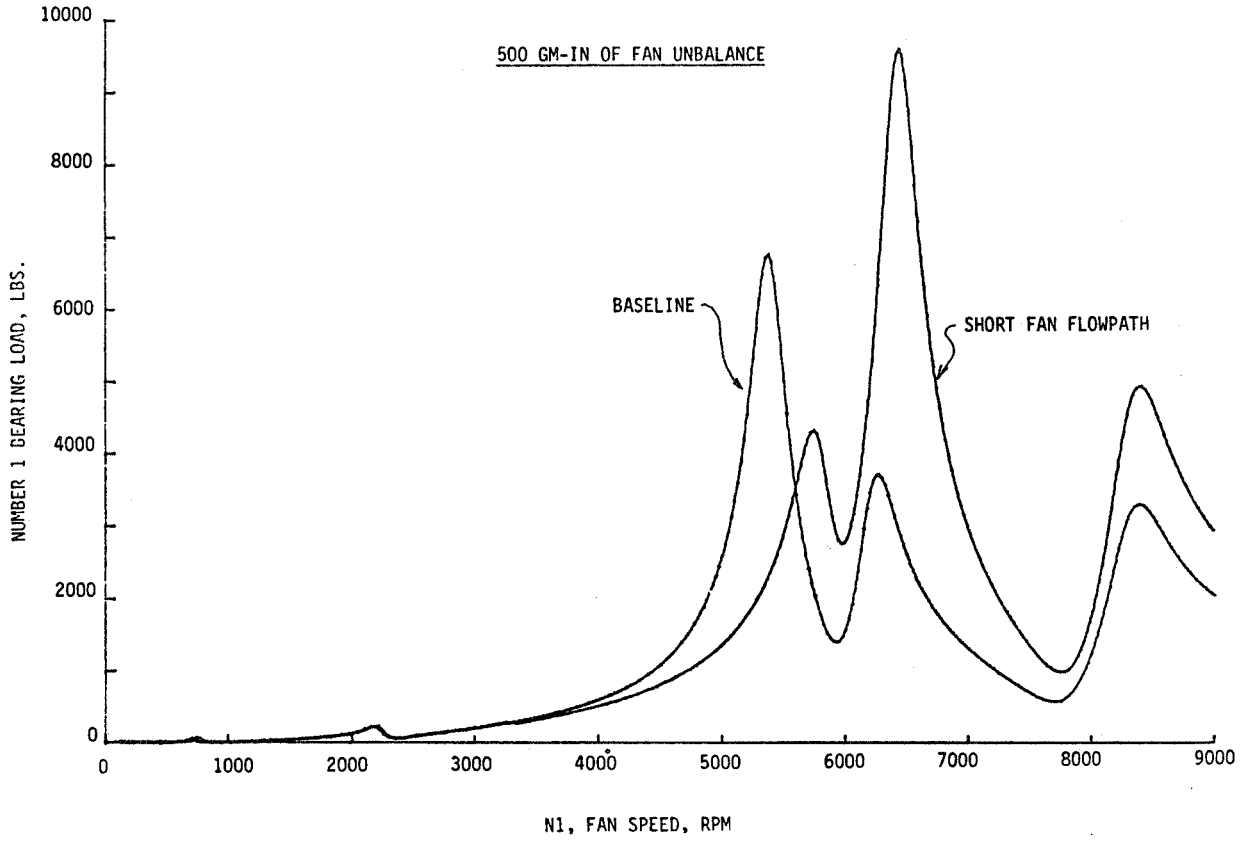

Figure 4.6-13. E^3 FPS Fan Synchronous Combined-Modes Frequency Response - No. 1 Bearing Load - Baseline vs. Short Fan Flowpath.

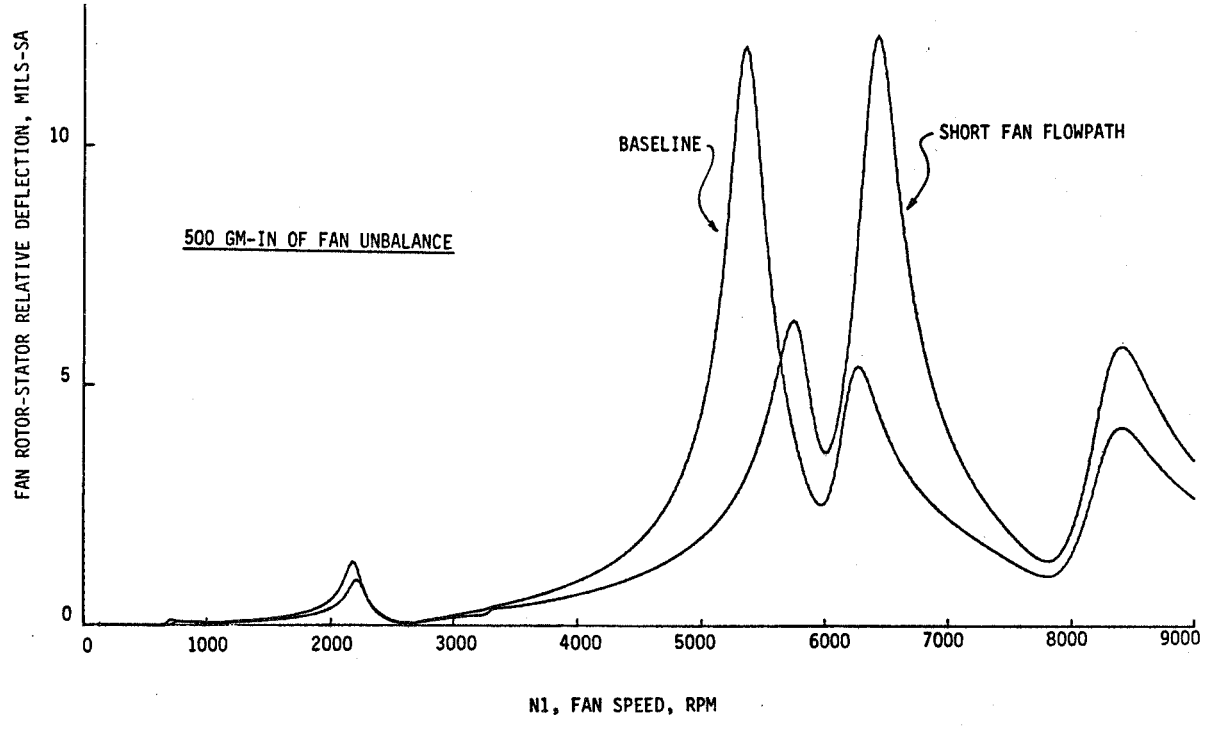

Figure 4.6-14. E^3 FPS Fan Synchronous Combined-Modes Frequency Response - Fan Relative Deflection - Baseline vs. Short Fan Flowpath.

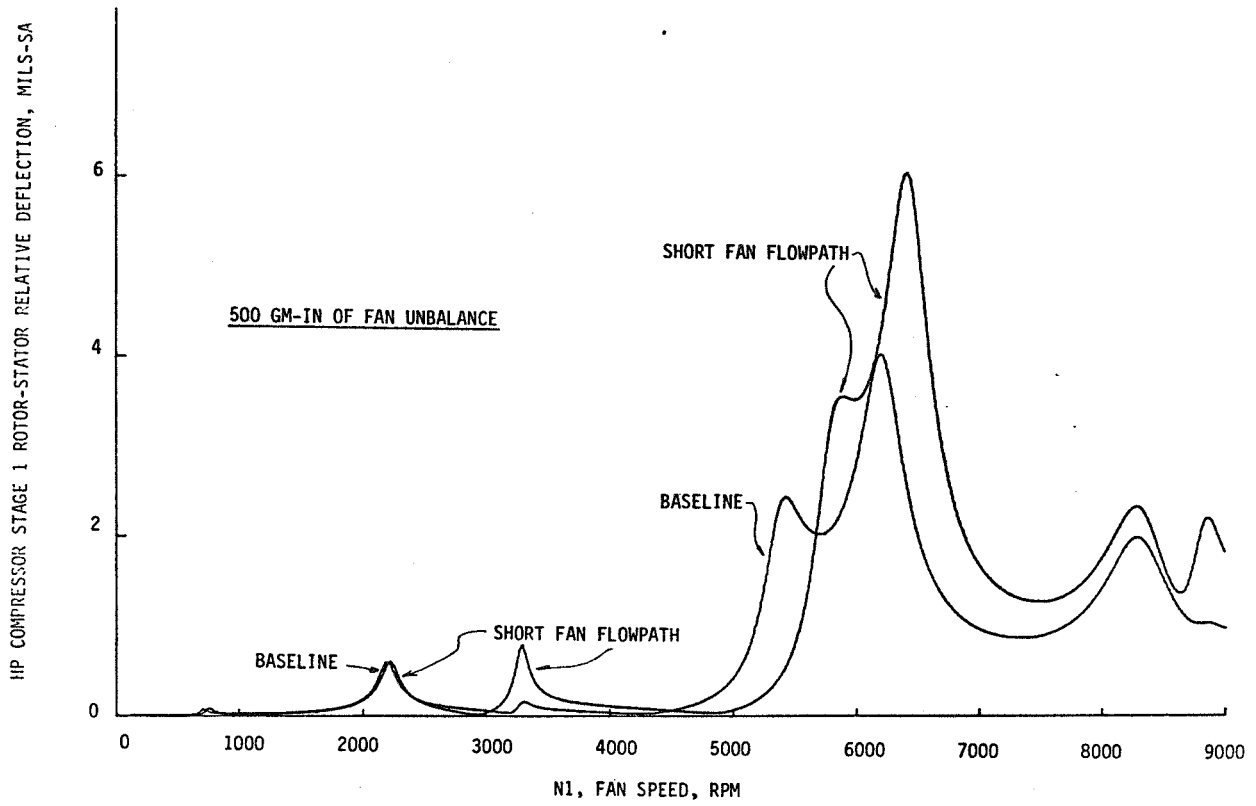

Figure 4.6-15. E^3 FPS Fan Synchronous Combined-Modes Frequency Response - HP Compressor Stage 1 Relative Deflection - Baseline vs. Short Fan Flowpath.

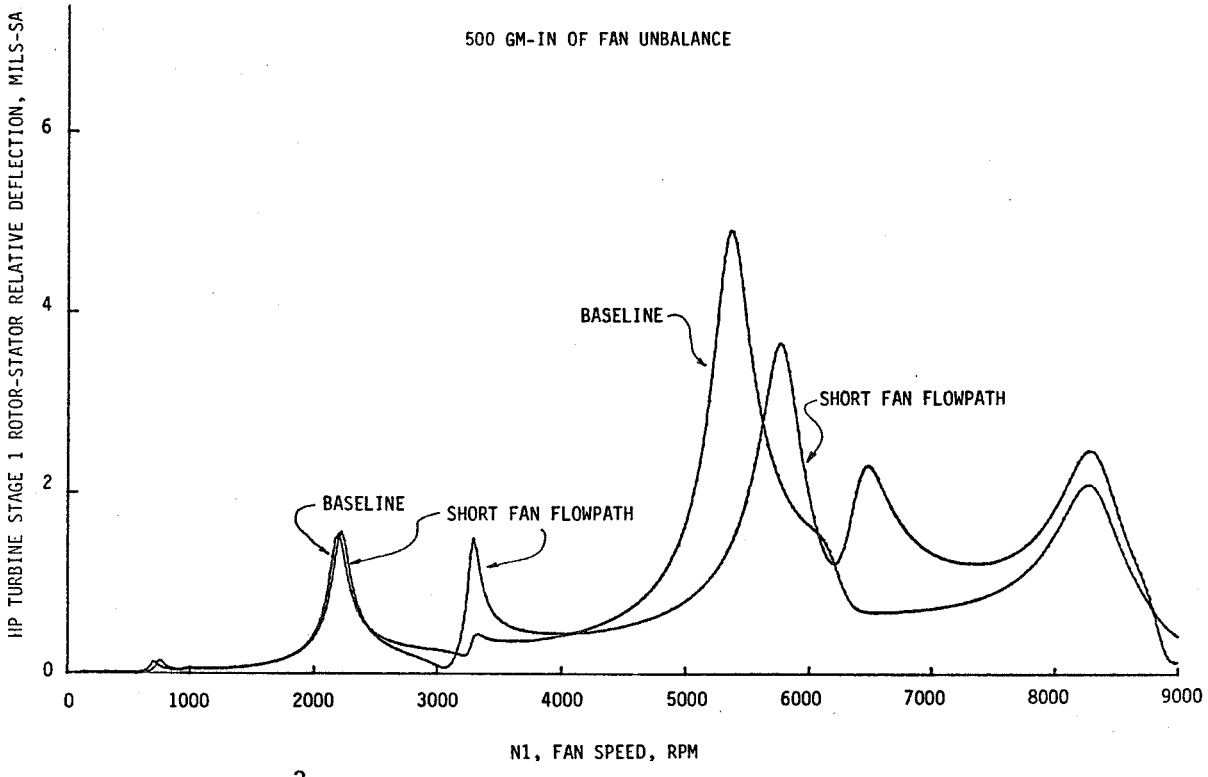

Figure 4.6-16. E^3 FPS Fan Synchronous Combined-Modes Frequency Response - HP Turbine Stage 1 Relative Deflection - Baseline vs. Short Fan Flowpath.

This study showed that an overall performance benefit of 0.25% in fan bypass efficiency and a weight savings of 12% for the fan and booster frame/stator module is feasible for the shortened fan configuration. Table 4.6-5 summarizes the projected weight savings. Overall design impacts and merit factors for the shortened fan configuration are presented in Table 4.6-6. The $45 million present-worth value indicates a sizable payoff in 1980 dollars compared to the estimated development cost of $2.5 million. The shortened fan configuration has some deficiencies which need to be more fully evaluated, including a slight increase in approach system noise of 0.45 EPNdB, a reduction in the growth capability of the engine, and the difficulty in designing a shortened fan frame with adequate radial and over-turning stiffness. Based on the assessment of the positive and negative tradeoffs associated with the shortened fan configuration, the conclusion has been reached that the benefits far outweigh the penalties in terms of overall engine system operation. Use of this technology improvement is recommended.

Table 4.6-5. Weight Savings Potential of Shortened Fan Configuration for the E^3 Engine.

	Weight Savings, lb
Outer Casing	70
Splitter	11
Support Cone	10
Fan Shaft	3
Fan Frame (Estimated at 10%)	86
Total Projected Savings	180

Table 4.6-6. Shortened Fan Flowpath.

Design Impacts	Direct	Secondary (Resizing)	Total
Δ Wt., lb	-185	0	-185
Δ Cost, $K	-19	0	-19
Δ Maint., $/flt.-hr	-.25	N.A.	-.25
Δ sfc, %	-.13	N.A.	-.13
Merit Factors	$-.52\ \Delta W_f$-%	-.85 Δ DOC-%	45 PW , $M
Ranking		$16\ \frac{PW \cdot P_s}{IDC}$	

4.7 HPC ACTIVE CLEARANCE CONTROL

Several alternative active clearance control (ACC) concepts were studied for the rear compressor casing cooling and compared to the current jet impingement cooling method on the E^3 FPS engine. The goal was to demonstrate the feasibility of concepts that improve ACC cooling and engine performance while reducing weight, manufacturing costs, and maintenance costs.

ACC Concepts Evaluated

Several casing cooling techniques were investigated, concentrating on fifth to tenth stage HPC casing cooling. Cooling effectiveness in cruise steady state was used as a selection criterion, in addition to weight, cost and ease of assembly. ACC operation in transients needs further study to determine the mode of operation that would minimize seal closure and rubbing during takeoff. The systems evaluated are described in the paragraphs that follow.

Fifth-Stage-Air Jet-Impingement Tube Rings

Casing cooling uses fifth-stage air, as in the current E^3 concept, but jet impingement comes from a set of holes in a series of parallel tube rings concentric with the casing, a scheme similar to that used in LP and HP turbine casing cooling in the E^3 FPS. The tubes are supplied through a common plenum.

This concept allows a decreased pressure drop in the cooling stream, and may present a simpler configuration than the slanted-hole jets in the E^3 FPS. The cooling flow, however, will be divided among the tubes, lowering cooling effectiveness. A manifold is still needed to collect the cooling air; this requirement may lead to a heavier configuration.

Mechanical Control Concepts

Several methods for active clearance control were contemplated, using mechanical control instead of casing cooling. The methods involve reducing casing growth or using in-growing rub seals that reduce rotor-casing clearances.

One method would use bimetallic springs to provide rub-seal inward growth, closing rotor-casing tip clearances during cruise. Figure 4.7-1(a) illustrates this concept schematically. The major drawback to this approach is that the seal intrusion into the smooth compressor flowpath causes an aerodynamic disturbance, and the benefits of tight clearance control are outweighed by the aero penalties of disturbance.

A similar concept uses the stage pressure differential to modulate seal growth inward and hence control rotor tip clearance. Again the large penalty due to the aerodynamic disturbance is prohibitive. Figure 4.7-1(b) illustrates this concept.

Graphite casings and other low-expansion materials can also be used as a mechanical means of reducing thermal growth, but their net effect is to increase running clearances because their transient response is also slow and they result in more rubbing during takeoff.

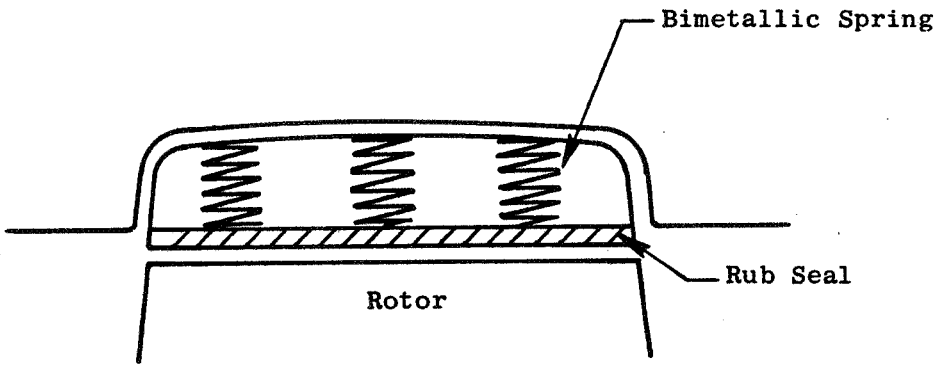

(a) Bimetallic Spring

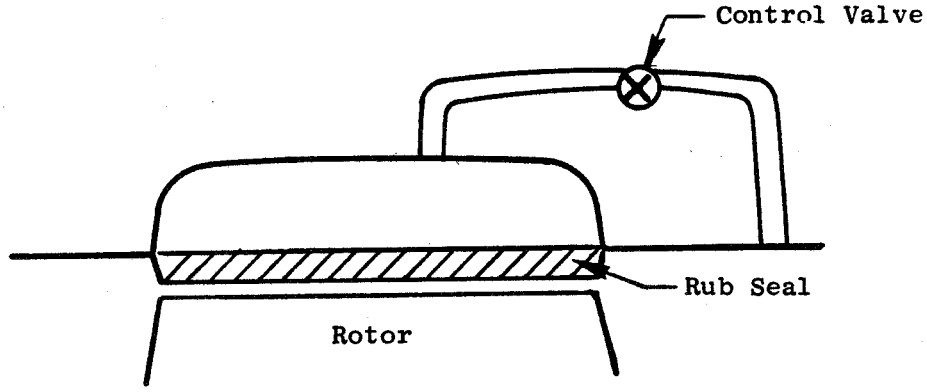

(b) Pressure Differential Control

Figure 4.7-1. Mechanical Active Clearance Control Concepts.

Organic-Fluid Heat Pipe Cooling

Heat pipes using liquid metals and organic fluids are an advanced technology finding many applications today in solar energy systems and other heat transport applications. Figure 4.7-2 shows a possible configuration using organic-fluid heat pipes (applicable in the 600 to 1000° F temperature range) for casing cooling. Dowtherm A is a suggested working fluid.

The heat pipe acts like a thermal transformer, allowing localized, effective cooling through a finned heat exchanger while the evaporation-condensation action of the fluid in the heat pipe (transported through gravitation or wicking action) maintains a uniform temperature in the heat pipe all around the casing. Typical temperature gradients across the heat pipe are on the order of a few degrees. This results in more-effective cooling, with a smaller pressure drop and less cooling flow needed at the light aluminum-finned heat exchanger. The resulting configuration is simple and easy to install, and would probably be quite light. Heat pipe technology has been proven in many applications and is quite reliable.

The only major drawback to this concept is the lack of experience in the aircraft industry in this unconventional area. For the small amounts of organic fluid needed, the safety considerations are minimal. But this concept will need further study and development to gain acceptability.

Insulation and Thermal Barrier Coatings

Several passive control techniques were studied that were aimed at reducing casing heating and the amount of cooling required. The use of high-temperature insulation such as Min-K in the shroud-casing clearances will cut down convection and radiation heating of the outer casing, thereby reducing the amount of cooling required. The use of thermal barrier coatings (TBC) such as zirconia on the casing outer flowpath will decrease the heating action from the compressor air. A 10-mil coating of zirconia, stabilized with yttria and applied over a 5-mil NiCrAlY bond coating, will cut the compressor air effective heat transfer coefficient by half.

The advantage of these passive methods is that they can be used to supplement other cooling concepts, reducing casing temperatures or reducing cooling requirements, as needed. They are simple, light, and reliable. Min-K barrier coatings are in an advanced stage of development at General Electric and other facilities and have been extensively tested for turbine-blade and other high-temperature applications.*

Alternatively, the reduced heating of the casing will reduce casing growth in transients and during takeoff, increasing rubbing problems and requiring wider cold clearances to compensate for increased transient closure.

---

*1. Girsaffe, Levine, and Clark, Thermal Barrier Coatings, NASA Technical Memorandum TM-78848, April 1978.

2. Francis S. Stepka, NASA Thermal Barrier Coatings - Summary and Update, NASA Technical Memorandum 79053, September 1978.

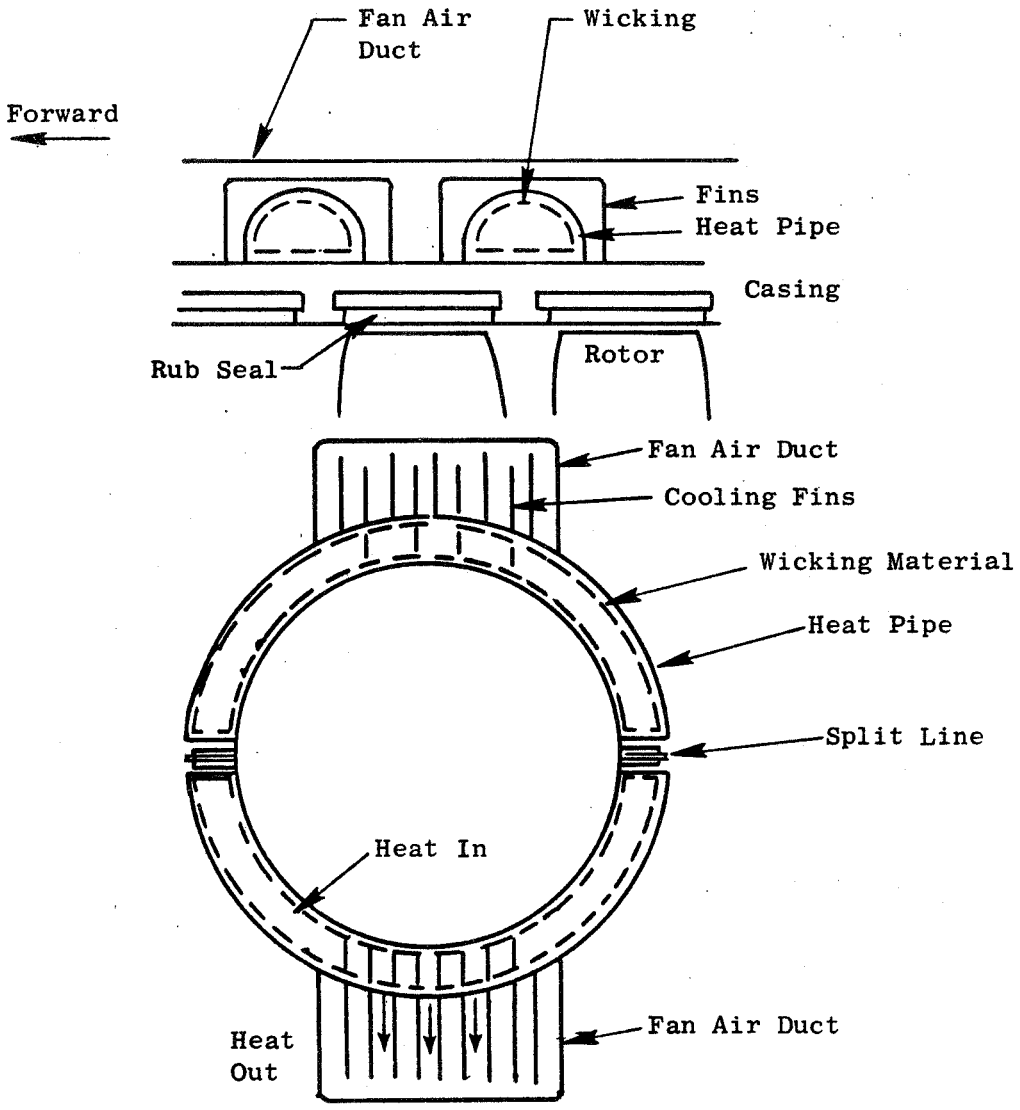

Figure 4.7-2. Organic Heat Pump Cooling Concept.

The net tradeoff is not immediately obvious and will require further detailed study of transient and steady-state response to find out whether the increased cooling compensates for the lower transient growth.

Fan Air Cooling

The use of low-cost, colder fan air in active clearance control has been demonstrated in the CF6 LP turbine ACC concept, and is contemplated for the current E^3 FPS LP and HP turbine active clearance control. Two methods were investigated; they are described in the paragraphs that follow.

Fan Air Jet-Impingement Tube Rings - Fan air impinging from holes in a series of parallel tube rings concentric with the casing provides cooling with a small pressure drop (a must when using fan air). The used air can flow out through the LP turbine exit struts and be discharged via the exit vent stinger. This removes the need for the pressure seal separating the aft and forward casing cavities. The tube rings are supplied through a common plenum. Fan air is intercepted by a modulated ram pressure recovery scoop, diffused and directed to the plenum; this scheme is similar to the current E^3 FPS LP turbine ACC fan air ducting. The design is simpler and lighter than the current fifth-stage impingement-cooling scheme, and could provide equivalent cooling.

The fan air, however, will divide among the tube rings, and its cooling effectiveness will be decreased. The penalty for the use of fan air would limit the amount of flow available. The scheme still looks viable; however, a further detailed study is required.

Fan Air Cooling with Baffle Configuration - Fan air flow can be directed axially over the casing for cooling using a thin metal baffle. Fan air can be directed either aft or forward, and ducted-in from a modulated ram pressure recovery scoop. The used fan air is then discharged into the compressor cavity for purging purposes and discharged through the LP turbine exit struts and the exit vent stinger.

This configuration was seen as the most promising, providing effective cooling coupled with a light, simple design. A fan air baffle configuration which has the potential of meeting the requirements of a high-bypass turbofan engine is shown in Figure 4.7-3. A ram-pressure recovery scoop off the pylon supplies fan air at 8.4 psi in cruise for LP turbine, HP turbine, and HP compressor cooling. The baffle is at low temperatures and can possibly be made of light aluminum. Fifth-stage bleed (for customer, and LPT cooling) and seventh stage bleed (for start, and HPT cooling) air uses threaded connections to large circular pipe manifolds for assembly. Alternative piping arrangements are possible.

The results assume a 1 pps fan air flow with the shown baffle arrangement. The main limit in this cooling concept is the small pressure drop allowed (from 8 psi down to 5.7 psi, assuming little ΔP through the LP turbine exit struts, and assuming the vent stinger is appropriately sized to discharge the cooling flows).

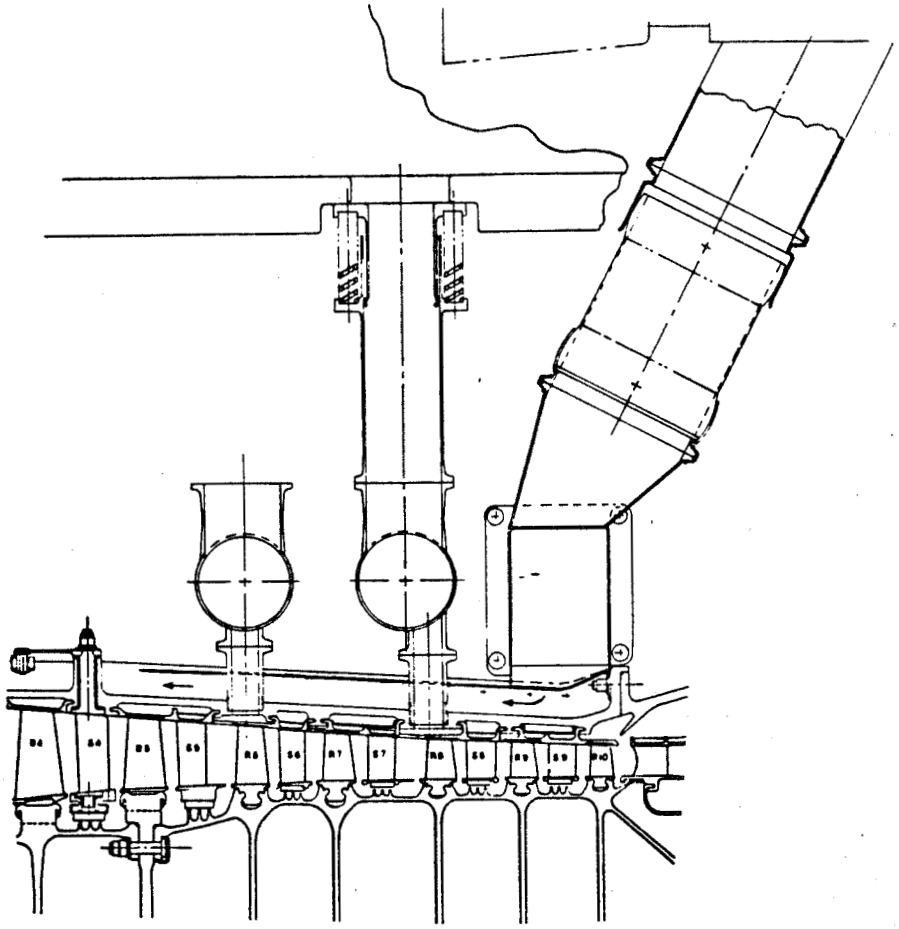

Figure 4.7-3. Fan Air Cooling Baffle Configuration.

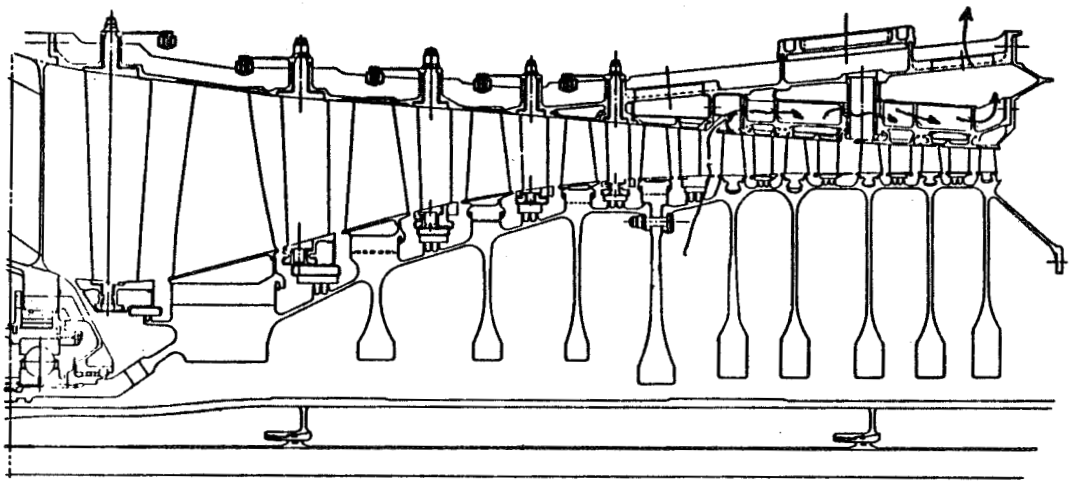

Figure 4.7-4. Current E^3 HPC Active Clearance Control Concept.

Although the heat transfer is limited by low fan-air velocities, the lower fan-air temperatures result in better cooling, especially in the sixth- and seventh-stage casing areas, where the fifth-stage air cooling effectiveness is low. The lower temperatures result in a 7-to-10-mil clearance closure.

Fan Air Cooling Performance Assessment

The current E^3 concept uses fan air for purging the compressor cavity, with 0.37 percent W25 flow to replace the air six times a minute. Of this 0.37 percent flow, 0.22 percent rejoins the fan stream, while 0.15 percent leaks through the pressure seal between the aft and forward cavities and exits through the LP turbine exit struts and the vent stinger, and some penalty is incurred. The proposed fan air cooling scheme will use 1 pps, or 1.47 percent W25, for cooling. A penalty is therefore assumed for 1.32 percent of the flow, which is equivalent to 0.435 percent in sfc penalty compared to the current E^3 FPS if the flow were dumped overboard. Since the flow exits through the vent stinger, some work is still done and the actual sfc penalty is 0.237 percent. As will be pointed out later, the 1 pps may result in overcooling and, along with baffle rearrangement, the fan cooling-air needed may be less, thereby reducing the sfc penalty.

In the E^3 FPS, no penalty was assumed for use of the fifth-stage air since the same flow is used for LP turbine cooling. However, a significant ΔP (from 53 psi to 44 psi) across the cooling holes reduces the cooling effectiveness of the air (along with a 30° F temperature rise), and therefore more air is needed for the same cooling in the LP turbine area. The penalty needs further evaluation, but this indicates that our analysis is conservative with potentially better performance than indicated.

Resulting Clearance Control

The cooling effect of the fan air results in a 7-to-10-mil clearance tightening, as indicated earlier. The current E^3 concept gives good clearance control in the eighth through tenth stages, with no control in the fifth stage and only slight control in the sixth and seventh stages. Our proposed configuration may therefore result in overcooling in the eighth through tenth stages. The design is very flexible, however, and fan air-flow baffle clearances can be adjusted to provide the needed amount of cooling. This needs further study.

Further study may consider the possibility of extending the baffle cooling to the lower stages (first through fourth). The tighter clearances in the fifth to tenth stages results in a 0.5 to 0.7 percent improvement in compressor efficiency, which translates to a 0.195 to 0.273 percent improvement in sfc. The figure varies, the actual value depending on stator seal clearance variations.

Weight Savings

The fan air baffle configuration is a simpler, lighter configuration than the E^3 FPS ACC scheme. Table 4.7-1 shows a preliminary tabulation of major component weights, showing a 78.7-lb weight savings.

Table 4.7-1. Baffle Configuration Weight Savings.

Current FPS Design			Fan Air Baffle Design		
Component	Material	Wt/lb	Component	Material	Wt/lb
1. Wishbone	M152	24	Aft Case	M152	72
2. Aft Baffle	M152	4	Baffle	Al	6
3. Aft Case	M152	65	Stage 5 Manifold	Ti	19
4. Forward Baffle	M152	3	Stage 7 Manifold	Ti	23
5. Outer Casing	M152	77	Rear Manifold	Ti	2
6. Stage 7 Manifold	M152	23	Fan Air Inlet Tube	Ti	10
7. Spool (44)	M152	5	Total Weight		132
8. Conduction Rings	M152	10			
Total Weight		211			

Wt. Savings = 79 lb

37 Percent

ACC Studies Summary and Conclusions

Fan Air Cooling Baffle Configuration

The scheme using cold fan air provides better cooling effectiveness than the current E^3 fifth-stage air jet-impingement scheme. The design shown in Figure 4.7-3 reflects several design iterations resulting in a simple configuration which is potentially cheaper to manufacture, assemble, and maintain. The 7-to-10-mil clearance control improvement gives a 0.5 to 0.7% improvement in compressor efficiency, or 0.2 to 0.27 % improvement in engine sfc. This improvement is offset by the sfc penalty of the fan air, which is .24%; therefore, the net sfc benefit is negligible. The payoff is in weight and costs.

Table 4.7-2 summarizes the overall performance benefits and penalties; Table 4.7-3 presents the overall design impacts and merit factors. The concept is an attractive alternative to the current E^3 scheme. Further studies are needed to better define system sizing, system components, and the resulting performance benefits. The above performance figures are considered to be conservative.

Alternative Concepts

Organic-fluid heat pipes are a state-of-the-art technology that looks promising for this cooling application, and need further study to establish a theoretical design and experimental feasibility.

The tradeoffs and performance benefits resulting from the application of high-temperature insulation and thermal barrier coatings in conjunction with the proposed cooling scheme need further study to establish transient and steady-state response characteristics.

As for "active" control logic, detailed transient analysis needs to be done to establish clearance control operational modes and modulating valve control schemes. In the proposed fan air cooling concept, the cooling air is not needed in transient (takeoff) operation since it will decrease casing expansion and increase transient rubbing.

Table 4.7-2. Fan Air Baffle Configuration Summary (Compared to Current E^3 FPS).

Summary of Overall Benefits

- Better Cooling Effectiveness
- 7-10 Mil Better Clearance Control Capability
- .5 to .7% Compressor Efficiency Improvement Possible
- Weight Saving Potential of 79 lb
- Reduced Manufacturing Cost

Summary of Penalties

- Increase in Fan sfc of 0.24%
- Threaded Bleed Connections

Table 4.7-3. HPC Active Clearance Control - Fan Air Cooling.

Design Impacts	Direct	Secondary (Resizing)	Total
Δ Wt., lb	-80	0	-80
Δ Cost, $K	-40	0	-40
Δ Maint., $/flt.-hr	-.20	N.A.	-.20
Δ sfc, %	0	N.A.	0
Merit Factors	$-.15\,\Delta W_f$-%	$-.34\,\Delta$ DOC-%	18 PW , $M
Ranking		$15\,\frac{PW \cdot P_S}{IDC}$	

4.8 ADVANCED FAN BLADE STUDIES

The objective of the advanced fan blade studies was to assess the weight, cost and performance benefits associated with alternate fan blade designs.

Throughout the studies the present E^3 FPS fan blade design was used as a basis for comparison. This is a 32-blade Ti 6-4 design with a shroud at 50% span. The removal of the mid span shroud in this design provides a performance benefit of .5% in bypass efficiency.

Four fan blade concepts were evaluated including the following:

- Shrouded Hollow Titanium - 32 Blades
- Unshrouded Polymeric Composite - 24 Blades
- Fiber-Reinforced Hollow Titanium - 28 Blades
- Wennerstrom Unshrouded Hollow Titanium - 20 Blades

The design of a large high-bypass fan blade is controlled to a great degree by frequency considerations, both flexural and torsional. Because of the inherent driving forces present in the engine and the amplitudes associated with low-order excitations, blade fundamental flexural frequencies must be high enough to avoid both 1/rev and 2/rev crossings. In addition the fundamental torsional frequency must be kept high enough to avoid instability ($R_V < 1.4$). These two constraints along with the mechanical design requirements of the blade/disk system constitute the basis for evaluating the various advanced blade designs.

Shrouded Hollow Titanium Blade

Hollow titanium blades can offer significant payoffs in weight over solid blades. The key, however, to a successful hollow titanium blade design is the ability to satisfy bird impact and the development of a viable manufacturing process which yields a cost-competitive blade. The hollow blade studies conducted utilized the E^3 fan blade external configuration and concentrated on the evaluation of various hollowing techniques to maximize the weight benefit and still meet the overall design requirements. A solid leading edge in the tip region and within the first 30% of the chord along the remainder of the leading edge was determined to be an essential approach for satisfying bird impact. This design yielded a weight payoff of 103 lb over the present FPS solid shrouded blade. This weight savings translates into a fuel-burned savings of .19%.

The manufacturing approaches that can be considered for such a blade design range from machined half shells which are diffusion bonded together, to a full superplastic formed/diffusion bonded SPF/DB process. The SPF/DB process is believed to represent the most viable approach to meeting the overall requirements of hollow titanium blades. Figure 4.8-1 shows a simplified SPF/DB process for a wedge-shaped simulated airfoil cross section. This process provides the potential for low-cost hollow blade manufacture and a consistent repeatable process.

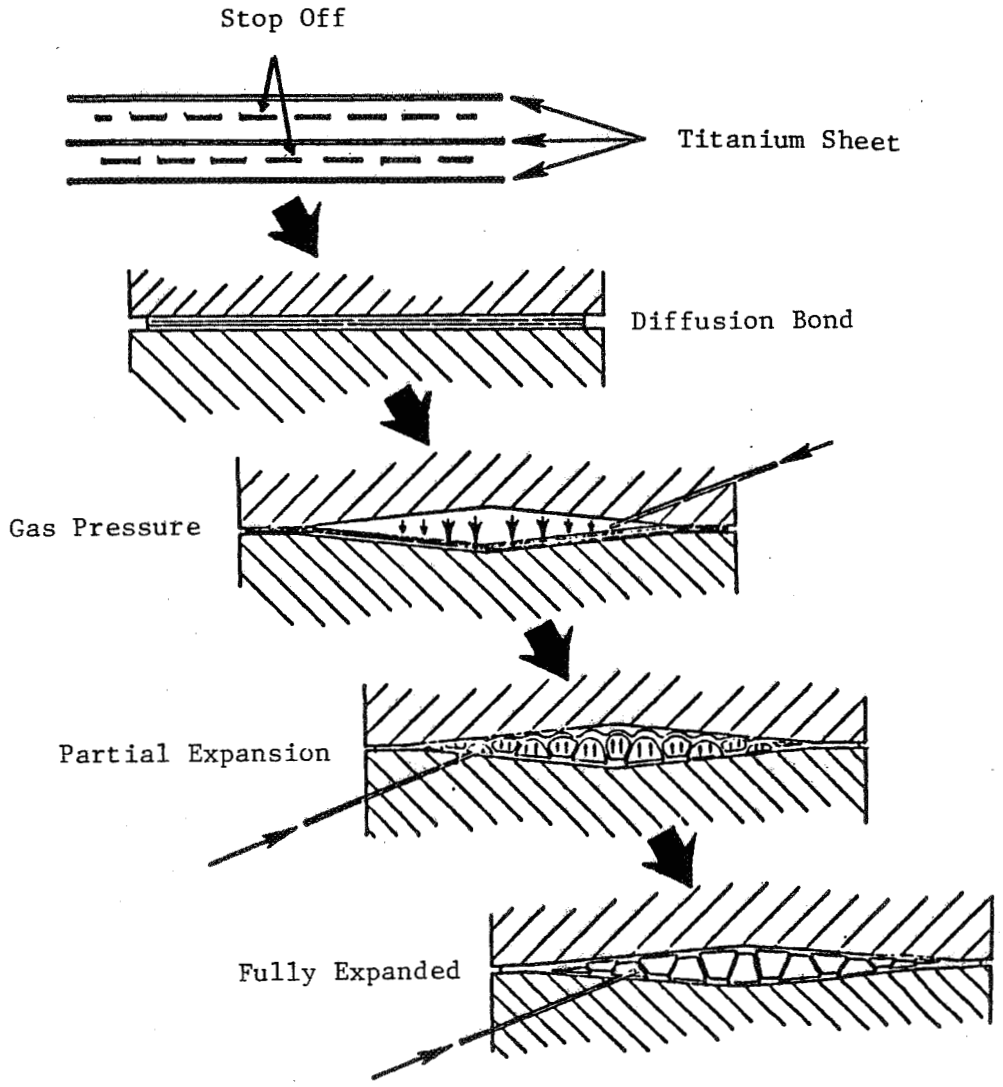

Figure 4.8-1. FOD Panel SPF/DB Process.

Unshrouded Polymeric Composite Blade

Polymeric composite blades offer the greatest potential for weight savings and cost savings over any other blade design. The limitations and risks, however, generally overshadow the potential payoffs. The greatest limitation is the inadequacy of the bird impact resistance of composite blades. Impact improvement programs to date have not shown a clear-cut solution to the impact problem. Some progress has been made with hybrid designs containing glass fibers and polyurethane interleaved design but much more work is required to perfect these concepts.

Other barriers that prevent the use of polymeric composites in large fan blades are their low flexural frequency characteristics compared to a shrouded metallic blade design. Current design practice requires that the blade's first flexural frequency be at least 15% above the 2/rev engine order line, to prevent excessive blade vibration. Polymeric composite blades in the unshrouded configuration cannot meet this requirement without going to very large chords and a low blade number per stage, which reduces the weight savings and lowers the overall benefit to the engine system.

Assuming that composite blades can eventually overcome the bird impact problem and become a viable candidate for fan blades, the low flexural frequency problem must be solved to allow its ultimate use in a production application. This can be accomplished in one of two ways:

- Developing the technology for making shrouded polymeric composite blades.
- Develop a highly damped blade design that allows low frequency operation through 2/rev in the design operating speed of the engine.

For the purposes of this study it was assumed that the blade could operate satisfactorily through 2/rev as a low-flex unshrouded blade. The resulting design uses 24 blades per stage. Weight savings was estimated to be 234 lb compared to the FPS design. Corresponding reduction in fuel burned was .4%, and a cost savings of $34K per engine set was projected in production quantities.

Fiber-Reinforced Hollow Titanium Blade

Fiber-reinforced hollow titanium is an emerging material that has the potential of offering renewed hope for the application of composites in large fan blades. This new material combined with superplastic forming and diffusion bonding techniques provides an added dimension in design flexibility, that of lightweight-core (hollow) configurations. For the purposes of this study SiC/Ti (silicon-carbide/titanium) composite material was used. Several other fibers are possible including B_4C and Borsic.

The results of a brief study to assess the potential benefits of SiC/Ti composite material in the E^3 fan blade are summarized in Table 4.8-1. Three conceptual blade designs of SiC/Ti Fiber-Reinforced Advanced Hollow Titanium (FRAHT) blades were studied and compared with the baseline design. The baseline design

Table 4.8-1. E^3 SiC/Ti Fan Blade Design Study.

Parameter	Baseline	Study No. 1	2	3
Rotor Speed, rpm	3,585	3,527	3,527	3,527
Blade Tip Speed, ft/sec	1,350	1,350	1,350	1,350
Blade Radius Ratio	0.35	0.35	0.35	0.35
Bypass Efficiency, %	87.9	88.4	88.4	88.4
Core Efficiency, %	88.5	88.5	88.5	88.5
Blade Max Temp., °F	275	275	275	275
Number of Blades	32	28	28	38
Blade Shroud	50% span	None	None	None
Blade Material	Titanium	Ti-SiC/Ti	Ti-SiC/Ti	Ti-SiC/Ti
Airfoil Features	Solid	Hollow	Hollow	Hollow
Solid t. leading edge, in.	-	1.5	3.0	3.0
Flexural Freq. Characteristics	Hi-Flex	Hi-Flex	Hi-Flex	Lo-Flex
Torsional Reduced Vel. par	1.24	<1.0	<1.0	1.0
Blade Wt., lb	14.8	13.5	15.9	7.9
Blade Stage Wt., lb	474.0	378.0	445.0	300.0
Disk Wt.,	309.4	255.0	310.0	250.0
Total Rotor Assy. Wt., (lb)	783.4	633.0	755.0	550.0
Containment Wt., lb	281.0	255.0	276.0	239.4
Total Wt., lb	1,064.4	888.0	1,031.0	789.4
Δ Wt. from Base, lb	-	176.4	33.4	275.0

uses 32 shrouded solid titanium fan blades with a conventional dovetail sized to satisfy bird-impact requirements. Figure 4.8-2 shows the basic SiC/Ti blade design study concept, which uses 28 unshrouded hollow blades with conventional axial single-tanged dovetails. The design has a solid titanium leading and trailing edge and dovetail, and SiC/Ti is used only in the midspan region of the blade. This approach was taken due to FOD considerations which indicate that a ductile material is desirable in the local impact region, namely the leading edge. The objectives of FRAHT blade designs 1 and 2 were to identify and evaluate designs which eliminated the midspan shroud and maintained the same aeromechanical stability characteristics as the baseline blade design. This was accomplished by reducing the number of blades, adding SiC/Ti, and making the blade hollow. The first flexural frequency of the blade is above the 2/rev excitation line at all speed conditions. (See Figure 4.8-3) It was found that a solid SiC/Ti airfoil could not satisfy this requirement and show a weight benefit. The difference between designs 1 and 2 is the length of the titanium leading edge. In design 1, this length is 1-1/2 inches while in design 2, it is 3 inches. Visual inspections of titanium blades impacted by medium-size birds have shown the leading edge gets bent and the bent portion extends back from the leading edge 1.5 to 3 inches, providing the rationale for looking at designs 1 and 2. The results of the preliminary study show that elimination of the midspan shroud could improve aerodynamic efficiency up to 0.4 percent relative to the present E^3 FPS design. For designs 1 and 2, the total rotor accessory and containment weight savings are estimated to be 176.4 pounds (16.6 percent) and 33.4 pounds (3.1 percent), respectively. Design 3 represents a minimum-weight design. This was accomplished by allowing the blade's first flexural natural frequency to drop so it crosses the 2/revolution excitation line at the engine 60 percent speed point as shown in Figure 4.8-4. The length of the titanium leading edge was set at 3.0 inches. Relieving the frequency requirement allowed increasing the number of blades in the stage to 38 shorter-chord blades (solidity parameter was held constant). Experience has shown that low-flex designs like design 3 are high risk and generally result in unacceptable blade response during engine operation.

Based on this brief study, several observations can be made. First, the increased stiffness of SiC/Ti is not great enough to allow the elimination of shrouds from solid fan blades - even with wider-chord blade designs - and still show a payoff in weight. However, since SiC/Ti is compatible with titanium, it is possible to identify hollow blade designs that take advantage of the desirable properties of each material. An added benefit is that the blade root centrifugal forces are reduced significantly by using the lower-density SiC/Ti and by incorporating hollow sections. This feature could be very significant for advanced high-tip-speed fan blades.

Considerable development effort is required before SiC/Ti composites can be proven for application in gas turbine engines.

Wennerstrom Unshrouded Hollow Titanium Blade

Recent advances in the aerodynamic design of low-radius-ratio fan and compressor blading have presented a need for the evaluation and conceptual design of hollow unshrouded blades. The aerodynamic design (Wennerstrom) is one that is characterized by high pressure ratio per stage, high stall margin, and hub efficiencies averaging 88 to 92%. Geometrically the blade requires thin leading

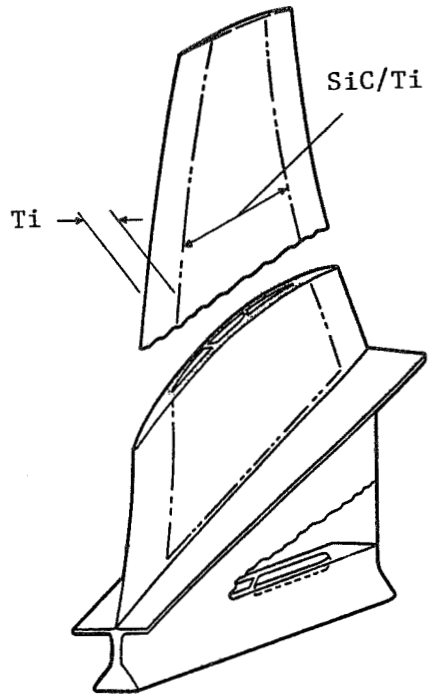

Figure 4.8-2. SiC/Ti Fiber-Reinforced Advanced Hollow Titanium (FRAHT) Fan Blade Conceptual Design.

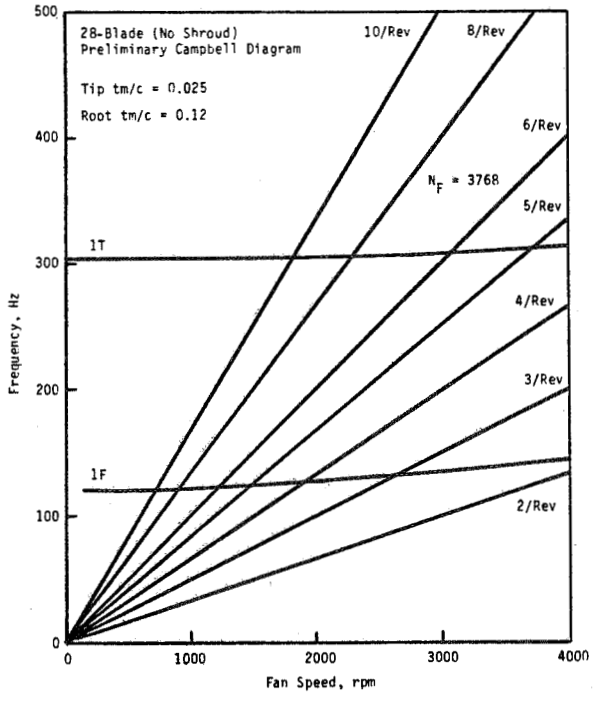

Figure 4.8-3. E^3 FRAHT Design No. 1.

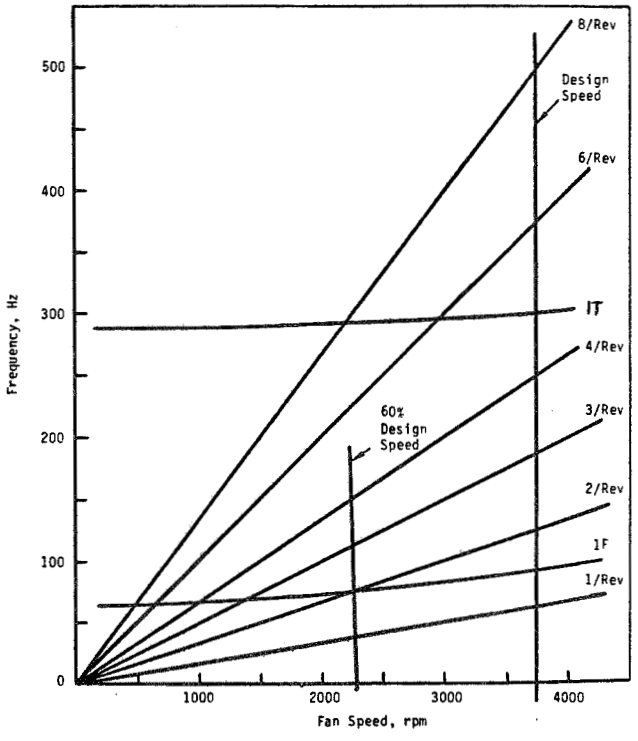

Figure 4.8-4. E^3 FRAHT Design No. 3.

edges, an unshrouded configuration to improve bypass efficiency levels, and low aspect ratio, both for improved stall margin and control of aeromechanical stimuli. These characteristics point toward a lower number of blades per stage and a greater stage weight. As with the unshrouded composite blade, the limiting constraints relative to the mechanical design of a hollow unshrouded titanium blade are flexural and torsional frequencies. To meet the aeromechanical requirements a 20-blade, wide-chord design is required. This design carries a weight penalty of 194 lb relative to the E^3 FPS design. The performance benefit of 0.5% in sfc is significant but is overshadowed by the weight and cost penalties associated with the hollow, wide-chord design. The overall effect on DOC yields a cost penalty rather than a savings, and relegates this concept to a poor ranking. As discussed earlier, the use of a low-flex blade design would allow the Wennerstrom design to be more competitive with the previously described blades and would offer a net payoff to the overall aircraft system.

Paramount to the design of a low-flex blade is the ability to design-in a means of damping out resonant response, especially at the 2/rev crossover point. A program is needed to develop techniques for the mechanical or material damping of a low flex blade.

Overall Design Impacts

The overall design impacts and merit factors for each of the advanced blades discussed are presented in Table 4.8-2. The fiber-reinforced hollow titanium blade design provides the greatest potential in terms of fuel savings, direct-operating-cost savings, and present-worth value.

Table 4.8-2. Advanced Fan Blades.

(a) Hollow Titanium Blade (32-Blade Shrouded Design)

Design Impacts	Direct	Secondary (Resizing)	Total
Δ Wt., lb	-103	0	-103
Δ Cost, $K	74	0	74
Δ Maint., $/flt.-hr	.10	N.A.	.10
Δ sfc, %	0	N.A.	0
Merit Factors	.19 ΔW_f-%	-.26 Δ DOC-%	13 PW, $M
Ranking		$2.4 \frac{PW \cdot P_S}{IDC}$	

(b) Polymeric Composite Blade (24-Blade Unshrouded Design) - Lightweight Core

Design Impacts	Direct	Secondary (Resizing)	Total
Δ Wt., lb	-234	0	-234
Δ Cost, $K	-34	0	-34
Δ Maint., $/flt.-hr	1.0	N.A.	1.0
Δ sfc, %	0	N.A.	0
Merit Factors	-.43 ΔW_f-%	-.81 Δ DOC-%	43 PW, $M
Ranking		$2.5 \frac{PW \cdot P_S}{IDC}$	

Table 4.8-2. (Concluded)

(c) 1-1/2" Leading Edge Fiber-Reinforced Hollow Titanium Blade (28-Blade Unshrouded Design)

Design Impacts	Direct	Secondary (Resizing)	Total
Δ Wt., lb	-176	0	-176
Δ Cost, $K	-14	0	-14
Δ Maint., $/flt.-hr	.30	N.A.	.30
Δ sfc, %	-.21	N.A.	-.21
Merit Factors	$-.6\ \Delta W_f$-%	$-.9\ \Delta$DOC-%	47 PW , $M
Ranking		$5.8\ \frac{PW \cdot P_s}{IDC}$	

(d) Wennerstrom Aero Design

Design Impacts	Direct	Secondary (Resizing)	Total
Δ Wt., lb	194	0	194
Δ Cost, $K	40	0	40
Δ Maint., $/flt.-hr	0	N.A.	0
Δ sfc, %	-.5	N.A.	-.5
Merit Factors	$-.33\ \Delta W_f$-%	$+.09\ \Delta$DOC-%	-4.6 PW , $M
Ranking		$-.53\ \frac{PW \cdot P_s}{IDC}$	

4.9 LOW-EMISSIONS SINGLE ANNULAR COMBUSTOR

Early in the E^3 program, testing of a prototype single annular combustor indicated that emissions requirements would probably not be met. The requirements being used were the standards for newly certified engines with an effectivity date of 1981. If CO and unburned hydrocarbons were held within limits, NO_x would be above limits. Or, if NO_x were held within limits, CO and unburned hydrocarbons would exceed their limits.

Therefore, to meet emissions requirements, a double annular combustor was designed for E^3. This used fuel nozzles arranged in inner and outer rings separated by a centerbody. All fuel nozzles would be used during start, then the inner nozzles would be shut off at low power levels such as idle and taxi, and then all nozzles would be used during flight.

A high price is paid for the emissions requirements. The double annular combustor is heavy, complex, and expensive. It requires a delicate start sequence in order to avoid locally over-temperaturing the turbine. The weight increase alone for the double annular combustor costs 5,000 gallons of fuel per year for each aircraft.

Development testing of the double annular is underway. Indications are that emissions goals will be met.

Now, however, emissions requirements are being relaxed. We expect to be able to meet the proposed standards, which have an effectivity date of 1984, with a single annular combustor.

It is important, therefore, to launch development of a low-emissions, single annular combustor. The development vehicle could be E^3 but the technology would be generic. Figure 4.9-1 and Table 4.9-1 summarize the benefits of this concept.

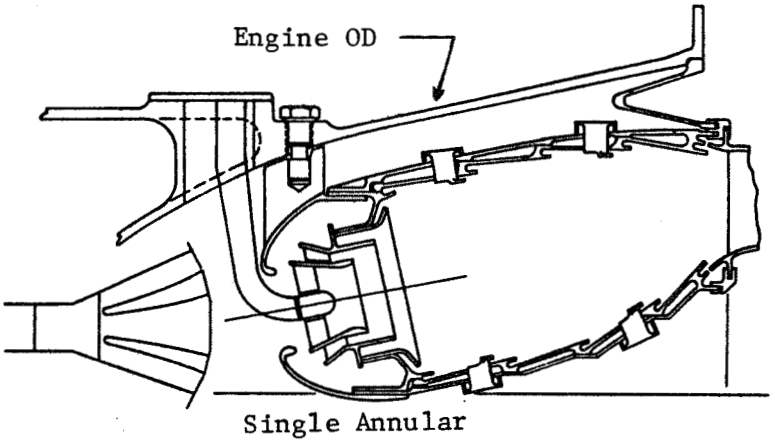

BENEFITS

- Lighter Weight
- Lower Cost

BARRIER PROBLEMS

- Emissions

PROBABILITY OF SUCCESS

- Design and Dev. - 95%
- Manufacturing - 100%
- Acceptance - 95%

Figure 4.9-1. Single Annular Combustor.

Table 4.9-1. Single Annular Combustor.

Design Impacts	Direct	Secondary (Resizing)	Total
Δ Wt., lb	-70	0	-70
Δ Cost, $K	-69	0	-69
Δ Maint., $/flt.-hr	-1.90	N.A.	-1.90
Δ sfc, %	0	N.A.	0
Merit Factors	$-.13\ \Delta W_f$-%	-.43 Δ DOC-%	23 PW , $M
Ranking		$11 \cdot \frac{PW \cdot P_s}{IDC}$	

4.10 COMPRESSOR BLISK

Integral bladed disks (blisks) are being considered for use on advanced engine designs primarily for weight and performance improvements. Performance improvements result from a combination of changes, including elimination of part span shrouds (where possible), platform step, gaps and dovetail leakage, as well as reduction of seal cavities between the rotors and stators. Tighter tip tolerances are also possible with blisks because the dovetail separation tolerance is eliminated, and because more accurate and reliable blade tip grinding is possible on blisk designs.

The weight savings in a blisk rotor results from eliminating the dead load of the blade platform, shank dovetail, and disk dovetail post. The reduction in rim dead load has a compounding effect, permitting a reduction in disk material.

In the study conducted in this program an assessment was made of the payoff associated with the use of blisks in Stages 1 through 4 of the E^3 FPS engine. The results indicate that a 26-lb weight savings and a 1% improvement in core efficiency are possible. Table 4.10-1 presents a summary of the overall design impacts and merit factors associated with the use of pressure-bonded blisks in the E^3 compressor. The major impact is the 0.4% improvement in sfc, which provides a significant payoff in terms of present-worth value.

Currently a common way to manufacture titanium blisks is to machine them from solid forgings. For all blisks but those of very small diameter such as the one on the T700 engine, this method is economically prohibitive. Other methods of blisk manufacture, such as pressure bonding, need to be explored and developed to make blisk manufacture feasible. A key factor in allowing this technology to be used in gas turbine engines is the development of adequate and economical repair procedures.

Table 4.10-1. Compressor Bonded Blisk.

Design Impacts	Direct	Secondary (Resizing)	Total
Δ Wt., lb	-26	0	-26
Δ Cost, $K	-4.3	0	-4.3
Δ Maint., $/flt.-hr	1.0	N.A.	1.0
Δ sfc, %	-.4	N.A.	-.4
Merit Factors	$-0.6\ \Delta W_f$-%	$-.56\ \Delta$DOC-%	30 PW , $M
Ranking		$3.2\ \frac{PW \cdot P_S}{IDC}$	

4.11 COMPOSITE VANES

The objective of this study was to assess the benefits of using composite materials for stator vanes in the E^3 FPS engine. The vanes selected for evaluation are shown in Figure 4.11-1 and include the booster stator assembly, the quarter-stage assembly, and the compressor inlet guide vane. The composite materials evaluated for this application are a graphite/glass hybrid-epoxy system having mechanical properties typical of those listed against titanium's in Table 4.11-1. The conceptual design of a composite vane assembly is shown in Figure 4.11-2. The total weight savings estimated for these applications is 75 lb; the detailed breakdown is shown in Table 4.11-2. Estimated cost savings for the 250th engine is $17K. In terms of fuel-burned savings the 75 lb is equivalent to 5400 gallons/aircraft/year. Table 4.11-3 presents the overall design impacts and merits factors for the composite vane applications. Weight and cost are the benefits which provide a present-worth value of $15 million in 1980 dollars.

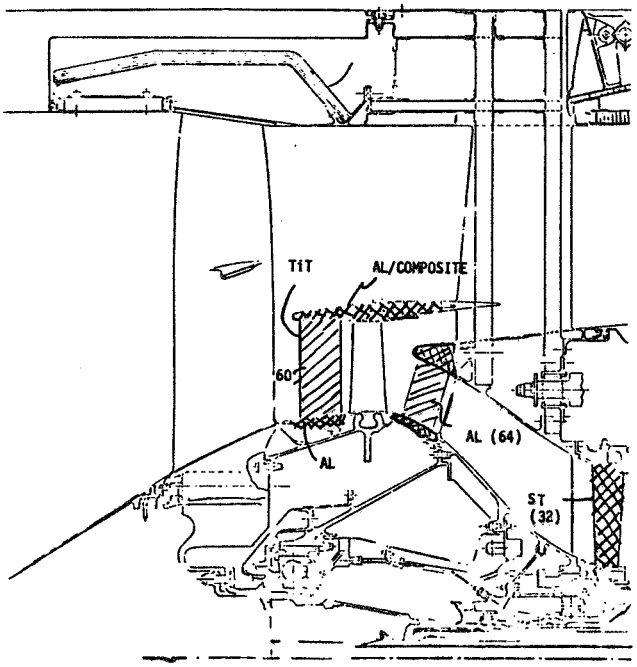

Figure 4.11-1. E^3 FPS Composite Vane Applications.

Table 4.11-1. Vane Material Properties.

	Titanium	Composite (0/35/0/-35) Layup
Density, lb/in.^{3}	0.161	0.057
Flex Modulus, E psi x 10^6	14.2	11.3
$\sqrt{E/\rho}$ psi x 10^6/lb/in.^{3}	9.4	14.2
Tensile Strength, ksi	117	104
Fatigue Strength, ksi	40	35
Vibratory Response, % (TF39 Stage 1 Blade)	100	60
Temp. Limit, °F	600	300

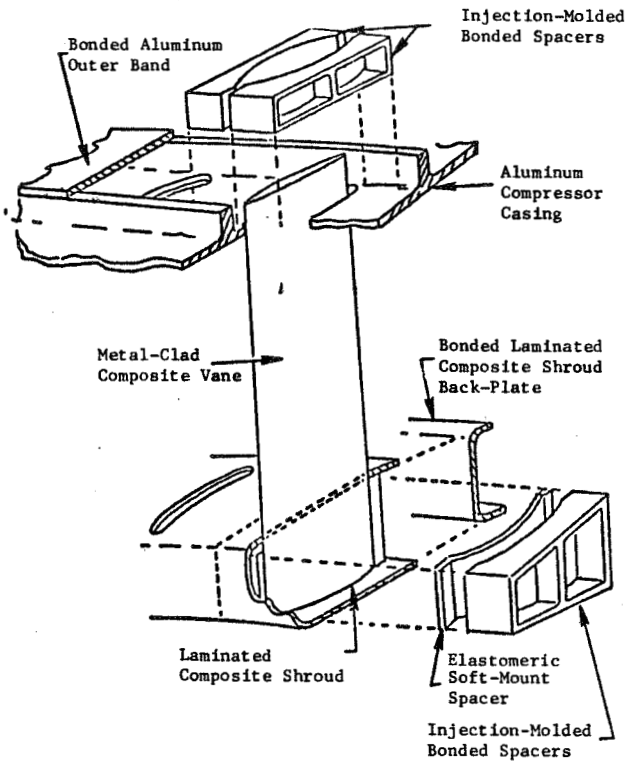

Figure 4.11-2. Composite Vane Conceptual Design.

Table 4.11-2. E^3 FPS Composite Vane Applications Weight Summary.

	FPS Config.	Composite Config.	Wt. Savings, lb
Stage 1 Vane	32	20	12
Inner Shroud	8	5	3
Splitter	62	37	25
1/4-Stage Assembly	62	37	25
Stage 1 IGV	29	19	10
	193	118	75

Table 4.11-3. Composite Vanes.

Design Impacts	Direct	Secondary (Resizing)	Total
Δ Wt., lb	-75	0	-75
Δ Cost, $K	-17	0	-17
Δ Maint., $/flt.-hr	0	N.A.	0
Δ sfc, %	0	N.A.	0
Merit Factors	$-.14\ \Delta W_f$-%	$-.28\ \Delta$DOC-%	15 PW , $M
Ranking		$5.1\ \frac{PW \cdot P_s}{IDC}$	

4.12 COMPOSITE SPINNER

Two approaches to the design and manufacture of a composite spinner for application in turbine engines have been assessed, including an injection-molded spinner and a resin-transfer-molded spinner. The material selected for the evaluation of the injection molded spinner is a 40% chopped-graphite-filled thermoplastic having a density of 0.048 lb/in.^{3}; it possesses good flow characteristics for injection molding. The thermoplastic is designated nylon 610. The graphite is a nominally 30-million modulus fiber which can be obtained from several sources, including Union Carbide. Hybrid combinations of graphite and glass can be achieved by mixing the two fibers.

Preliminary material properties for this material are shown in Table 4.12-1. These data are preliminary and are representative of injection-molded panels with some directionality and alignment of the fibers in the test direction; transverse properties may be lower than those presented. The data show that the RT tensile strength and modulus are 27 ksi and 2.5 x 10^6 psi, respectively, with approximately a 50% reduction in strength at a temperature of 180° F. The low tensile elongation values indicate that impact characteristics will be the limiting constraint in this application.

The second approach evaluated is a resin-transfer-molded composite spinner which uses Kevlar, glass, or a graphite/glass fabric. The manufacturing method allows the use of a dry fabric in combination with a low-viscosity resin system. The dry fabric preform can be locally reinforced by stitching prior to the resin transfer process. This material system/manufacturing process offers major benefits, including strength levels approaching two to four times those of the chopped-fiber-filled thermoplastic material, higher stiffness, better dimensional control and improved impact resistance.

In order to determine the stresses in a composite spinner, a direct-substitution stress analysis was conducted using an existing E^3 fan rotor model. In this model, composite material properties were substituted for current aluminum alloy properties. A summary of the stresses for the spinner that were obtained from this computer run is presented in Table 4.12-2; the spinner design is illustrated in Figure 4.12-1. The summary shows that for the injection-molded design all stresses are below 8 ksi, the predominant stress being in the tangential direction. Corresponding stresses in the current aluminum spinner design are also shown.

Table 4.12-3 lists the cyclic and life requirements for the spinner, together with the maximum fan rpm and the maximum temperature. The maximum temperature of 132° F for the spinner corresponds to the takeoff condition, which constitutes less than 2% of the overall life requirement.

Both of these composite spinner designs offer cost and weight benefits over the existing aluminum spinner. For the resin-transfer-molded design, projected 250th-part cost and weight savings are 62% and 34%. Table 4.12-4 summarizes the design impacts and merit factors for the composite spinner. The development of composite flange design concepts and manufacturing techniques is required in order for the cost and weight benefits to be fully realized.

Table 4.12-1. 40% Graphite, Chopped-Fiber-Filled Nylon 610 Thermoplastic (QC 1008).

Flexural Properties

Temp., °F	Strength, 10^3 psi	Modulus, 10^6 psi
-70	55.5 - 64.8 (59.3)	3.19 - 3.58 (3.34)
0	55.3 - 60.5 (56.0)	3.19 - 3.51 (3.30)
73	43.0 - 45.8 (44.0)	2.53 - 3.05 (2.77)
180	27.9 - 29.6 (28.6)	1.70 - 1.80 (1.74)
255	22.8 - 23.7 (23.2)	1.47 - 1.49 (1.48)

Tensile Properties

Temp., °F	Strength, 10^3 psi	Modulus, 10^6 psi	Elong., %
-70	---	---	---
0	33.0 - 37.9 (35.9)	2.80 - 3.99 (3.43)	1.28 - 1.71 (1.48)
73	25.5 - 28.3 (27.0)	2.37 - 2.58 (2.49)	2.03 - 2.21 (2.14)
180	14.7 - 17.3 (15.8)	1.49 - 2.67 (2.15)	1.07 - 2.71 (1.63)
255	11.3 - 13.4 (12.2	1.20 - 2.11 (1.81)	1.13 - 2.76 (1.69)

Table 4.12-2. Comparison of Spinner Stresses, Max Climb, Case 41 - 3539 rpm.

	Composite		7075 Aluminum	
Spinner	Meridional psi	Tangential psi	Meridional psi	Tangential psi
1	0	0	0	0
2	0	159	0	334
3	0	900	-40	1894
4	0	1260	-63	2660
5	77	1663	240	3510
6	-1585	2167	-4186	4126
7	-867	2873	-2577	5672
8	810	5040	-567	11,020
9	1242	6131	2109	14,400
10	-150	7321	-563	21,410
11	-3220	7333	-2702	22,580
12	802	6844	3467	21,630
13	0	6513	0	21,230

Table 4.12-3. Life Requirements for Spinner at the Critical Mission Points.

	Max Fan rpm	Cycles	Life, hours	Spinner Max Temperatures, °F
Takeoff	3731	1,224	2,448	132
Max Climb	3926	12,960	25,920	83
Max Cruise	3836	29,376	58,752	5
Reverse Thrust	3543	288	576	59
Approach	2741	3,064	6,128	80
Remaining Mission (Max)	2318	25,088	50,176	80
		72,000	144,000	

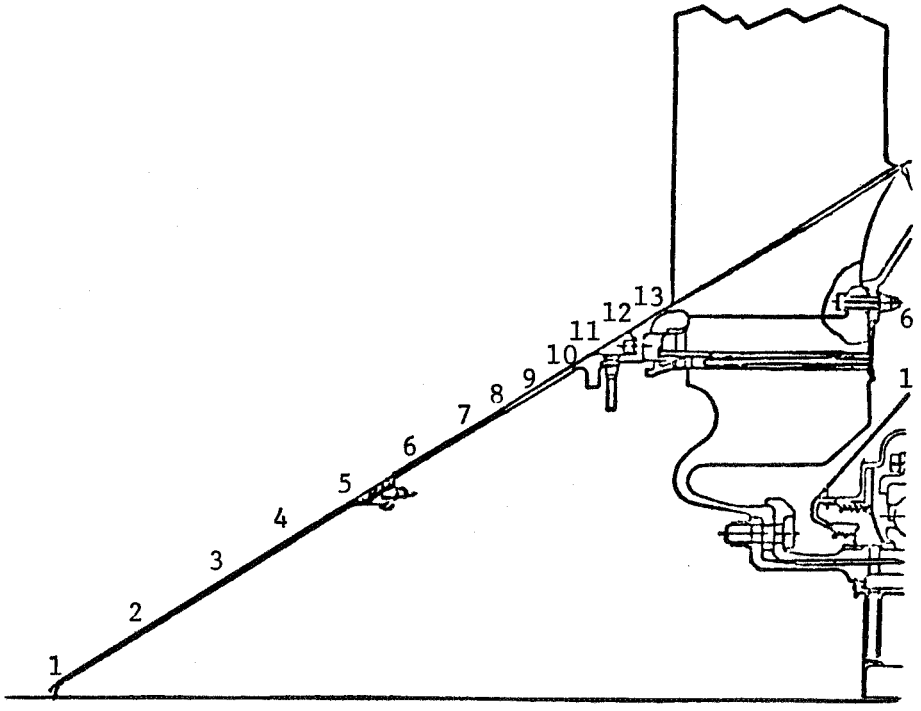

Figure 4.12-1. Composite Spinner Conceptual Design.

Table 4.12-4. Composite Spinner.

Design Impacts	Direct	Secondary (Resizing)	Total
Δ Wt., lb	-7	0	-7
Δ Cost, $K	-4.1	0	-4.1
Δ Maint., $/flt.-hr	0	N.A.	0
Δ sfc, %	0	N.A.	0
Merit Factors	$-.013\ \Delta W_f$-%	$-.03\ \Delta$DOC-%	1.5 PW, $M
Ranking		$3.9\ \frac{PW \cdot P_s}{IDC}$	

4.13 COMPONENT EFFICIENCY IMPROVEMENT

Efficiency can be improved by many technologies besides aerodynamics. Historically, a large number of efficiency improvements have resulted from technology advances in materials, cooling, structures, manufacturing, and other fields. Efficiency can be increased through improvements in (1) heat transfer and cooling designs, which are affected by materials; (2) airfoil configuration and shrouds, which are affected by vibration analysis and tuning; and (3) rotational speeds, windages, and aerodynamic configuration, which are affected by advances in materials, structural design, and manufacturing. Some aerodynamic developments, such as the Wennerstrom fan, require advances in other areas before they can be practically used in an engine.

In this study, the benefits due to arbitrary improvements in aerodynamic efficiency were analyzed. This was done to show what an improvement in each component is worth. It provides a means for comparing aerodynamic improvements and for comparing efficiency improvement programs with other technology programs.

A 1% η improvement was assumed for each rotating component and a 5% improvement in mixing effectiveness was assumed for the mixer. These represent major technical advancements. A series of development tests for each component would be necessary to achieve such improvements. Development costs were assumed, admittedly arbitrarily, without specific development programs in mind. In this analysis the important criterion is the performance payoff in terms of fuel burned, direct operating costs, and present worth, rather than the return on investment for a specific program. The development cost assumptions are reasonable, so a very general comparison of returns can be made.

Table 4.13-1 shows the benefits to be realized from performance improvements. Figure 4.13-1 and Table 4.13-2 summarize the benefits of all component improvements combined. Cycle performance effects on the engine are covered in Section 4.1.

Table 4.13-1. Combined Benefits of Component Performance Improvements.

	Fan Bypass	Fan Hub	Compressor	HP Turb.	LP Turb.	Mixer	Combined
For an improvement of:	1% η	1% η	1% η	1% η	1% η	5% Mix. Effect.	
The following benefits may be realized:							
% Δ sfc	-.75	-.2	-.75	-.8	-.8	-.3	-3.6
Δ Fuel Burned, %	-1.04	-.28	-1.04	-1.10	-1.10	-.41	-5.0
Δ Fuel Burned, Gallons Per Aircraft Per Year	40,000	11,000	40,000	43,000	43,000	16,000	193,000
Δ % DOC For $2/G Fuel	-.96	-.26	-.96	-1.02	-1.02	-.38	-4.6
Δ % DOC For $1/G Fuel	-.68	-.18	-.68	-.73	-.73	-.27	-3.3
Present Worth For $2/G Fuel	$64M		$50M	$54M	$54M	$20M	$242M
Present Worth For $1/G Fuel	$32M		$25M	$27M	$27M	$10M	$121M
For an initial development cost of	$4.5M		$8.5M	$4M	$4.5M	$3M	$24.5M
and a probability of success of	80%		80%	80%	80%	80%	80%
The following payoffs may be realized:							
$\frac{PW \times PS}{IDC}$ for $2/G	11		5	11	10	5	8
$\frac{PW \times PS}{IDC}$ for $1/Gal	6		2	5	5	3	4

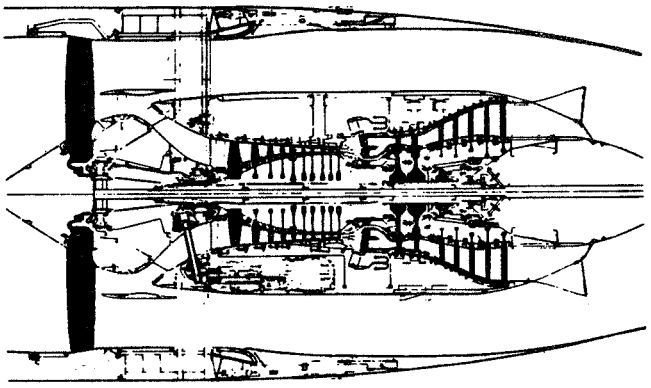

BENEFITS

- Improved sfc

BARRIER PROBLEMS

- Substantially Improve Highly Developed Components

PROBABILITY OF SUCCESS

- Design and Development - 80%
- Manufacturing - 95%
- Acceptance - 95%

Figure 4.13-1. Component Efficiency Improvements (+1%).

Table 4.13-2. Benefits of Component Efficiency Improvements (+1%).

Design Impacts	Direct	Secondary (Resizing)	Total
Δ Wt., lb	0	-74	-74
Δ Cost, $K	0	-18	-18
Δ Maint., $/flt.-hr	0	N.A.	0
Δ sfc, %	-3.6	N.A.	-3.6
Merit Factors	$-5.1\ \Delta W_f$-%	-4.9 Δ DOC-%	257 PW $M
Ranking		$8.4\ \frac{PW \cdot P_S}{IDC}$	

4.14 VARIABLE-AREA NOZZLE, MIXED-FLOW EXHAUST

Specific fuel consumption on a mixed-flow turbofan engine can be improved at part power over a range of Mach numbers by reducing the exhaust nozzle area. This raises the fan operating line and improves the fan efficiency. The magnitude of the improvement for a mission can vary, depending on the time spent at low power. This is discussed in Section 4.1.3.6 of this report.

The benefits analysis was conducted for a nozzle with a translating centerbody which can vary the area. Preliminary analysis indicated that a weight increase of about 130 lb would be required with an additional plug drag loss equivalent to about 0.1% of thrust. As indicated in the referenced section, a short-range commercial mission would result in an sfc savings equivalent to 0.5%, but this would be reduced by the 130 lb weight penalty, resulting in a net savings of 0.3%. If the time at loiter power were increased from the reference mission, the fuel savings could increase substantially from that shown.

The evaluations of the reference mission are summarized in Figure 4.14-1 and Table 4.14-1.

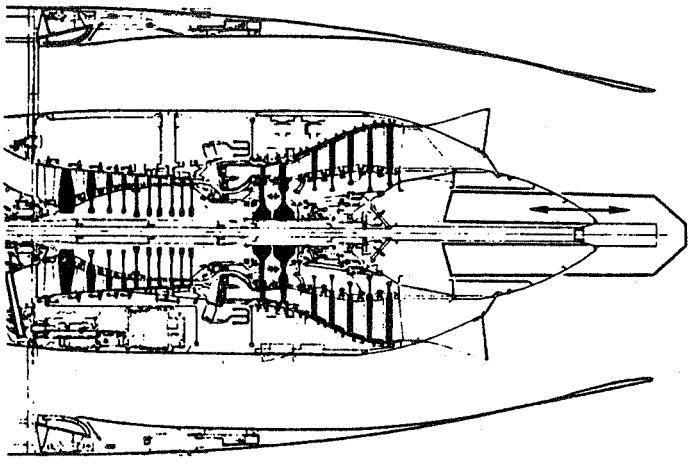

BENEFITS

- Improves sfc At Cruise, Loiter and Approach

BARRIER PROBLEMS

- None

PROBABILITY OF SUCCESS

- Design and Dev. - 95%
- Manufacturing - 95%
- Acceptance - 95%

Figure 4.14-1. Variable Area Nozzle (A_8).

Table 4.14-1. Variable Area Nozzle (A_8).

Design Impacts	Direct	Secondary (Resizing)	Total
Δ Wt., lb	130	0	130
Δ Cost, $K	+41	0	+41
Δ Maint., $/flt.-hr	+.50	N.A.	+.50
Δ sfc, %	-.50 (Effective / Average)	N.A.	-.50
Merit Factors	-.46 Δ W_f-%	-.12 Δ DOC-%	6 PW , $M
Ranking		7.6 $\frac{PW \cdot P_s}{IDC}$	

4.15 TURBOMACHINERY 3D AERO ANALYSIS

Turbine through-flow vector aerodynamic analyses treat the flow as being axisymmetric. Viscous effects are represented on a gross basis by circumferentially averaged mainstream pressure losses and sometimes, for secondary flow, by perturbations in pressure, temperature, and flow angle to represent the circumferentially averaged effects of secondary flow. Though computational development has been underway at some institutions, a practical analysis does not exist. Yet, 3D flow dominates some areas. Proper treatment of this flow has the potential of significantly improving efficiency.

The 3D flows of concern are radial and cross-channel flows of boundary-layer air under the influence of mainstream pressure gradients. These occur in the channel between airfoils and repeat in each channel in a blade row. The 3D effects can concentrate large quantities of low-pressure air into certain corners of the channel, where they can cause separation of the mainstream. Also, they can coalesce into vortices which alter the flow angle into the downstream blade row.

There are two difficulties in viscous 3D analyses. The first, the establishing of an analytical method, has been fairly well met. The second difficulty is developing the analysis and computer code so that the calculation can be executed in reasonable amounts of computer time. This has not been accomplished.

Figure 4.15-1 illustrates the complexity of real flows. Table 4.15-1 summarizes the benefits of this concept for the LP turbine component.

The technology under consideration is aerodynamic analysis. It is directly applicable to fans, compressors, HP turbines and LP turbines. Potentially it could also apply to mixers and flow around bodies in inlets, ducts, and nozzles.

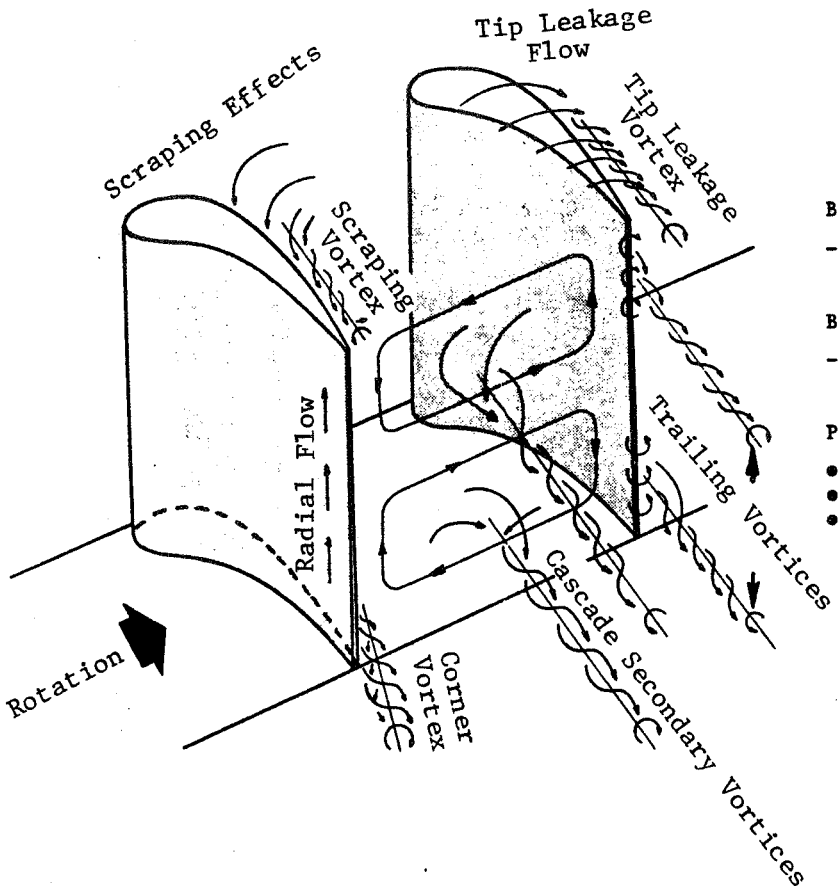

Figure 4.15-1. Secondary Flows and Vortices in a Turbine Rotor.

Table 4.15-1. Low Pressure Turbine Aerodynamics - 3D Aero.

Design Impacts	Direct	Secondary (Resizing)	Total
Δ Wt., lb	0	0	0
Δ Cost, $K	0	0	0
Δ Maint., $/flt.-hr	0	N.A.	0
Δ sfc,%	-.2	N.A.	-.2
Merit Factors	$-.28\ \Delta W_f$-%	-.26 Δ DOC-%	14 (PW , M)
Ranking		$7\ \frac{PW \cdot P_s}{IDC}$	

4.16 LPT FLARED FLOWPATH

Long-duct engines such as the E^3 use a convoluted mixer to mix the fan and core streams prior to their expansion through the exhaust nozzle. The subject of this section is integration of the LP turbine flowpath, frame, and mixer flowpath. This improvement weighs more but is sufficiently more efficient that there is a net reduction in fuel burned of 13,000 gallons of fuel for one aircraft each year.

The flared LP turbine with integrated frame and mixer is a design refinement. It is now being incorporated into the E^3 flight engine configuration. Figure 4.16-1 and Table 4.16-1 summarize the benefits of this concept.

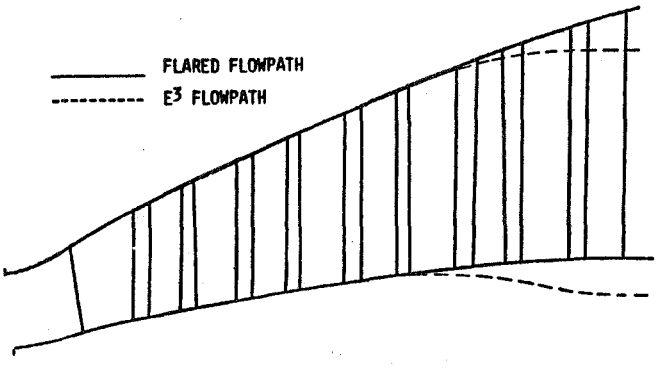

BENEFITS

- Better Mixer Performance
- Better LPT Performance

BARRIER PROBLEMS

- None

PROBABILITY OF SUCCESS

- Design and Dev. - 95%
- Manufacturing - 95%
- Acceptance - 95%

Figure 4.16-1. Low Pressure Turbine - Flared Flowpath.

Table 4.16-1. Low Pressure Turbine - Flared Flowpath.

Design Impacts	Direct	Secondary (Resizing)	Total
Δ Wt., lb	+74	0	+74
Δ Cost, $K	+2.6	0	+2.6
Δ Maint., $/flt.-hr	0	N.A.	0
Δ sfc, %	-.36	N.A.	-.36
Merit Factors	$-.34\ \Delta W_f$-%	-.17 Δ DOC-%	9 (PW , $M)
Ranking		$5.6\ \frac{PW \cdot P_s}{IDC}$	

4.17 LPT ORTHOGONAL BLADING

Modern low-pressure turbines use highly sloped outer walls with essentially radial blading. As a result, the blading is not normal to the outer wall, a condition considered to be deleterious to aerodynamic performance. Performance should improve if the blading could be swept forward to make the tip region more normal to the outer wall.

There should be negligible weight or cost penalties in such a system. Orthogonal blading is judged to be worth 0.1 to 0.2% $\Delta\eta$, which yields 0.1% better sfc.

In a turboprop or geared-turbofan application, higher rpm reduces the number of stages, making the tip slope much steeper. In this case, the efficiency gain due to orthogonal blading would be much larger. Also, because of the higher speed, the dynamic problems would be more severe.

Figure 4.17-1 and Table 4.17-1 summarize the benefits of this concept.

Successful execution of orthogonal blading in a shrouded low-pressure turbine requires application of existing and more sophisticated structural and dynamic analyses in areas beyond current experience. To develop the technology, a design would have to be executed and a 3D analysis made for deformation and creep as well as stress. This should be followed by hot pull tests and cyclic spin pit tests. In a parallel program early in this activity, an air turbine rig performance test should be conducted to establish the performance improvement. If all preceding results are positive, the concept would be demonstrated in an engine test.

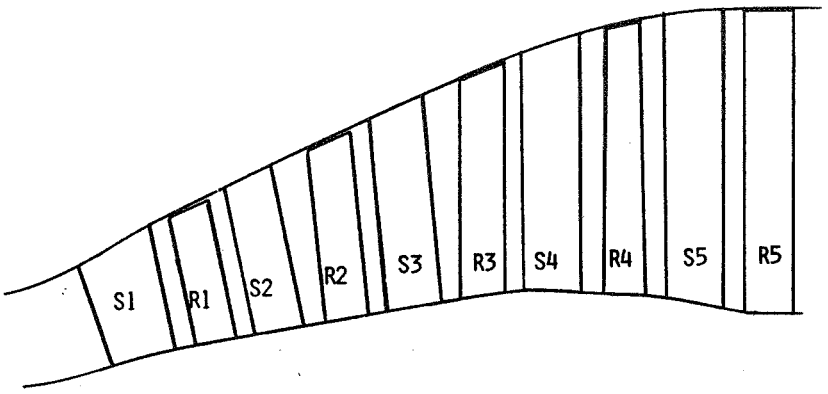

BENEFITS

- Lighter Weight
- Lower Cost

BARRIER PROBLEMS

- Canted Stacking Axis

PROBABILITY OF SUCCESS

- Design and Dev. - 80%
- Manufacturing - 95%
- Acceptance - 80%

Figure 4.17-1. Low Pressure Turbine Aerodynamics - Orthogonal Flowpath.

Table 4.17-1. Low Pressure Turbine Aerodynamics - Orthogonal Flowpath.

Design Impacts	Direct	Secondary (Resizing)	Total
Δ Wt., lb	0	0	0
Δ Cost, $K	0	0	0
Δ Maint., $/flt.-hr	0	N.A.	0
Δ sfc, %	-.1	N.A.	-.1
Merit Factors	-.14 ΔW_f-%	-.13 Δ DOC-%	6.7 (PW , M)
Ranking		$2 \frac{PW \cdot P_s}{IDC}$	

4.18 ADVANCED FUEL DELIVERY SYSTEM

4.18.1 Introduction

The Advanced Fuel System is a new approach to the type of fuel pumps, control valves, and fuel nozzles used on aircraft jet engines. The desirability of this change begins with the need for more heat sink in the engine fuel to permit waste heat recovery from other engine systems in order to improve sfc. A common solution is found for this objective and for the possible need for fuel system compatibility with broadened-specification or synthetic fuels.

The technologies involved with these changes have evolved over the years from early engine designs, previous fuel system programs, and similar components used on augmented jet engines. These are also new areas of component design and development which will require special emphasis. The major concern, however, is the integration of these fuel system improvements with other parts of the engine and aircraft. This applies particularly to the engine combustor in the case of fuel nozzle design and the aircraft air systems and fuel tanks for waste heat recovery. Consequently, a program devoted to this effort will be needed. Because of the broad-reaching impact of these system changes, it will also be necessary that such a program be initiated well in advance of new engine and aircraft development.

4.18.2 Background

In June of 1980 General Electric Company completed a 7-year program for the Naval Air Propulsion Center entitled the Lightweight Fuel Delivery System (LWFDS). This program resulted in the successful design and development of a new engine fuel system offering significant advantages in terms of fuel contamination resistance and improvement in weight, cost, and reliability. The results did not totally meet the Navy's objective of a filterless fuel system, but would enable use of coarse rather than fine filtration and afford a higher tolerance to fuel contamination. The system successfully ran on the GE23 (ATEGG) engine and showed favorable results during fuel system and combustor rig tests which included transient performance, suction feed, contamination, temperature rise, blow-out limits, and nozzle flow distribution.

New emphasis on this system approach is now resulting from interest in synthetic fuels and improved sfc as the result of waste heat recovery.

The Lightweight Fuel Delivery System is shown in Figure 4.18-1. The basic differences between this and a conventional system, Figure 4.18-2, are:

- A single high-speed centrifugal fuel pump for both main and augmentor fuel systems
- Flat-plate shear-type fuel valves instead of sleeve valves in the fuel metering assembly

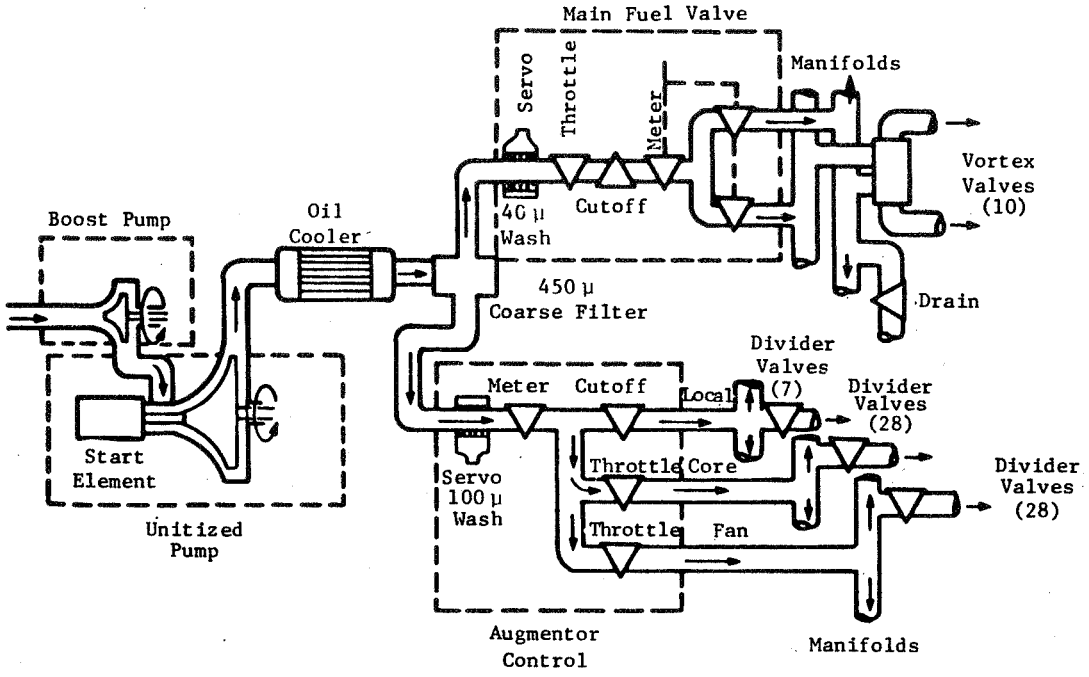

Figure 4.18-1. Advanced Lightweight Fuel Delivery System.

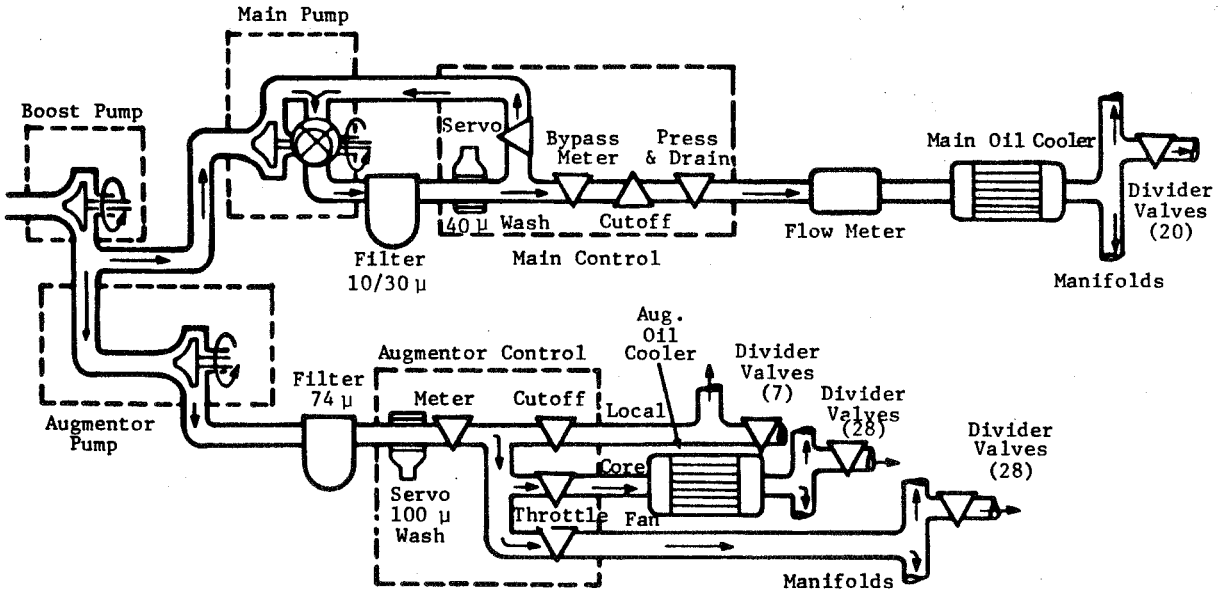

Figure 4.18-2. Conventional Fuel Delivery System.

- A single oil cooler for both main and augmenter flows located upstream of the flow split to these systems
- No-moving-part vortex fuel distribution valves for the main system for use with an air-atomizing combustor
- A single coarse-micron rated filter for main and augmenter flows
- Compatibility with conventional or electronic fuel controls

The Advanced Fuel System is shown in Figure 4.18-3. This system is similar to the LWFDS but intended for use on a non-augmented engine including commercial applications.

4.18-3 Technical Discussion

Sfc Improvement

The advanced fuel system does not result in a significant direct benefit measurable in terms of sfc. Except for potential saving in weight and cost, mostly attributed to the use of fewer combustor nozzles, there is no direct decrease in fuel consumption. What the system does achieve is the ability to utilize other engine systems which may offer significant sfc improvement. These systems may generally be classified as waste heat recovery systems. The objective of these systems is to eliminate or reduce sfc penalty associated with air cooling and to return engine thermal energy to the fuel.

In the past, before fuel consumption became such a premium factor in the design of jet engines, it was customary to use fan air or outside ram air to cool just about everything which could not be cooled by fuel. This practice resulted in air cooling of electric generators, engine bleed air for air conditioning and anti-ice, and other special systems. Ram air cooling is bad because it increases airplane drag. Fan bleed air cooling is worse because it includes both ram drag (into engine inlet) and loss of thrust (from fan duct nozzle). The result is fuel burned to provide component and system cooling instead of thrust.

This situation can be overcome by eliminating air cooling and using fuel as the heat sink. This results in an actual decrease in fuel consumption because thermal energy put into the fuel raises its sensible heat and increases the energy available for combustion. Examples of this technique are the fuel-cooled generators on present day engines. These systems improve cruise sfc by approximately 0.35%.

A more advanced system with potentially greater fuel savings is offered by the NASA/GE E^3 Waste Heat Recovery System. This system shown in Figure 4.18-4 uses fuel to cool the compressor bleed air which is used for air conditioning and airframe anti-icing. For E^3 the cruise sfc improvement is 0.8%.

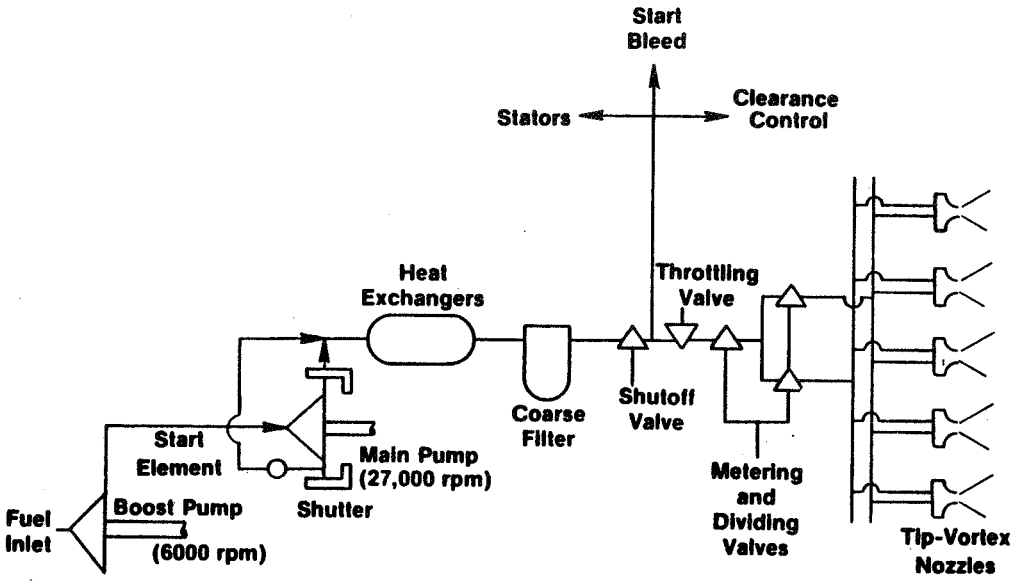

Figure 4.18-3. Advanced Fuel System.

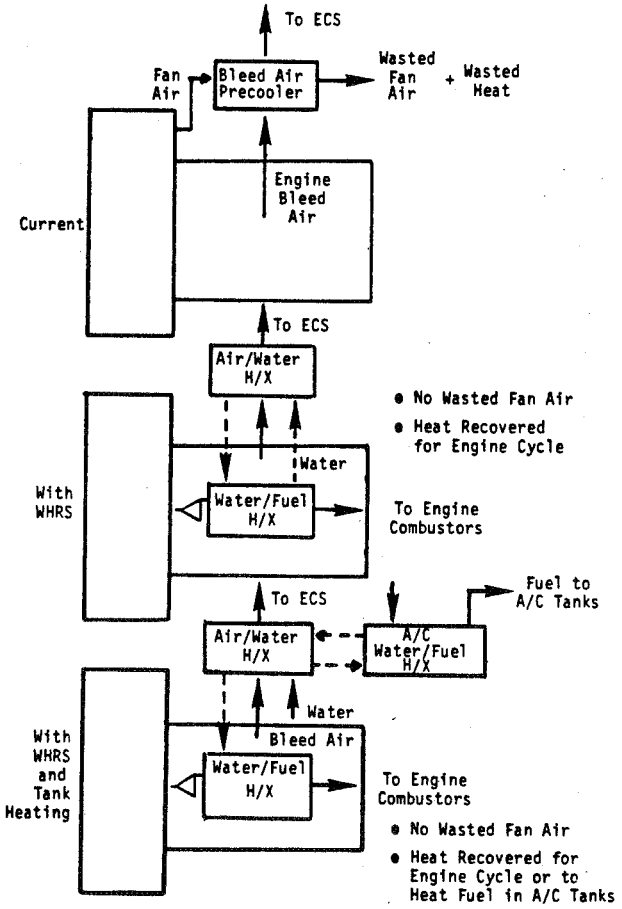

Figure 4.18-4. Environmental Control System (ECS) Waste Heat Recovery System (WHRS).

Figure 4.18-5 shows the situation which arises as heat is put into the fuel. The figure is intended to show three considerations: (1) the effect of adding heat to the fuel for waste heat recovery, (2) the effect of synthetic fuels on fuel temperature limits, and (3) the improvements offered by the Advanced Fuel System. Computerized analysis was used to obtain these results. The generator (IDG) waste heat recovery system is included in the fuel heat load in all cases.

Today's conventional fuel system uses a gear-type engine fuel pump and fuel nozzles with check and shutoff valves located near the hot combustor casing. Because of the need for excess flow capacity, the gear pump generates considerable heat which results in high fuel temperature rise at low engine power (descent). The nozzle valves require close clearances which impose fuel temperature limits to avoid gumming and coking. These nozzle limits are based also on the fact that GE engines do not require scheduled cleaning of nozzles and valves.

Using JET-A fuel, the nozzle fuel inlet limit of 275°F is reached during descent. With synthetic fuel, a limit of 235°F is assumed based on 40°F reduction in thermal breakpoint (coking). In this case the nozzle fuel inlet is over limit by 17°F at cruise and by 40°F during descent. For the conventional system it must be concluded, then, that: (1) no additional heat sink is available at descent power even with JET-A, (2) 23°F (1000 BTU/min.) of heat sink is available at cruise using JET-A, and (3) both descent and cruise are over limit using synthetic fuel. Consequently conventional engine systems do not offer much potential for more advanced forms of waste heat recovery or compatibility with synthetic fuels.

The Advanced Fuel System improves this situation. Fuel heat sink is increased by reducing the fuel system's internal heat rejection and by increasing the fuel nozzle temperature limits. The fuel pump is made more efficient by eliminating bypass flow recirculation. The nozzle limits are increased by removing mechanical valves from the engine hot section.

The gear-type fuel pump is replaced by a centrifugal pump. A well designed conventional centrifugal pump running at high speed (27000 rpm) will reduce the cruise fuel temperature rise by 17°F. During descent, a reduction of 106°F can be achieved if the pump includes a diffuser shutter. Without the shutter, the reduction is 91°F. Figure 4.18-5 shows the result (180°F) with the shutter. All of the results shown in the figure assume the use of a conventional low-speed centrifugal boost impeller (for gear or centrifugal main pump).

Because a centrifugal main pump cannot develop sufficient pressure at low cranking speeds to start the engine, a special starting element is required. This may be in the form of the vane-pump start element developed for the LWFDS pump and shown in Figure 4.18-6. A small electric-motor-driven starting pump could also be used.

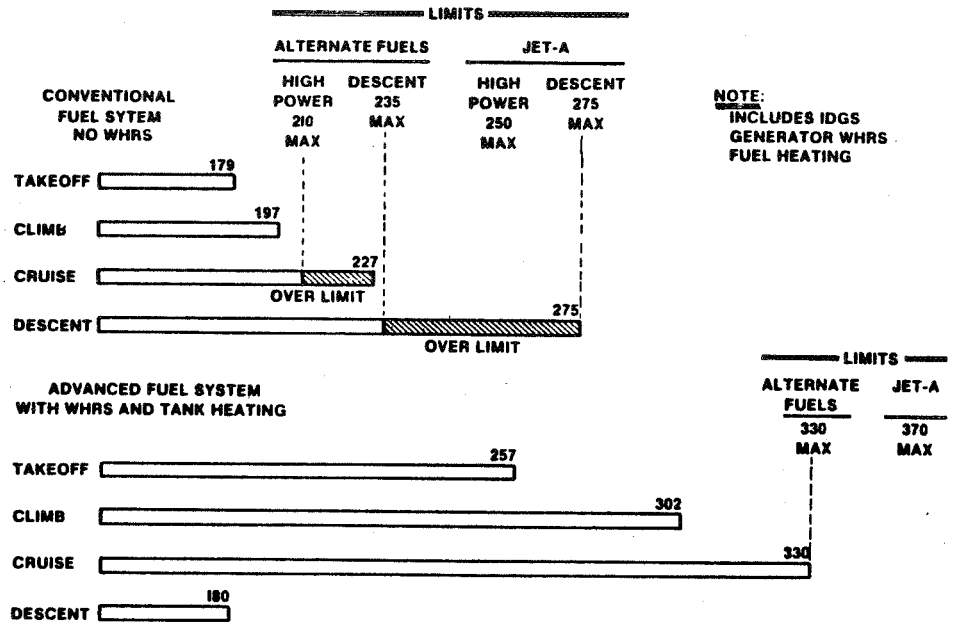

Figure 4.18-5. Effects of Waste Heat Recovery, Synthetic Fuels, and Advanced Fuel System on Nozzle Fuel Inlet Temperature.

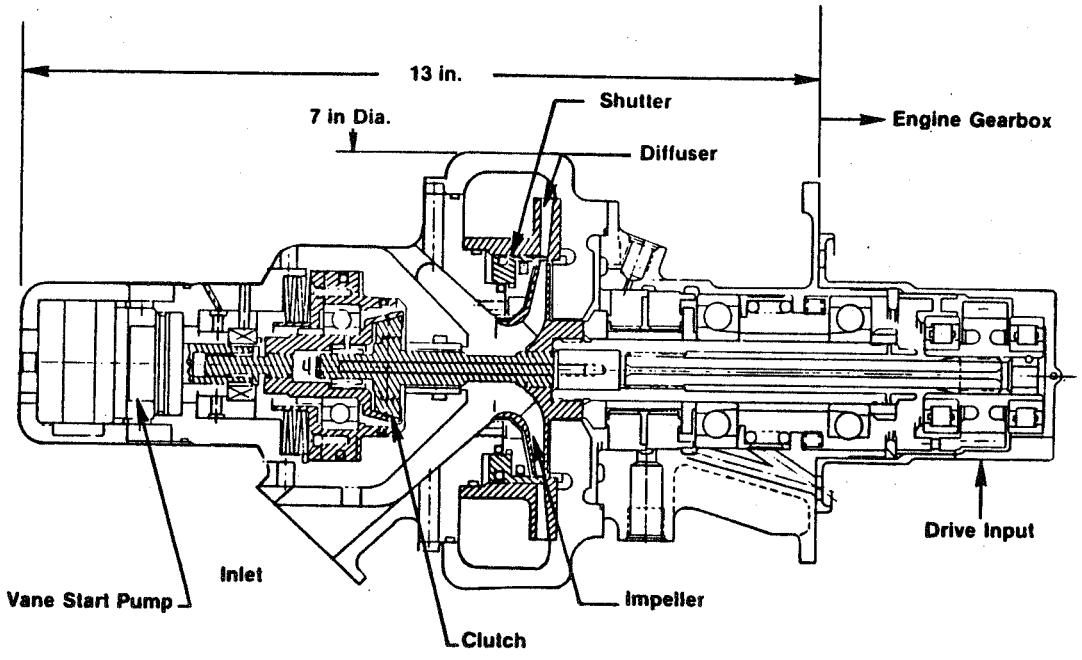

Figure 4.18-6. Main Fuel Pump of LWFDS.

Basically the pumping system is straightforward and requires only a change in pump drive speed and change in the fuel metering device from a bypassing system to a throttling system. Both of these changes are supported by the technology used for many years for augmentor fuel systems.

In order to eliminate mechanical valves from the engine hot section a different approach can be taken to nozzle fuel distribution. Whether fuel pressure atomizing or air atomizing, the nozzles must address four basic considerations, which are: (1) uniform distribution of fuel around the engine, (2) adequate atomization for lightoff and flame propagation, (3) stable combustion, and (4) a relationship between flow and impedence which permits adequate control of flow.

The dark line in Figure 4.18-7 shows the typical shape of a fuel nozzle flow versus ΔP operating line. Below minimum idle (500 lb/hr), ΔP is sufficient to overcome the effect of gravity head between the top and bottom of the engine and nozzle-to-nozzle flow variations. Above idle, the shape of the operating line permits adequate flow control and distribution. Depending on the nozzle and combustor design, these results are achieved by a combination of nozzle orifice impedence and mechanical valves.

The same-shape operating line can be produced by fluidic valves or fluidic nozzles. This concept was used in the LWFDS program and has been used on many early jet engines such as the General Electric J47. The basic design, referred to as a vortex nozzle, is shown in Figure 4.18-8. Each nozzle includes a vortex spin chamber and receives two separate input flows. During engine lightoff and low power, only the tangential flow stream is used. Flow enters the spin chamber tangentially and spins to the center, then out through the atomizing orifice. The pressure drop across the spinning vortex aids the orifice in obtaining adequate ΔP for flow distribution. Above idle power, the radial flow stream comes on-line. This stream must mix with the tangential stream before exiting the nozzle tip. As a result, a scheduled relationship between tangential flow and radial flow establishes the nozzle flow versus ΔP characteristic. Now only flow control valves are required for each flow stream (tangential and radial) and these valves can be located upstream in the fuel system away from the engine hot section. In the vortex nozzles the spin velocity, on the order of 250 fps, tends to self-clean the nozzle, and the nozzle openings may be larger than those required for conventional nozzles.

Referring back to Figure 4.18-5, the lower set of fuel temperature results includes the improvements discussed above. Fuel pump temperature rise is decreased and nozzle coking limits are increased. Now it is possible to add considerable heat to the fuel via a waste heat recovery system. The ECS waste heat recovery system offering 0.8% cruise sfc improvement was used for this analysis. Since the generator heat is also included, the total sfc improvement as the result of fuel heating is 1.15 percent. During descent, where engine thrust is not relevant to sfc, no heat is added to the fuel because air cooling is available for the generator, and the aircraft fuel tank is used for ECS cooling. The reduction in descent fuel nozzle inlet temperature (180° F instead of 275° F) does pay off in terms of nozzle coking because at idle there is very little fuel available to cool the nozzle internally. The hot casing temperature tends to drive up the temperature of the nozzle surface

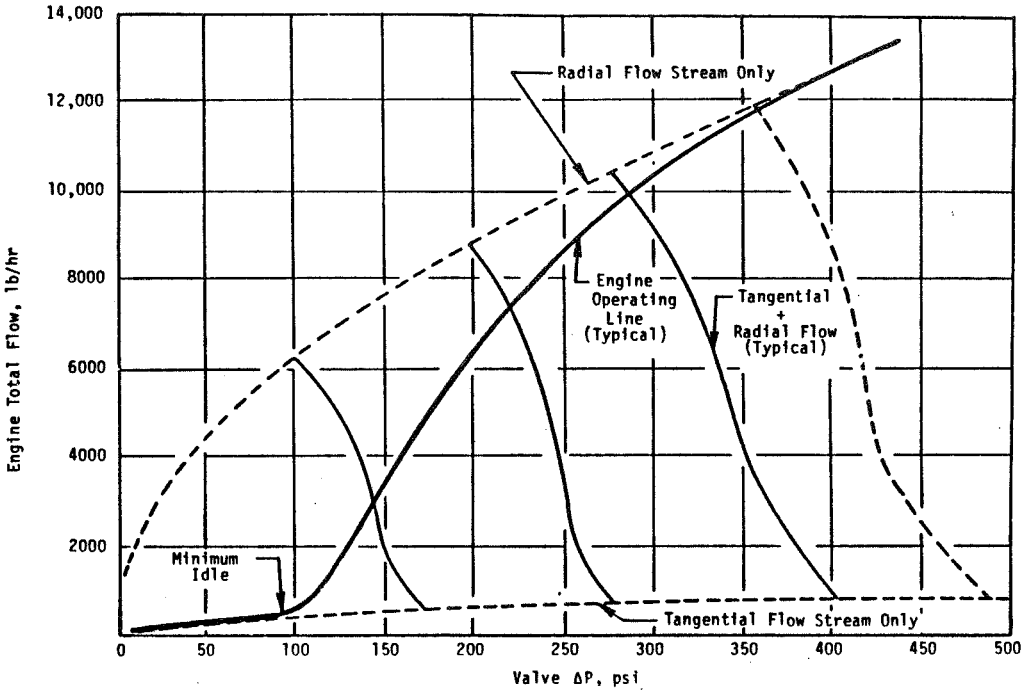

Figure 4.18-7. Vortex Nozzle Flow Characteristics.

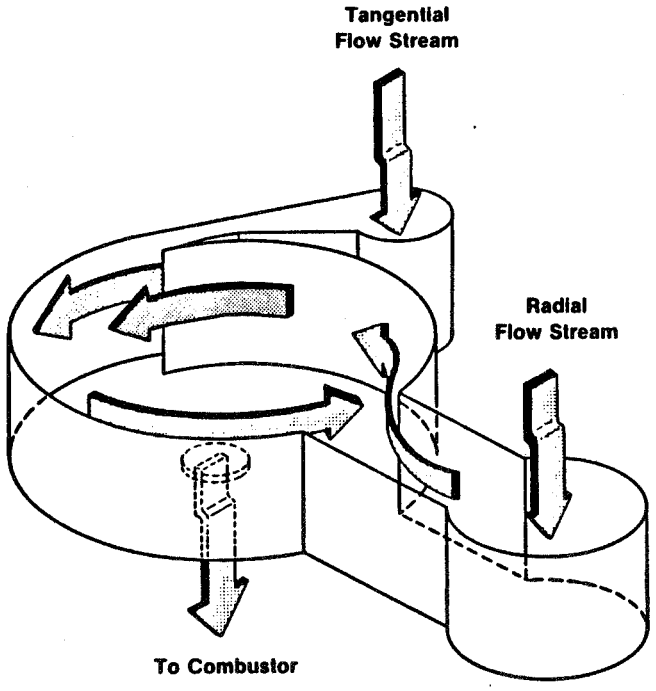

Figure 4.18-8. Vortex Fuel Nozzle.

in contact with fuel, particularly during the transient cooldown of the casing after a power reduction from cruise to idle.

Fuel Compatibility

In addition to sfc improvement by providing a heat sink for waste heat recovery, a second major benefit of the Advanced Fuel System is compatibility with broadened-specification or synthetic fuels. It has already been explained how the vortex nozzle permits higher fuel temperature limits and reduces coking. Other features which enhance fuel compatibility are:

- Insensitivity to low-lubricity fuels
- Less sensitivity to gumming and coking in control valves
- Fuel tank heating in combination with waste heat recovery

It is a widely debatable issue as to whether or not JET-A fuel properties will ever deviate significantly from current specifications. There are a number of uncertainties involved in the prediction of future energy sources and aircraft fuel priorities. Likewise it is certain that interest in fuel property relaxation will continue, if only from the standpoint of increasing the options available in the event that sufficient incentive were to arise for the use of broadened-specification fuels. Consequently the issue is not one of predicting what will happen, but whether or not the options in the form of new technology are worth achieving.

The aircraft fuel compatibility issue can be categorized in three areas: (1) the airframe, which primarily concerns tank heating to accommodate increased fuel freezing point; (2) the combustor, which is concerned with higher metal temperature, durability, and emissions; and (3) the engine fuel system, which influences both the airframe and combustor and has its own unique problems.

Considering shale oil as an example, the first problem is low hydrogen content which increases smoke in the combustor and results in higher metal temperatures. In order to minimize this problem and also as a consequence of the processing of shale crude to form clean distillates, hydro-treating is used. Hydro-treating removes natural impurities and sulfur, of which relatively little is present in shale in the first place. The result is a fuel that, though clean, may have low lubricity. Gear-type fuel pumps are already known to experience rapid wear when used with hydro-treated fuels. The centrifugal pump used in the Advanced Fuel System would be inherently immune to this problem.

The second problem with shale oil is its high nitrogen content. Nitrogen increases fuel coking (thermal instability). Improving the combustor nozzle design and moving mechanical valves out of the hot combustor environment is one way to improve this situation.

A way around this problem is the valve design used in the LWFDS program and shown in Figure 4.18-9. Conventional sleeve valves require close clearances to limit leakage. They may also require rotation as well as translation to avoid jamming. The newer shear-type valve design uses flat plates which are spring-loaded together. LWFDS valves of this type exhibit zero leakage, provide self-cleaning, and can ride over contaminants. Valve position feedback is easier with shear-type valves because linear transducers can be used instead of rotational transducers. Fuel flow rate for engine control purposes can be determined directly from metering valve position.

The third problem is high freezing point. The NASA/GE E^3 program identified and analyzed a form of waste heat recovery system which would provide aircraft tank heating in addition to sfc improvement. This system simply extends the heat transfer loop (between the hot engine bleed air used for air conditioning and the engine fuel) to the aircraft wing. On those rare occasions where tank heating is required, the system valves and controls direct heat input to tank fuel instead of engine fuel. Fast tank heating reserve is provided by switching momentarily from midstage engine compressor bleed to compressor discharge bleed. Figure 4.18-10 shows the tank heating capability of the WHRS. The freezing point of the fuel is assumed to correspond to Experimental Referee Broadened Specification (ERBS) fuel. The minimum allowable temperature includes a 5°F allowance required by the FAA.

Tables 4.18-1 and 2 summarize the benefits of this concept.

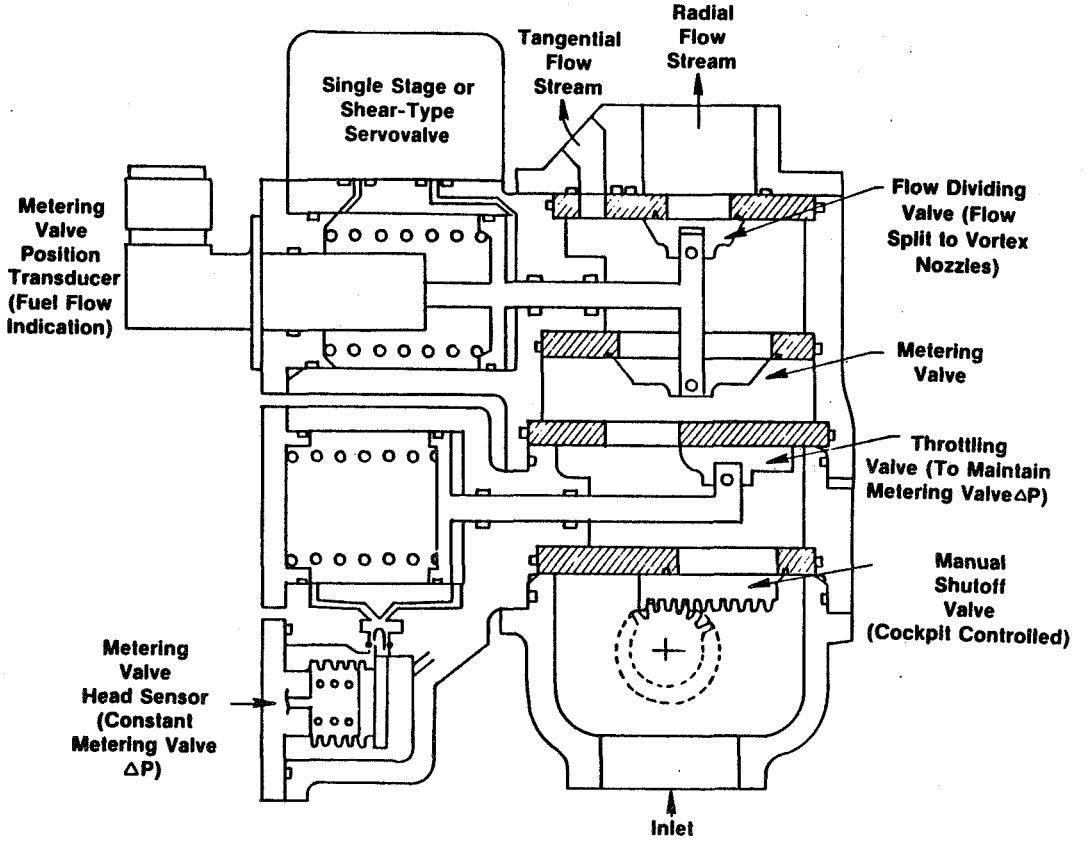
Radial Flow Stream
Tangential Flow Stream
Single Stage or Shear-Type Servovalve
Metering Valve Position Transducer (Fuel Flow Indication)
Flow Dividing Valve (Flow Split to Vortex Nozzles)
Metering Valve
Throttling Valve (To Maintain Metering Valve ΔP)
Manual Shutoff Valve (Cockpit Controlled)
Metering Valve Head Sensor (Constant Metering Valve ΔP)
Inlet

Figure 4.18-9. Fuel Metering Assembly with Shear-Type Valves.

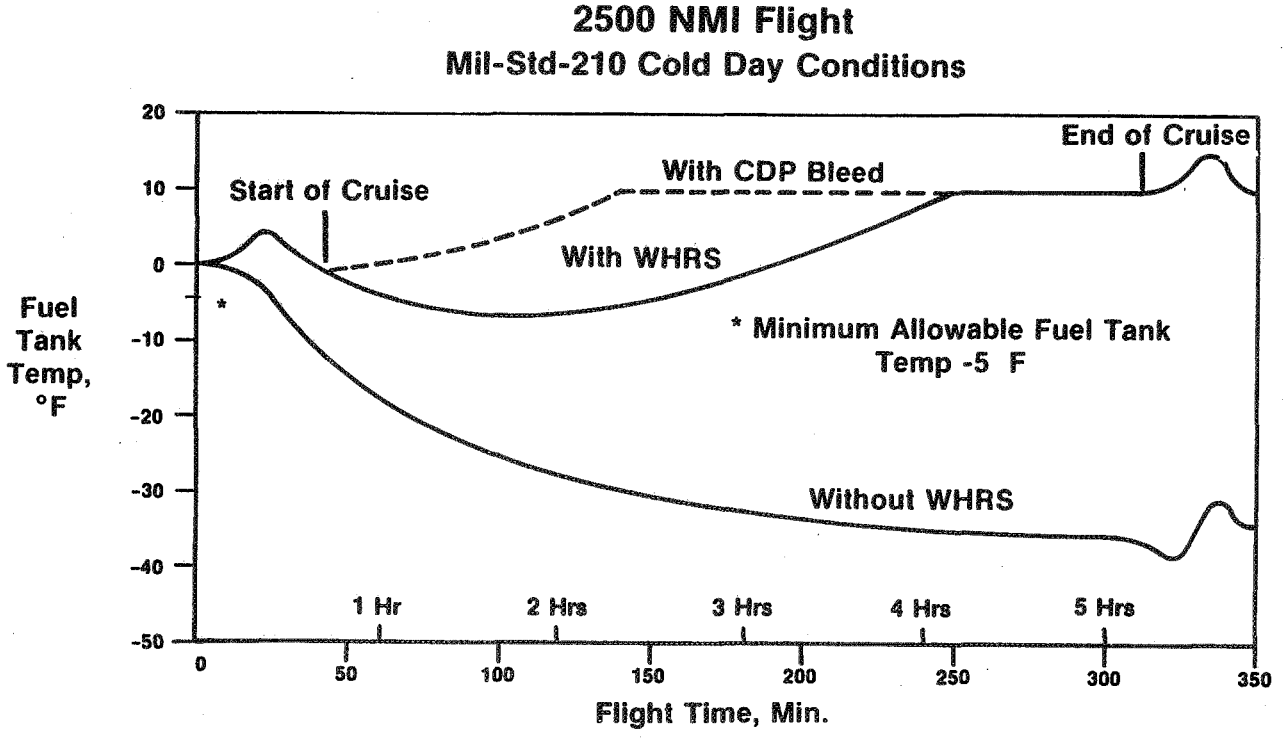

Figure 4.18-10. ECS Waste Heat Recovery System Tank Heating with High-Freeze-Point Fuel.

Table 4.18-1. Advanced Fuel Delivery System.

Benefits

- Permits Use of Broader-Range Fuel Properties
- Provides Heat Sink for Waste Heat Recovery and Reduced sfc

Barrier Problems

- Non-Conventional Pumps, Valves, and Fuel Nozzles

Probability of Success

- Design and Dev. - 95%
- Manufacturing - 95%
- Acceptance - 95%

Table 4.18-2. Advanced Fuel Delivery System Benefits.

Design Impacts	Direct	Secondary (Resizing)	Total
ΔWt., lb	-28 (+53)	0	-28 (+53)
ΔCost, $K	-6 (+13.6)	0	-6 (+13.6)
ΔMaint., $/Flight-Hour	0	N.A.	0
Δsfc, %	0 (-.8)	N.A.	0 (-.8)
Merit Factors	(-1.0) -.05 ΔW_f-%	(-0.8) -.11 ΔDOC-%	(43) 5.5 PW - $M
Ranking Factor		$1.1 \frac{P\ W\ \cdot\ Ps}{IDC}$ (8)	

( ) Including E^3 FPS Waste Heat Recovery System (WHRS) Without Fuel Tank Heating

4.19 ADVANCED SECONDARY POWER SYSTEM

4.19.1 Summary

This study was initiated to evaluate the feasibility and identify potential payoffs of an engine-mounted generator/starter concept which meets the requirements of the new-technology concept "all electric" airplane.

The rare-earth samarium cobalt (SmCo) permanent-magnet (PM) generator/starter extracts electric power from the high-pressure (HP) rotor of the main propulsion engine and also provides starting (motoring) of the turbofan engine. The electric power supply includes all secondary power for both the aircraft and the engine, including power normally used for hydraulic pumps and power supplied by bleed air. Among the objectives of this study were to establish the potential payoffs, feasibility, and conceptual configuration of the generator/starter, and to decide where to locate the electric secondary power system on the engine. The results of this study conclude that the external engine generator/starter (EEG/S) system is a feasible approach and offers potential advantages over today's typical secondary power systems (SPS). The primary potential advantages of the EEG/S system over conventional SPS are:

- Higher engine efficiency through the elimination of customer bleed air. This advantage will increase with the future trend toward higher-bypass-ratio turbofan engines.

- Higher reliability through the elimination of engine-mounted accessories like pneumatic starters, air start valves, hydraulic pumps, constant-speed drives, and equipment associated with these items. Increased reliability of the solid-rotor PM machine construction over conventional wound-rotor generators.

- Less maintenance, because there would be only one type of secondary power, thereby reducing the amount of conversion and distribution equipment and eliminating the possibility of leaky hydraulics.

- Easy accessibility (maintainability) for LRU replacement of engine-gearbox-mounted generators and engine accessories.

- Better access to the engine periphery due to elimination of hydraulic pipes, the elimination of starter air ducts, and a reduction in the number of accessories.

- Easier packaging and mounting of the accessory unit because of its smaller size.

The weight of the EEG/S system compared to the conventional SPS constitutes a weight penalty of about 150 lb per engine for a dual ac/dc system that would include the cycloconverters. However, it is the weight of the total aircraft system, with its associated distribution system and end-user equipment, that determines the overall system weight payoff (or penalty) compared to conventional aircraft.

A determination of the overall effect and payoff of the electrical secondary power generation system, therefore, cannot be made by the engine designer or electrical system designer, and requires the support of the aircraft manufacturers. The feedback received from the aircraft manufacturers focuses on the following EEG/S advantages:

1. The elimination of titanium ducts in the nacelles, pylons, wings, and fuselage.

2. A significant cost and weight reduction accompanying the elimination of the titanium ducts.

3. An impressive reduction in long-range mission fuel, resulting from the elimination of customer bleed demands on the engine.

4. A higher degree of operational flexibility and efficiency, resulting from an all-electric environmental control system (ECS) using motor-driven compressors.

5. A synergistic relationship between the demands of ECS and engine starting. The enlargement of the generator to meet the ECS power requirements puts the generator in the right ball-park as a generator/starter for the engine.

6. The elimination of the pneumatic start system and its components.

7. The elimination of a major hydraulic system (with the problems of leakage, contamination/maintenance support, etc.) and its necessary design/test hours.

8. The elimination of acquisition costs, labor/material costs, and installation costs associated with 7.

9. Reduced engine installation/removal time (due to a single electrical umbilical).

10. Opportunity for using 60 Hz and/or 400 Hz ac for ground power support.

11. Reduced logistic support and reduced capital-investment in ground power facilities.

The EEG/S system for the E^3 consists of two 150 kVA channels per engine.

The two SmCo generator/starters are mechanically connected to the HP rotor and run at 24,000 rpm at takeoff conditions.

The power delivered would be either 115/200V 400 Hz ac, 270V dc, or both.

The study demonstrates the feasibility and good potential of the electric secondary power system as applied to high-bypass turbofans and the all-electric airplane.

4.19.2 Introduction

Studies by the major aircraft companies on the subject of the "all-electric" airplane concluded that the concept is feasible and offers substantial advantages in manufacturing cost, operating cost, overall weight, and maintainability/reliability.

The development of high-energy permanent magnets of the rare-earth cobalt type has made high-power generators and motors attractive for aircraft secondary-power generation and user equipment.

The General Electric Company has recently completed a study under USAF Contract F33615-77-C-2018. This study consisted of integrating a generator/starter internally on the engine rotor shaft, providing both secondary electric power and engine starting. The integrated engine generator/starter (IEG/S) has been analyzed and conceptually designed for three power levels and three engine categories. The preliminary layouts and supporting analysis of the rare-earth, permanent magnet (PM) machine concluded that the IEG/S concept is a technically feasible approach to secondary power extraction and engine starting. One advantage to this approach is the potential for eliminating the engine gearboxes.

Variable Speed Constant Frequency (VSCF) Starter/Generator Systems using samarium cobalt (SmCo) machines have been developed by the General Electric Company. A 150 kVA PM Starter/Generator - VSCF System using rare-earth SmCo magnets was developed for the Air Force. The operation of this system was successfully demonstrated in early 1978.

The success of the 150 kVA PM effort resulted in a major follow-on program with 60 kVA starter/generator units which are to be flight-tested on the A-10 aircraft. This program was initiated in August 1978 and will culminate in an extensive one-year service test beginning in 1982.

4.19.3 Design Objectives

The objectives of this study are to investigate and define the applicability, optimal location, and conceptual configuration of rare-earth SmCo permanent-magnet generator/starters for secondary power generation. In addition to the functional and performance aspects of the secondary power generator system, considerable attention shall be given to maintainability, reliability, and system safety.

4.19.4 Design Requirements

This study considers the twin-engine airplane with the E^3 FPS engine as the base for all investigations. The power requirements of two 150 kVA generators per engine were specified by both Boeing and Lockheed. The overload capability of the generators for short periods of time is:

1.5 x 150 = 225 kVA for 5 minutes

2 x 150 = 300 kVA for 5 seconds

This capability also applies for starting considerations.

Electric engine starting time shall be equivalent to pneumatic starting.

4.19.5 Technical Discussion

4.19.5.1 Electric System

The PM SmCo generators developed by General Electric on the previously mentioned USAF programs would be excellent for use in high voltage dc systems as well as for operation with cycloconverter-type starter and ac generating systems. The choice of the type of power to be employed in the aircraft is very much a function of the total aircraft system requirements. Tradeoffs must be made considering the effects on the aircraft utilization equipment, the power distribution system, and overall reliability, size, weight, and cost. In any case, the engine gearbox/generator interfaces are largely the same: high pad speed (12,000 to 24,000 rpm) and an integrated system for cooling and lubrication. A number of recent studies have been made on aircraft systems employing high voltage (270V) dc as the primary power source. From a generating system point of view, the power conditioner required for converting the generator output to dc would be simpler than the conditioner required to convert the output to three phase, 400 Hz. This advantage may be largely offset if the generator is to be used as a starter, since the power conditioner employed must be capable of performing the start function. If a cycloconverter is used for this purpose, there is little additional penalty to using the system in both the start and ac generate modes, since power can be handled in either direction. Figure 4.19-1 shows a hybrid electric power system for both ac and dc power supply.

4.19.5.2 Comparison of Design Concepts

Secondary electric power generation by mechanical extraction from the main engine has been considered by two methods:

1. Integrating the generator/starter into the HP rotor system of the engine.

2. Using a shaft-driven externally mounted generator/starter.

Integrated Engine Generator/Starter (IEG/S) - The optimum location of the IEG/S in a high-bypass turbofan engine is in the forward sump area (between fan and compressor) of the engine, as shown in Figure 4.19-2. The PM machine rotor is mounted directly onto the HP-shaft extension. The generator stator is supported by the fan casing and is cooled by engine oil. Engine protection is provided in the form of an electric (fused) safety disconnect. In a military application, the best potential for the IEG/S concept is in a high-performance military aircraft with near-sonic or supersonic operation. The elimination of the accessory gearbox from low-bypass engines or pure jets (single spool) usually results in a frontal area reduction in fuselage or nacelle, thereby reducing drag and improving the overall aircraft performance.

The absence of those characteristics in dual-spool high-bypass engines (E^3) for commercial aircraft makes the IEG/S concept less attractive and makes options like gearbox-driven PM generator/starters look more favorable, especially where two generators are required per engine.

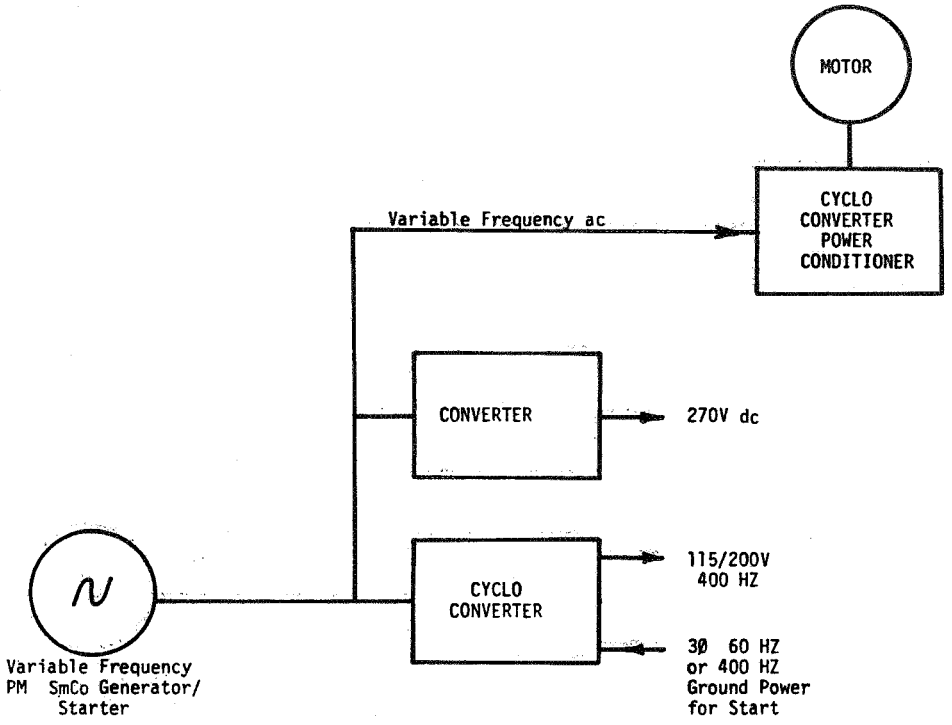

Figure 4.19-1. Hybrid Electric Power System.

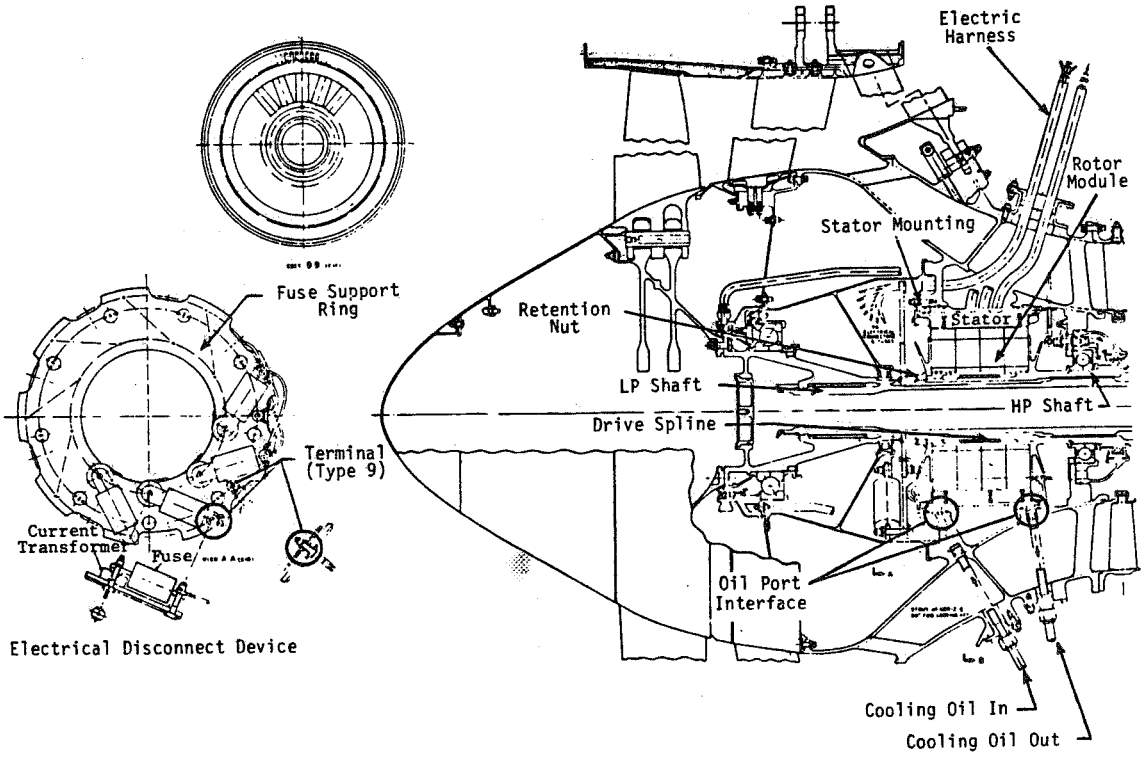

Figure 4.19-2. Integrated Engine Generator/Starter.

External Engine-Mounted SmCo Generator/Starter (EEG/S) - This arrangement, shown in Figure 4.19-3, allows the selection of optimum generator speed and provides good accessibility, redundant (dual) system option per engine, and the application of present state-of-the-art PM machines with minimum development risk.

Two PM generator/starters and engine accessories (fuel and lube pump) are driven from a core-mounted gearbox which is located in the area between the fan-bypass duct and the compressor casing aft of the fan frame.

This hybrid accessory power system was selected as the best candidate for reliable operation, high efficiency, and minimum weight. (The use of electric motors to drive pumps adds weight.)

4.19.5.3 Description

Figure 4.19-3 shows the mechanical arrangement of the accessory drive system located in the six o'clock position aft of the fan frame. The accessory package is enclosed in a cavity which is accessible from below through the cowl doors.

Figure 4.19-4 shows the packaging arrangement and pad speeds of the two 150 kVA SmCo generator/starters and the engine accessories driven by the auxiliary gearbox (AGB).

The dual electric system, which seems favored by the aircraft companies for use on the twin-engine E^3 airplane, is shown in Figure 4.19-5 for one engine.

Power Generation - Several types of electric power systems can be used with a variable-frequency output source resulting from the varying shaft speed of the PM generator.

The system schematic presented in Figure 4.19-5 will serve as a working base for a 150 kVA system having an 80 percent 270V dc power supply, a 20 percent 400 Hz ac power supply, and a 30 kw variable-frequency ac supply that will go to the environmental control system. The actual schematic will depend on the electrical system ultimately selected by the customer. That is, the schematic will depend on whether the system is to use dc power, ac power, or both; and if both, will depend on the ac/dc ratio.

Starting - Ground starting is accomplished by connecting the converter to either a 400 Hz power source from a start-cart or a three-phase 60 Hz current from a wall plug.

The starting capability is provided by the application of power from the converter to the generator output windings. Sensors (Hall probes) are used to detect the angular relationship between the rotor poles and phase windings, functioning as the commutator, such that power can be applied to the proper phase to achieve the required engine starting torque.

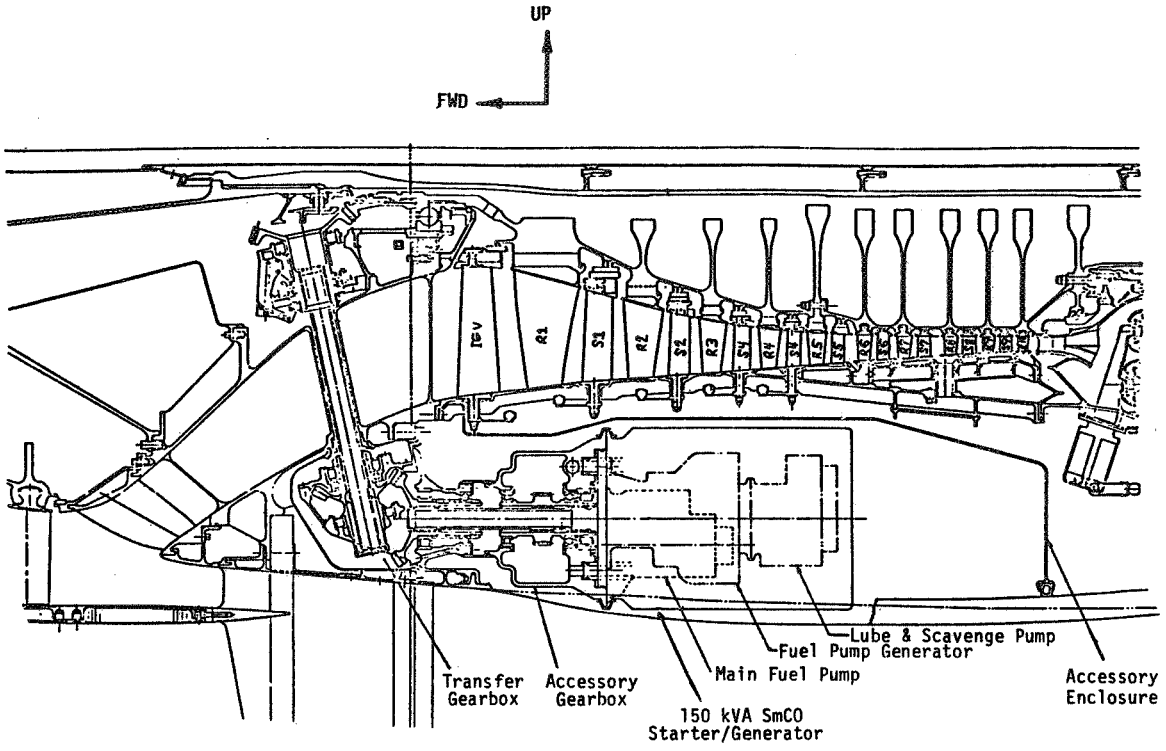

Figure 4.19-3. Mechanical Arrangement of Accessory Drive System.

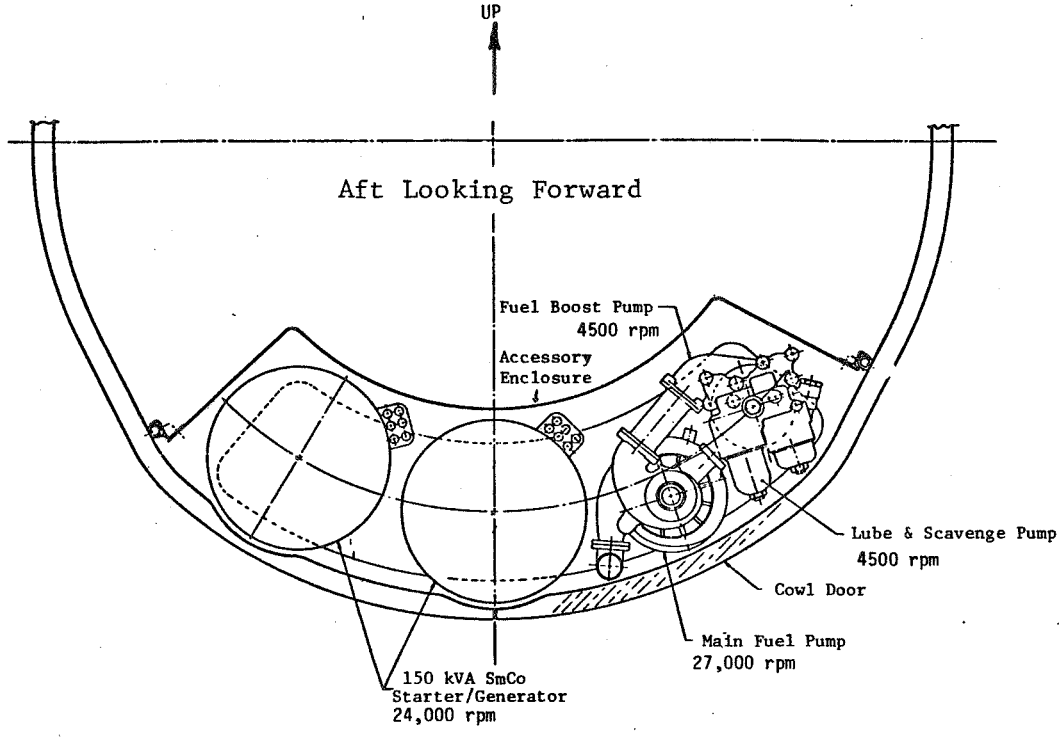

Figure 4.19-4. Packaging of Generator/Starters and Engine Accessories.

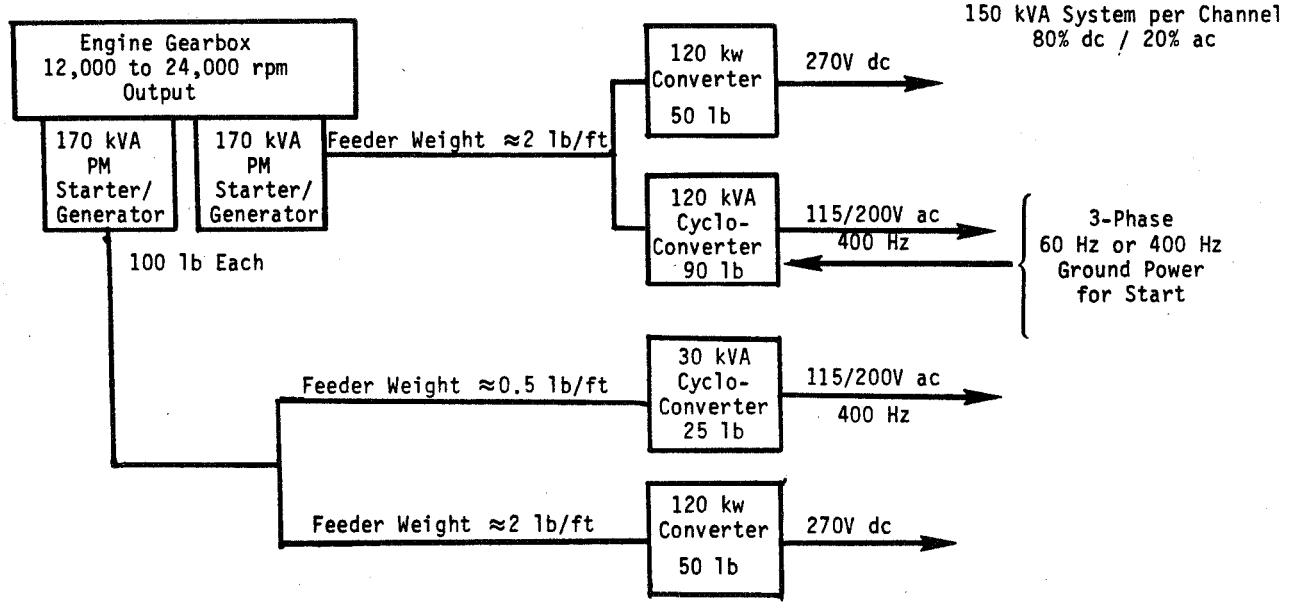

Figure 4.19-5. Post-E^3 SPS Configuration for One Engine.

The PM machine functions as a brushless dc motor and provides starting of the E^3 engine. A 120 kVA start system was assumed to be adequate for starting the E^3 FPS engine in 35 seconds. This assumption, however, has to be verified by analysis.

The PM machine/cycloconverter combination provides the capability to generate power as well as to perform engine starting in the air. The type of starting under consideration is a cross-start whereby one channel of the electrical system provides the essential electrical bus power as well as the electrical power to start the engine.

4.19.5.4 Description of Interface Between Selected Generator/Starter and Engine

The PM generator/starter is an oil-cooled 150 kVA generator/starter similar to the one developed under Air Force Contract F33615-74-C-2037. Thus, the concepts in design and manufacturing techniques have been established from test and/or operational experience with rare-earth/cobalt permanent magnet Variable Speed Constant Frequency (VSCF) generator/starters.

The generated voltage and power output are functions of speed. Therefore, the generator is designed to be capable of delivering rated load over the speed range of 12,000 to 24,000 rpm and meeting overload requirements at the base (idle) speed. At higher speeds the generator has the capability of delivering power exceeding specification requirements.

The winding is cooled by engine oil circulated in discrete channels around the stator frame.

This type of starter/generator is considered inherently more reliable than conventional, wound-rotor-type ac generators since the generator does not contain rotating windings, eliminates the use of rotating rectifiers, has but one output winding, and is simplified by using substantially fewer parts.

A cross-sectional view of this generator/starter, with identification of components as referenced and described herein, is shown in Figure 4.19-6.

The rotor is a 14-pole ring segment design with seven ring segments, each 1.00 inch long and 6.50 inches in diameter. Each segment is constructed to contain the permanent magnets and the metallic members and to provide the required magnetic path and mechanical strength. The ring segments are aligned and assembled onto a shaft and held in place with a shrink collar.

4.19.5.5 Safety Disconnect

Because a permanent-magnet machine lacks excitation control, there is no way to turn off the excitation when a fault occurs. Faults in the cycloconverter and at the output terminals of the converter can be disconnected within the converter. Faults in the high-frequency cables between the input terminals of the cycloconverter and the generator, as well as faults within the generator, cannot be deenergized without special devices. The disconnect is especially

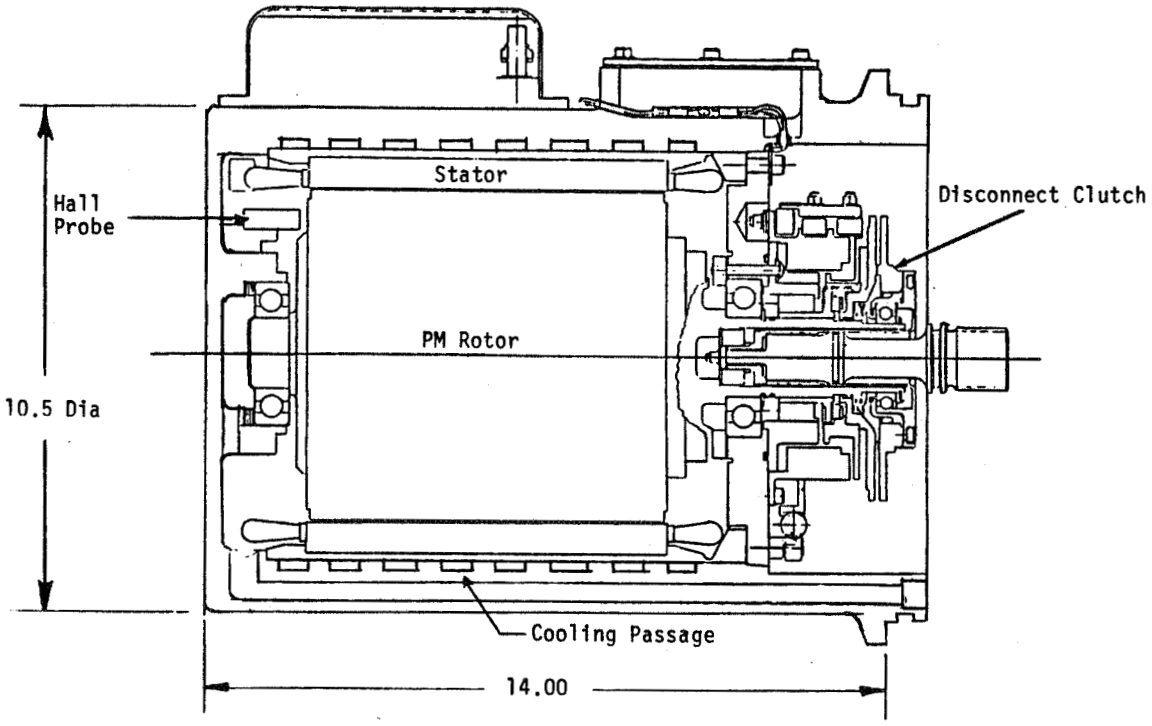

Figure 4.19-6. 150 kVA SmCo Starter/Generator Cross Section.

required in a PM machine, where in the event of an internal machine fault or feeder fault, the electrical power output must be interrupted without affecting normal engine operation. Maximum short-circuit current levels for a short at the generator terminals can reach five per unit for a symmetrical three-phase short and up to nine per unit for an unsymmetrical fault (that is, a line-to-neutral short), creating tremendous heating. In order to limit the time duration of these short-circuit currents, a means to interrupt, eliminate, or reduce the short-circuit currents must be included within the system.

The disconnect could be either an electromagnetic-actuated mechanical clutch such as the one used in the 150 kVA USAF development program, or another suitable type of clutch which would disconnect the generator rotor from the drive shaft at the time of failure detection.

4.19.6 System Comparison

The EEG/S system will be compared to the baseline E^3 FPS accessory configuration.

4.19.6.1 Weight

It is assumed that the accessory drive system weight would be the same for both configurations. This weight is therefore not entered into the comparison. A weight comparison with the baseline is shown in Table 4.19-1.

4.19.6.2 Reliability

Only items which differ from one system to the other are compared in Table 4.19-2.

The E^3 EEG/S accessory system has less than one-fifth the replacement occurrence of the baseline.

4.19.6.3 Efficiency

Figure 4.19-7 shows a comparison of the power extraction efficiency using airbleed versus mechanical shaft power. The values shown are the specific fuel consumption penalties at cruise for the E^3 bypass ratio. It can be seen that the use of mechanical shaft power extraction is the approach that allows the more efficient fuel consumption. If concern over sfc drives bypass ratios higher in the future, power extraction penalties imposed by bleed will become more severe. For example, a 1.8 lb/sec airbleed from the fifth-stage E^3 compressor is equivalent to 300 hp. If this 300 hp would be extracted by mechanical shaft power, the result would instead be a net improvement of 1.5% in Δ sfc at cruise. Therefore a substantial improvement in engine sfc results from the implementation of the electric secondary power extraction system by eliminating or reducing bleed air from the engine.

Table 4.19-1. Weight Summary, Baseline and EEG/S.

Baseline - E^3 FPS	Weight (lb)	E^3-EEG/S	Weight (lb)
FADEC (2)	20	FADEC (1)	12
--	--	Fuel Boost Pump	6
Main Fuel Pump	18	Main Fuel Pump (Centrif.)	22
Fuel/Oil Heat Exch.	9	Fuel/Oil Heat Exch.	9
--	--	Fuel/Air Heat Exch. (EEG/S)	18
Fuel Control Valve	6	Fuel Control Valve	9
Overspeed Limiter	6	Overspeed Limiter	6
Lube Pump	17	Lube Pump	17
PM VSCF Generator, 90 kVA	80	PM Generator/Starter 150 kVA (2)	200
Cycloconverter, 90 kVA	75	ac Cycloconverter, 120 kVA (1) + 30 kVA (1)	115
Control Alternator	7	--	--
--	--	dc Converter, 120 kVA (2)	100
Hydraulic Pump (2)	59	--	--
Hyd. Tubing (Engine)	4	--	--
Air Starter	48	--	--
Air Starter Valve	16	--	--
Air Ducts (Starter)	6	--	--
Electrical Cable, 5 ft (1)	4	Electrical Cable, 5 ft (2)	10
Total	375	Total	525

ΔWeight = 150 lb penalty (over baseline) per engine

Table 4.19-2. Reliability of E^3 FPS vs. E^3-EEG/S - Replacements per 10^6 Hours.

Item	LRU'S*	Baseline E^3 FPS		E^3-EEG/S	
PM Generator	40	40		80	(2)
ac Cycloconverter Generation	80	80	(1)	--	-
dc Converter	60	--		120	(2)
ac Cycloconverter Start/Generation	100	--		200	(2)
Air Starter	179	179	(1)	--	
Air Start Valve	171	171	(1)	--	
PM Control Alternator	100	40		--	
Hydraulic Pump	890	1780	(2)	--	
Total Removals per 10^6 hours		2290		400	

* Line Replaceable Units

35K/0.8M/Std Day
Constant Thrust

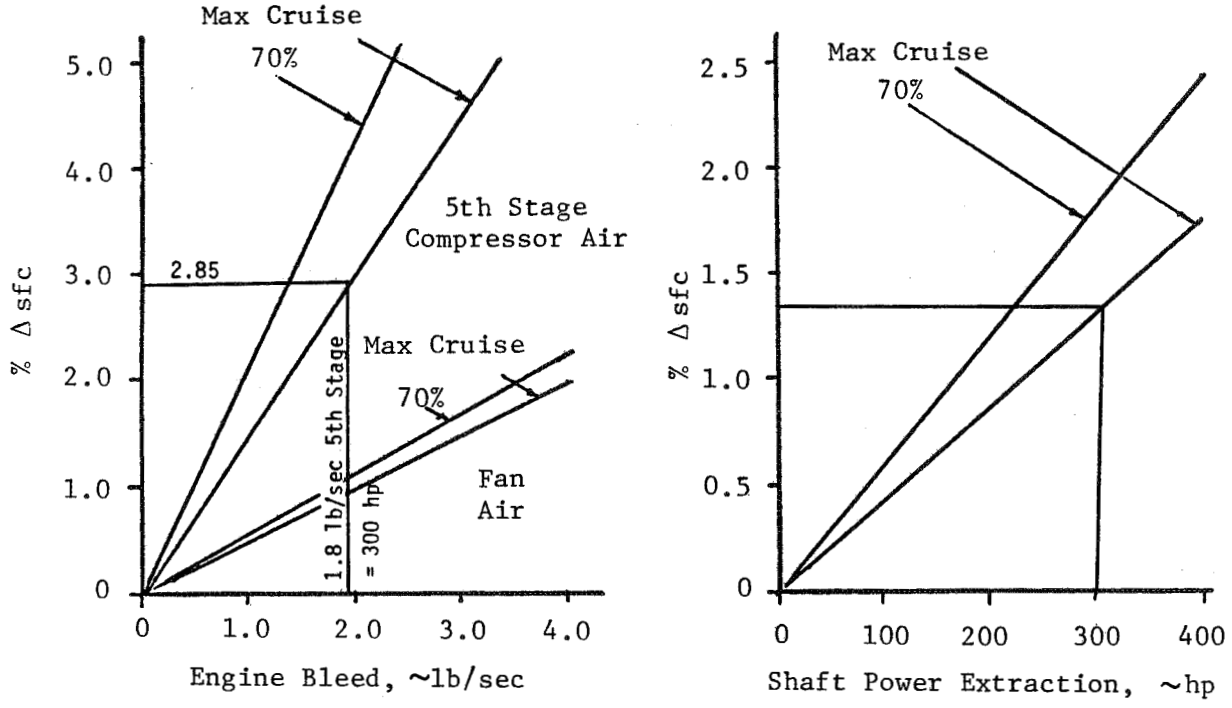

Figure 4.19-7. Bleed Air and Shaft Power Extraction Penalties on sfc for E^3 FPS.

4.19.6.4 System Payoff Comparison

The comparison does not include the total impact on the aircraft, which is beyond the scope of this study. The impact of replacing hydraulic lines and actuators with larger-sized electrical cables and electric motors is not included. More accurate comparisons do require consideration of the impact on the total aircraft and require the participation of the airplane designer in the study.

In Table 4.19-3, major design characteristics that affect the engine alone (as opposed to the airplane) are compared for the baseline engine and the E^3 engine equipped with an electric secondary power system. Containment of the generator rotor was not addressed but needs to be studied. The benefits of this concept are summarized in Table 4.19-4.

Table 4.19-3. System Payoff Results - Comparison Between Baseline and E^3-EEG/S.

	Baseline	E^3- EEG/S
Weight	Base	+150 lb
SPS Reliability MTBF (hours)	436	2500
Engine Δ sfc % - Bleed Air Elimination	Base	1.0 to 1.5% improvement
Maintenance	Base	Less

Table 4.19-4. All-Electric Aircraft Engine SPS Benefits.

Design Impacts	Direct	Secondary (Resizing)	Total
ΔWt., lb	150	-47	103
ΔCost, $K	+25	-10	15
ΔMaint., $/Flight-hour	-.10	N.A.	-.10
Δsfc, %	-1.5	N.A.	-1.5
Merit Factors	-1.9 ΔW_f-%	-1.5 ΔDOC-%	81 PW - $M
Ranking Factor	$\frac{57 \text{ PW} \times \text{Ps}}{\text{IDC}}$		

4.20 EXHAUST NOZZLE LOAD ISOLATION AND ALIGNMENT JOINT

BACKGROUND

Propulsion systems must frequently provide thrust deflection for vertical or short takeoff and landing operations and/or in-flight maneuvering. In such instances, it is generally desirable to transfer nonaxial thrust loads to the aircraft by means of a mounting point at or near the plane of thrust deflection. With a relatively long afterburner-type engine and a conventional two-point mount system, either the compressor overhang or the distance between fore and aft mounts becomes quite large. This results in an inordinate increase in weight to stiffen the engine to the extent necessary to prevent loss of clearances and rubs between static and nonrotating engine components under normal load conditions.

An alternate approach to the problem of long spans or overhangs with excessive engine bending is to retain the conventional two-point mount system on the gas generator and add a third mount point to accommodate the nonaxial thrust loads. A typical problem, however, is that the third mount point is usually located near the aft end of the aircraft fuselage or near the trailing edge of the wing, where the aircraft structure is relatively "soft" or flexible with respect to the forward engine mount points; this, in turn, imposes an indeterminate bending moment on the engine. The solution is to incorporate a higher degree of flexibility in the engine structure by means of a flexible joint such that all of the nonaxial thrust loads are transmitted to the aircraft via the third mount point. This requires a knowledge of the aircraft deflections under various loads.

In addition to those installations that require thrust deflection, there are instances where it is desirable to maintain a close alignment and/or minimum clearance between the exhaust nozzle and adjacent aircraft structure. An example might be the need to maintain aerodynamic alignment of the exhaust flow over or under a surface of the wing to provide lift enhancement. With a suitable lightweight flexure joint, consideration could be given to attachment of the exhaust nozzle exit to the aircraft structure to maintain the desired alignment.

TECHNICAL CONCEPT

The conventional approach to a flexible joint for industrial piping is to utilize a bellows with pivot- or gimbal-type structures to transmit axial loads. Since the bellows transmits little or no load itself, the resultant joint is heavier than desired for aircraft engine applications. In addition, the bellows is subject to a variety of distortions and failure modes.

A promising approach to a flexible joint in gas turbine exhaust systems is shown in Figures 4.20-1. The figure illustrates the application of the flex joint to a typical deflected-thrust system with a soft mount aft of the conventional engine mounts. The flexible joint is essentially a portion of a spherical ball-type joint. Since the two mating spherical surfaces are rotatable with respect to each other, both torsional rotation and angular deflection of the exhaust system can be accommodated.

At present, the design is limited to metal temperatures in the 300-500° F category, such as would be found in the afterburner of a mixed-flow turbofan engine like the F404. This limitation is established by the requirement for low surface friction which is provided by the coating. A low surface friction is very important since the magnitude of the moment transmitted across the flange is a function of the coefficient of friction of the flange rubbing surfaces, the ΔP across the duct, and the cube of the radius of the duct.

CONCEPT DEVELOPMENT

In anticipation of a future urgent need for a lightweight flexible joint such as described above, a one-third-scale model of an F404-size joint was designed and fabricated to investigate the feasibility of a low-friction joint under simulated ΔP conditions.

The resultant one-third-scale model has been hydrostatically proof-tested at flange loads equal to those found on the F404, and torque measurements have been made at internal pressure loads comparable to those which would be experienced during VTOL operations. These limited tests have indicated that low friction and the desired flexibility were attained, warranting further development.

The next step in the development of this flexure joint is to design, fabricate, and test flight-weight, full-size hardware under representative engine operating conditions.

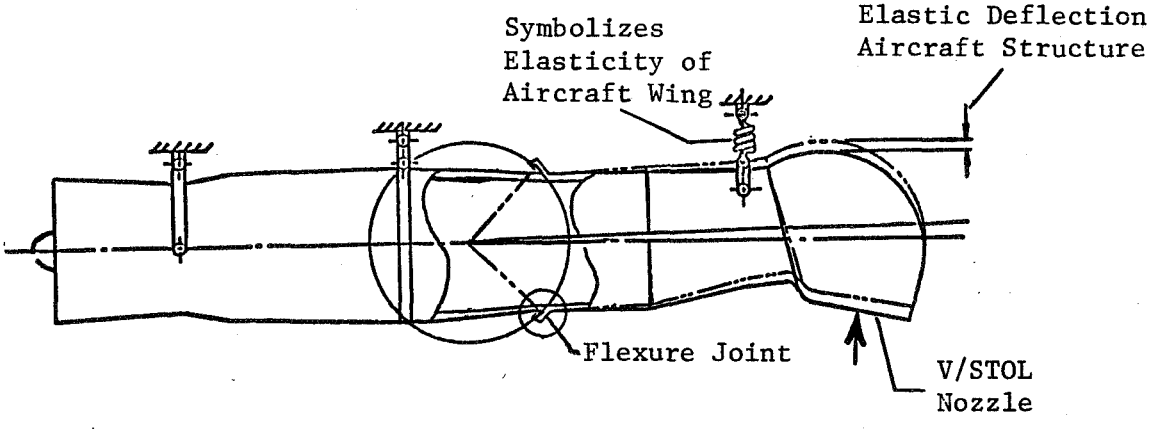

Figure 4.20-1. Spherical Flexure Joint for Three-Mount Engine Systems.

5.0 RECOMMENDED TECHNOLOGY PROGRAMS

5.1 SUMMARY

The advanced technology concepts which have significant payoff beyond the E^3 FPS were discussed in Section 4. The programs for these recommended technologies are presented here. To facilitate cross referencing, the program identification numbers in this section are essentially common with those of Section 4.

The common format includes the program title, objectives, major tasks, and schedule. The potential payoffs for developing each concept are shown as (a) the fuel savings per aircraft year year, (b) the present ΔDOC reduction, and (c) the present-worth ranking parameter. The estimated probability of successfully developing and incorporating the concept is also included.

The recommended structural and life analysis technology programs are presented separately in Section 6.

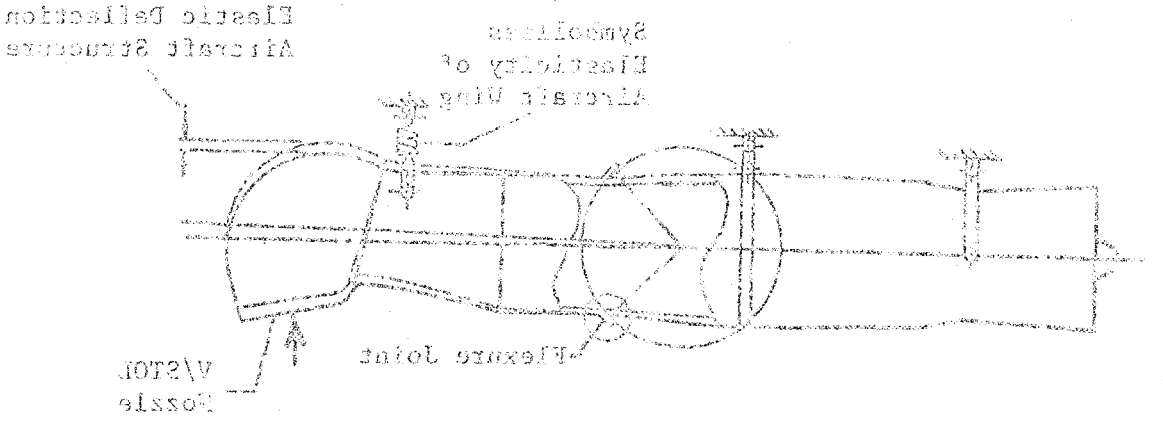

Program Title: HPT Metal Cooling Improvements

Identification Number 5.2

Objective: Increase cooling air effectiveness.

Potential Payoff

a) Gal. Fuel Savings Per Aircraft Per Year 47,000

b) % Δ DOC -1.2

c) PW x Ps / IDC 58

Tasks

Schedule, Months

- Select Technology and Assess Payoff
- Assess and Test Configuration Changes
- Assess and Test Heat Transfer
- Test and Demonstrate in Engine

Elapsed Time 3 Yrs.

Probability of Success 90%

Identification Number 5.3

Program Title: HPT Modulated Cooling Flow

Objectives: Develop hardware and control system to modulate HP turbine cooling air.

Potential Payoff

a) Gal. Fuel Savings Per Aircraft Per Year 36,000

b) % Δ DOC -.8

c) PW x Ps / IDC 40

Schedule, Months

Tasks

- Define Strategy and Requirements
- - Design and Build
  - Modify E^3 to Accept
- Bench Test
- Engine Test

Elapsed Time 2 Yrs.

Probability of Success 95%

Program Title: HPT Metal Temperature Improvement

Identification Number 5.4

Objective: Increase temperature capability of hot-section materials by 100^{0} F.

Potential Payoff

a) Gal. Fuel Savings Per Aircraft Per Year 153,000

b) % Δ DOC -4.7

c) PW x Ps / IDC 41

Tasks

Schedule, Months

- Metallurgical Studies
- Pilot Material Pour and Bar Test
- Develop Coating
- Pilot Airfoil Fabrication and Bench Test
- Engine Airfoil Fabrication and Test

Elapsed Time 5 Yrs.

Probability of Success 70%

Program Title: Metal Coating Improvements

Identification Number 5.5

Objectives: Improve life and temperature capabilities of hot-section coatings.

Potential Payoff

a) Gal. Fuel Savings Per Aircraft Per Year 31,000

b) % Δ DOC -.75

c) PW x Ps / IDC 17

Tasks

Schedule, Months

- Select Coating Candidates
- Comparison Bench-Test Candidates Select Prime Candidates
- Hot Rig Test Airfoils Coated with Prime Candidates
- Coat Engine Hardware and Engine Tests

Elapsed Time 3 Yrs. Probability of Success 65%

Program Title: Shortened Fan Flowpath

Identification Number 5.6

Objective: Develop shortened fan configuration to save weight and cost and improve performance.

Potential Payoff

a) Gal. Fuel Savings Per Aircraft Per Year 20,000

b) % Δ DOC -.85

c) PW x Ps / IDC 16

Tasks	Schedule, Months
• Conduct Detailed Design Studies	6
• Develop Shortened Fan Frame Technology	18
• Demonstrate Technology by Engine-Testing Potential Technical Barriers	6
• Fan Frame Design/Stiffness	___

Elapsed Time 24

Probability of Success 90%

Program Title: HP Compressor Active Clearance Control

Identification Number 5.7

Objective: Provide an improved method for clearance control using fan air.

Potential Payoff

a) Gal. Fuel Savings Per Aircraft Per Year 5800

b) % Δ DOC -.34

c) PW x Ps / IDC 15

Tasks

Schedule, Months

- Conduct Detailed Design Study
- Demonstrate Heat-Transfer/Design Adequacy on Rig Test
- Build Engine Hardware and Test

Elapsed Time 24

Probability of Success 85%

Program Title: Advanced Fan Blade

Identification Number 5.8

Objectives: Identify and develop lightweight fan blade.

Potential Payoff

a) Gal. Fuel Savings Per Aircraft Per Year 24,000

b) % Δ DOC -.88

c) PW x Ps / IDC 5.8

Tasks

Schedule, Months

- Conduct Design Studies to Identify Most Promising Advanced Blade Designs
- Develop Analytical Tools for Evaluating Designs
- Manufacture Prototype Blades for Testing
- Transition Technology into Engine Hardware

Elapsed Time 3-4 Yrs

Probability of Success 60%

Program Title: Low-Emissions Single Annular Combustor

Identification Number 5.9

Objective: Develop single-annular combustor for anticipated 1984 EPA emissions standards.

Potential Payoff

a) Gal. Fuel Savings Per Aircraft Per Year 5000

b) % Δ DOC -.43

c) PW x Ps / IDC 11

Tasks

Schedule, Months

- Design
- Develop by Rig Test

Elapsed Time 3 Yrs.

Probability of Success 95%

Program Title: Compressor Blisks

Identification Number 5.10

Objective: Develop manufacturing technology for compressor blisks to achieve lower weight and reduced leakage.

Potential Payoff

a) Gal. Fuel Savings Per Aircraft Per Year 23,000

b) % Δ DOC -.56

c) PW x Ps / IDC 3.2

Tasks

Schedule, Months

- Conduct Detail Design Studies to Determine Blisk Configuration and Associated Weight/ Perf. Benefits
- Conduct Cost Analysis to Determine Lowest Manuf. Approach
- Assess and Develop Low-Cost Diffusion Bonded/ Pressure Bonded Disks
- Manuf. & Engine Test Compressor Blisk

Elapsed Time 36

Probability of Success 70%

Identification Number 5.11

Program Title: Composite Vanes

Objective: Apply composite vanes in E^3 engine for weight/cost benefits.

Potential Payoff

a) Gal. Fuel Savings Per Aircraft Per Year 5400

b) % Δ DOC -.28

c) PW x Ps / IDC 5.1

Schedule, Months

Tasks

- Conduct Design Studies to Identify Engine Configuration
- Manufacture Prototype Hardware for Bench Testing
- Conduct Piggyback Engine Testing

Elapsed Time 18

Probability of Success 85%

Program Title: Composite Spinner

Identification Number 5.12

Objective: Develop composite spinners for commercial use.

Potential Payoff

a) Gal. Fuel Savings Per Aircraft Per Year 500

b) % Δ DOC -.03

c) PW x Ps / IDC 3.9

Tasks

Schedule, Months

- Conduct Preliminary Design Studies
- Design, Build & Test Prototype Spinner
- Develop Composite Flange Attachment Techniques
- Build Full-Scale Engine Hardware for Testing

Elapsed Time 12

Probability of Success 90%

Program Title: Component Efficiency Improvement

Identification Number 5.13

Objective: Improve component efficiency.

Potential Payoff

a) Gal. Fuel Savings Per Aircraft Per Year 197,000 b) % Δ DOC -4.9 c) PW x Ps / IDC 8

Tasks

Schedule, Months

- Select Most Promising Components
- Evaluate Aero and Structural Potential Improvements
- Design, Build, and Rig Test

Elapsed Time 5 yrs. Probability of Success 80%

Program Title: Variable-Area Nozzle Mixed Flow

Identification Number 5.14

Objective: Develop a variable-area nozzle for a mixed-flow turbofan.

Potential Payoff

a) Gal. Fuel Savings / Per Aircraft Per Year — 18,000

b) % Δ DOC — -.12

c) PW x Ps / IDC — 7.6

Tasks

Tasks	Schedule, Months
• Select Aircraft and Mission	1
• Optimize and Design	2
• Mechanical System Model Tests	6
• Aero Model Tests	9 (Concurrent)
• Fabricate and Engine Test	12

Elapsed Time 24

Probability of Success 95%

Program Title: Turbomachinery 3D Aero Analysis

Identification Number 5.15

Objectives: Establish practical 3D aero analysis and computer code.

Potential Payoff

a) Gal. Fuel Savings Per Aircraft Per Year 11,000

b) % Δ DOC -.26

c) PW x Ps / IDC 7

Tasks

Schedule, Months

- Select Analytical Method
- Select Representation of Viscous Effects
- Develop Computer Code
- Aero Test Verification of Analysis

Elapsed Time 3 Yrs.

Probability of Success 50%

Program Title: LPT Flared Flowpath

Identification Number 5.16

Objective: Integrate LPT/frame/mixer aero design

Potential Payoff

a) Gal. Fuel Savings Per Aircraft Per Year 13,000 b) % Δ DOC -.17 c) PW x Ps / IDC 6

Tasks

Schedule, Months

- No Program Necessary - Is Being Incorporated into E^3 FPS

Elapsed Time 0

Probability of Success 100%

Program Title: LPT Orthogonal Blading

Identification Number 5.17

Objectives: Develop aero and structural technology for orthogonal blading in a low-pressure turbine.

Potential Payoff

a) Gal. Fuel Savings Per Aircraft Per Year 5300

b) % Δ DOC -.13

c) PW x Ps / IDC 2

Tasks

Schedule, Months

- Select Application - Turbofan or Turboprop Engine
- Conduct Studies, Analysis, and Design
- Air Turbine Test η Effect
- Structural Tests

Elapsed Time 3 Yrs.

Probability of Success 80%

Program Title: Advanced Fuel Delivery System

Identification Number 5.18

Objectives: Provide engine compatibility with broadened-specification and synthetic fuels.

- Increased Nozzle Coking Tolerance
- Low-Lubricity Fuel Compatibility
- Waste Heat Recovery and Fuel-Tank Heating Capability

Potential Payoff

a) Gal. Fuel Savings Per Aircraft Per Year 2000

b) % Δ DOC -0.11

c) PW x Ps / IDC 1.1 (10 with WHRS)

Tasks	Schedule, Months
• Establish Preliminary Design; Req'm.	9
• Detail Design, Fab., Test Components	24
• Manufacture System Test Hardware	9
• System Tests, Including Engine Transient and Steady-State Simulations Using Breadboard FADEC	21

Elapsed Time 60

Probability of Success 95%

Identification Number 5.19

Program Title: Secondary Power Generation System for the All-Electric Aircraft

Objectives: Design, develop, and test SPS with SmCo generator starter, including safety disconnect, dc converter, and cycloconverter, for commercial aircraft use.

Potential Payoff

a) Gal. Fuel Savings Per Aircraft Per Year 73,000

b) % Δ DOC -1.5

c) PW x Ps / IDC 57

Tasks	Schedule, Months
• Analysis and Preliminary Design	5
• Final Design of Mechanical, Electrical System	4
• Fabricate 3 Sets of Flight-Type Hardware Component and System Test	12
• Preflight Bench Test	3
Elapsed Time	24

Probability of Success 70%

Program Title: Exhaust Nozzle Load Isolation and Alignment Joint

Identification Number 5.20

Objectives: Demonstrate lightweight, flexible exhaust duct joint for isolating engine from bending moments induced by nonaxial thrust. Achieve critical aerodynamic alignment of exhaust nozzle relative to adjacent aircraft structures.

Tasks	Schedule, Months
• Model Tests of Joint	
- Pressure Test	Complete
- Vibration Test	Pending
• Full Scale - Flight-Weight Design, Fabricate and Rig Test	12

Elapsed Time 12

Probability of Success 90%

6.0 STRUCTURAL AND LIFE ANALYSIS PROGRAMS

Structural and life analysis programs are by nature generic and not necessarily associated on a one-to-one basis with the advanced design concepts identified in this report. A review of these advanced design concepts has resulted in the identification of thirteen needed analytical methods programs. The advanced design concepts are listed with their needed structural and life analysis technologies in Table 6.0-1. It is clear from this tabulation that, while five of the design concepts do not require further technology development, most of the remaining thirteen will need methods development in two or more areas. These structural methods needs are discussed below.

Table 6.0-1. Advanced Design Concepts and Required Structural Analysis Programs.

STRUCTURAL AND LIFE ANALYSIS PROGRAMS / ADVANCED CONCEPTS	HPT Metal Cooling Improvements	All-Electric Aircraft	HPT Metal Temp. Improvement	Modulated Cooling Flow	HPT Coating Improvements	Shortened Fan Flowpath	HPC A.C.C. - Fan Air	Single Annular Combustor	Component Efficiency Improvement	Variable A_8 Nozzle	3D Aero Analysis	Advanced Fan Blade, Fiber-Reinforced Ti, 1.5"	LPT Flared Flowpath	Composite Vanes	Composite Spinner	HPC Blisk, Bonded	LPT Orthogonal Blading	Advanced Fuel System
6.1 Improved Interface Between Heat Transfer and Stress Analysis	●		●	●	●		●	●	●				●				●	
6.2 Simplified Frame Analysis						●												
6.3 Verification of Airfoil Stresses and Deformations																	●	
6.4 Dovetail Design Verification Program	●		●									●	●				●	
6.5 Analysis Tools for Predicting Fabrication Effects	●		●													●		
6.6 Structural, Life Analysis, and Test Techniques For Coatings			●		●													
6.7 Anisotropic Turbine Blade and Vane Life Prediction			●															
6.8 Component Fatigue and Rupture Damage Measurement	●		●	●	●			●				●				●	●	
6.9 Extend Manson-Halford Damage Curve Life Analysis Methodology	●		●	●	●								●			●	●	
6.10 Incorporate Damping into Vibration Analysis of Fan Blades												●		●				
6.11 Time-Sharing Program for the Analysis of Turbomachinery Vibration						●	●											
6.12 Transient Blade-Out Modal Analysis						●	●						●			●		
6.13 Transient Analysis and Design Criteria for Engine Seizure Loads						●	●									●		

6.1 IMPROVED INTERFACE BETWEEN HEAT TRANSFER AND STRESS ANALYSIS

Thermal stresses are often life-limiting in gas turbine components; however, it is so tedious and time-consuming to transform temperature data calculated using heat-transfer analysis computer programs to the data input for finite-element stress analysis computer programs, that simplified and less-accurate temperature distributions are often used to minimize cost and project time. A major reason is the incompatibility of the finite-difference mesh used for a time-dependent heat transfer analysis and the finite-element mesh used for the time-independent stress analysis (Figure 6.1-1).

One possible solution is to substitute a finite-element analysis for the finite-difference heat transfer analysis. This would allow use of the same finite-element mesh for both analyses. The resulting analysis is in general more detailed and costly than necessary for the temperature calculation; it is also too coarse and hence insufficiently accurate for the stress analysis.

A more flexible solution is to use the computer to transfer the temperature data, making the necessary interpolations and the small corrections needed to account for the small discrepencies which usually occur between the two models.

As shown in Table 6.0-1, this program would greatly facilitate nine of the proposed technology concept programs by making possible more accurate predictions of thermal stress in the feasibility and design stages.

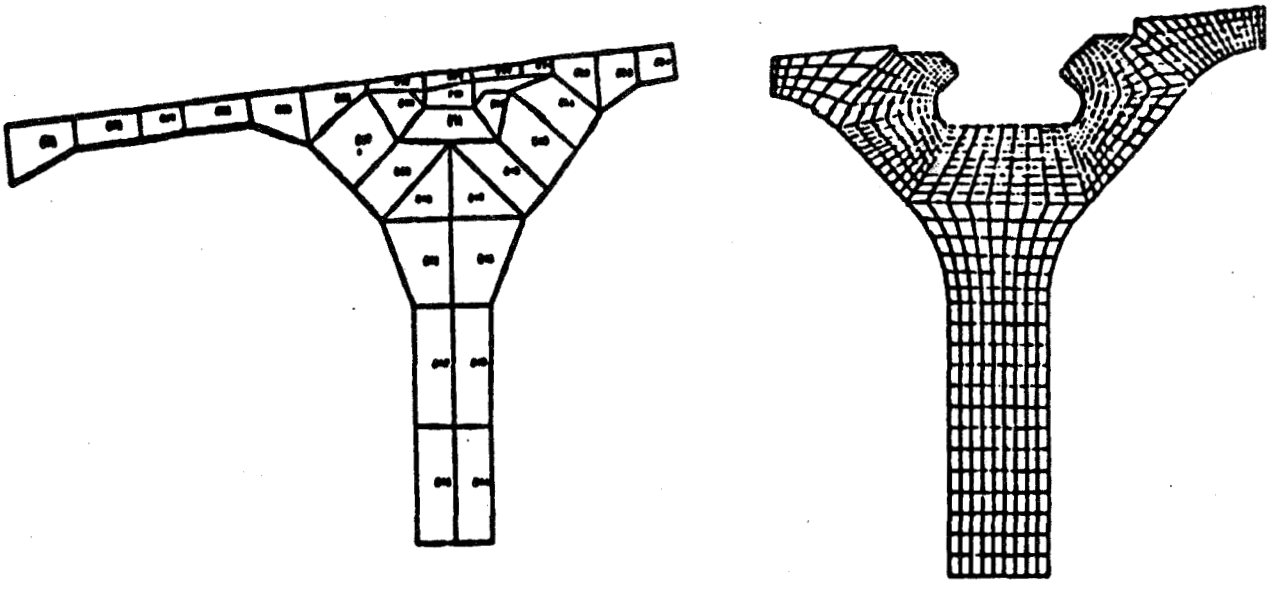

Heat-Transfer Model

Stress Model

Problem: Take temperature data from heat-transfer program and automatically generate temperature data required for thermal stress analysis when the two programs may use completely different meshes.

Significance: Large savings in man-hours currently required to set up thermal stress calculations, plus more accurate results than previous methods.

Figure 6.1-1. Automatic Interface Between Heat-Transfer Program and Stress Analysis Program.

Identification Number 6.1

Program Title: Improved Interface Between Heat Transfer and Stress Analysis

Objective: Eliminate the need for identical 3-dimensional thermal and stress finite-element models for greater analytical flexibility. The heat-transfer finite-difference model and the stress finite-element model can each be optimized independently. Also, mesh refinements in the stress model would no longer require rerunning the heat-transfer results.

Tasks	Schedule, Months
• Develop interface to perform consistent interpolation between different analytic meshes	6
• Program method for greatest computational efficiency	4
• Demonstrate on proposed designs for "Metal Cooling Improvements" task	2

Elapsed Time 12

Probability of Success 100%

6.2 SIMPLIFIED FRAME ANALYSIS

Successful development of a Shortened Fan Flowpath Program will require numerous feasibility and tradeoff fan frame structural analyses to optimize the design. This is not practical with current engine frame analysis techniques, which are laborious and costly, commensurate with the complexity of the structures being dealt with (Figure 6.2-1). Improved methods, verified by component structural tests, are vital to successful completion of the Shortened Fan Flowpath Program.

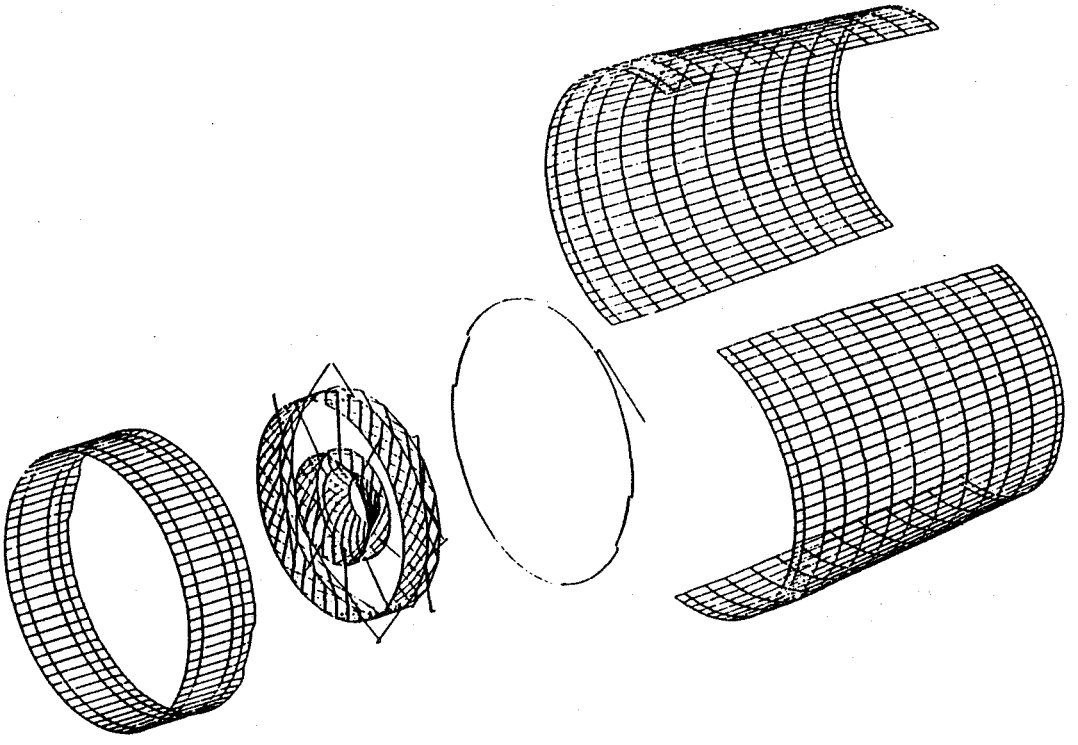

Figure 6.2-1. Fan Structural Analysis Model.

Program Title: Simplified Frame Analysis

Identification Number 6.2

Objective: Provide the designer with a simple way of evaluating frame stiffnesses and stresses, including the effect of the strut-ring joints and the surrounding casings. Currently these jobs require a considerable expense in both engineering labor and computer dollars.

Tasks	Schedule, Months
• Verify results from analytical model	10
• Program method as design tool	5
• Demonstrate use on proposed shortened fan flowpath design.	3

Elapsed Time 18

Probability of Success 95%

6.3 VERIFICATION OF AIRFOIL STRESSES AND DEFORMATIONS

Development of accurate stress analysis methods for fan, compressor, and turbine blades has been made possible by the development of three-dimensional finite-element methods. Although, in principle, any 3D configuration can be modeled geometrically, the resulting calculated stresses are often very inaccurate because of the inherent limitations imposed by the finite-element method, which approximates a continuous deformation field by a patchwork of "best-fit" assumed displacement functions. Consequently, development and verification of finite-element techniques, such as those used to successfully model the airfoil-platform junction shown in Figure 6.3-1, are needed to predict the efforts of shroud and shank flexibility, as well as friction effects. For a radical blade design, such as that needed for the Low Pressure Turbine Orthogonal Blading, these methods are essential.

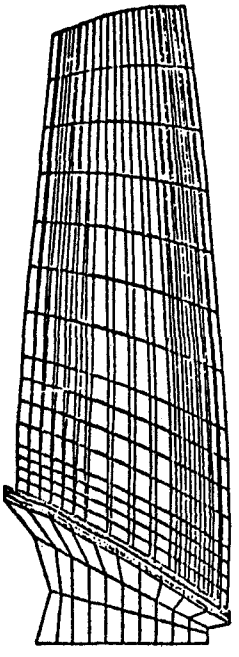

3D Finite-Element Model

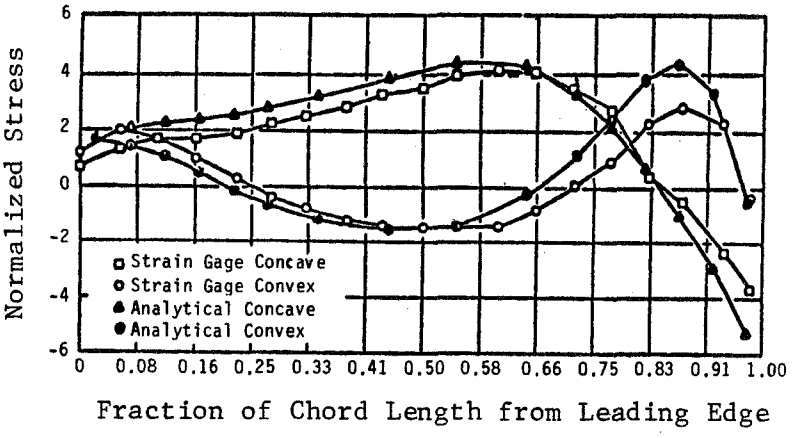

Fan Blade Stress Comparison

Significance: Techniques developed for joining airfoil to platform give us a demonstrated analytical method for prediction of end effect stresses.

Figure 6.3-1. Prediction/Correlation Fan Blade End-Effect Stresses.

Identification Number 6.3

Program Title: Verification of Airfoil Stresses and Deformations

Objectives: Establish and verify methodology to permit the analysis of 3D airfoils with shroud connections. Current limitations involve knowledge about friction effects as well as shank flexibility. Also, correct solutions tend to be extremely expensive.

Tasks	Schedule, Months
• Outline finite-element modeling scheme to include shroud connection	6
• Verify from existing engine data	3
• Identify significant parameters	3
• Determine and program method for reduced costs	6

Elapsed Time 18

Probability of Success 90%

6.4 DOVETAIL DESIGN VERIFICATION PROGRAM

Dovetails represent yet another complex three-dimensional configuration for which easily applicable and experimentally verified analysis methods do not exist. Development of these methods is needed to ensure the success of new design concepts based on (1) High Pressure Turbine Cooling Improvements; (2) Metal Temperature Improvement, particularly through the use of directionally solidified or monocrystal metals; and (3) Advanced Fiber-Reinforced Hollow Titanium Blades. This development should be based on a combined experimental-analytical approach, such as that which yielded the results shown in Figure 6.4-1.

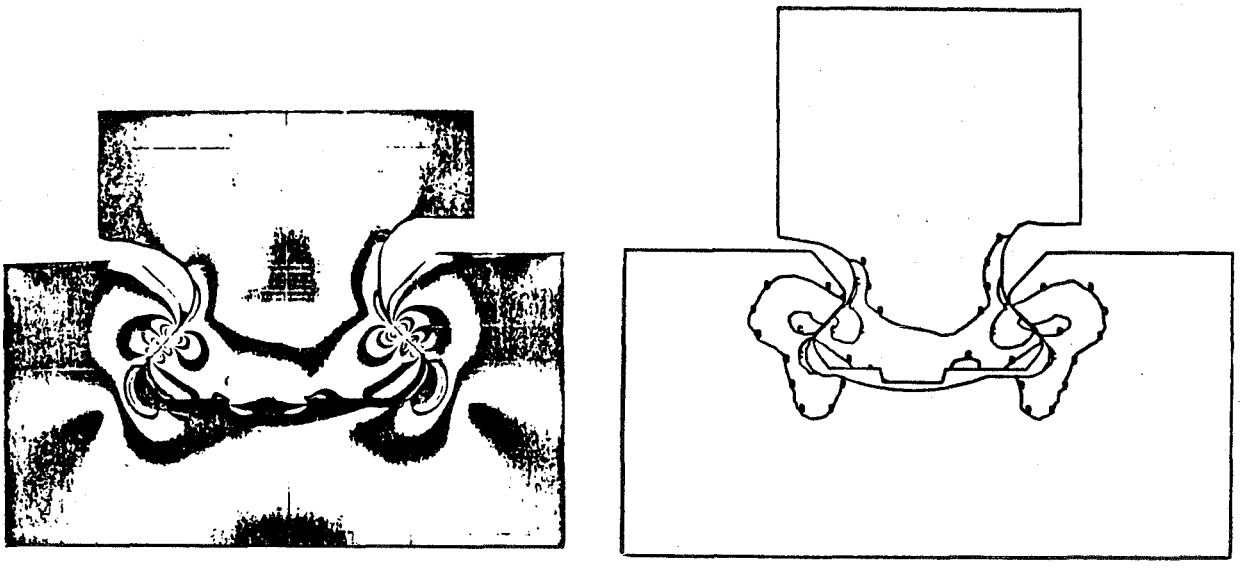

Photoelastic Results

Analytic Results

Figure 6.4-1. Comparison Between Analytic and Photoelastic Data.

Identification Number 6.4

Program Title: Dovetail Design Verification Program

Objective: Allow the designer to analyze gas turbine fan, compressor, and turbine blade dovetails in a timely fashion, based on proven methods which correctly account for 3D effects and friction.

Tasks	Schedule, Months
• Develop specialized 3D mesh generator for dovetails	4
• Verify model with experimental data	4
• Perform sensitivity study to establish significant design parameters	4

Elapsed Time 12

Probability of Success 90%

6.5 ANALYSIS TOOLS FOR PREDICTING FABRICATION EFFECTS

The improvement in stress and life analysis methods which has made it possible to design components with higher stresses and smaller margins of safety has, paradoxically, made it imperative to take into account all of the stress-inducing factors, including those which, up to now, have been ignored. Among these are the residual stress-strain distributions resulting from manufacturing processes. Thus, Figure 6.5-1 shows the residual stress distributions, as a function of depth from the surface, in a 0.4-inch-diameter bar for two different shot-peening intensities: "standard" and "heavy". The data points represent x-ray strain measurements, and the curves are the results of elastic-plastic stress analyses which were matched to the data to provide the complete stress-strain distributions. The value of fitting this analytical result to the data is shown in Figure 6.5-2. This figure shows axial stress as a function of radius from the center of the 0.4-inch-diameter bar. The initial residual stress distribution (square symbols) is the same as in Figure 6.5-1. The bar is then loaded and the calculated elastic-plastic stress is shown as the curve defined by the circles. Unloading to zero strain on the bar resulted in a calculated stress redistribution shown by the curve through the triangular symbols. What is of particular interest here is that the subsurface residual tensile stress peak between r=0.183 inch and r=0.193 inch is eliminated, and the residual compressive peak at r=0.1985 inch is increased. This analysis simulated metal behavior at a stress concentration where the increase in the compressive peak would be desirable. A similar analysis of the heavy peen specimen did not show this beneficial effect.

Combined analytical-experimental analyses of this type are needed to determine the influence of fabrication effects on such advanced concepts as HPT Metal Cooling Improvement, HPT Metal Temperature Improvement, and the Bonded HP Compressor Blisk.

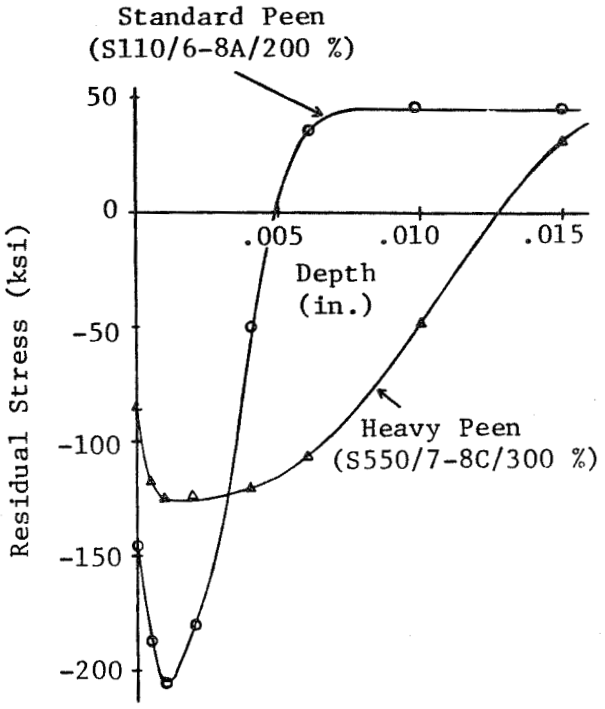

Figure 6.5-1. Residual Stress Distributions in Shot-Peened Surfaces.

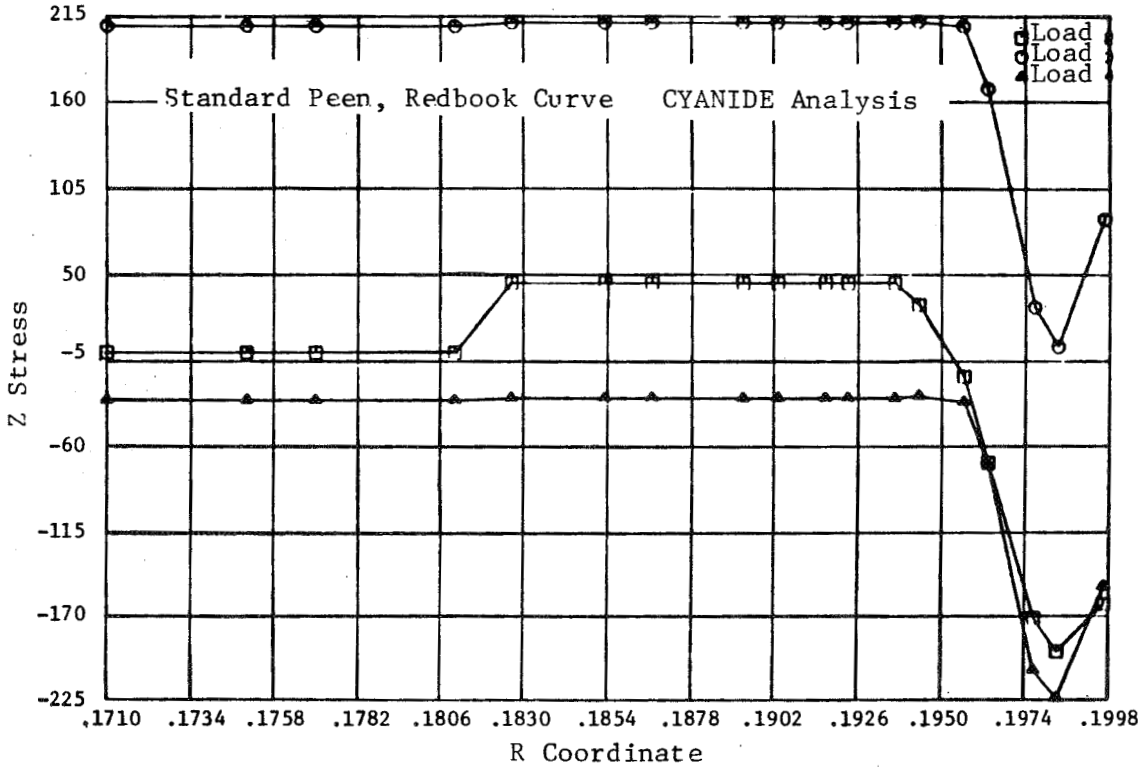

Figure 6.5-2. Effect of Strain-Controlled Cyclic Load on Residual Stress Distribution.

Program Title: Analysis Tools for Predicting Fabrication Effects

Identification Number 6.5

Objective: Provide the necessary analytical tools whereby the residual stresses and strains and deformations occurring due to aircraft gas turbine engine fabrication techniques can be predicted and taken into account for performance and durability projections.

Tasks	Schedule, Months
• Develop material property test techniques for manufacturing processes - Phase change - Ultra-high temperature, up to melting	18
• Accumulate material property data	24
• Develop theoretical analysis techniques	24
• Develop analysis computer programs	36
• Verify techniques and tools	15

Elapsed Time 60

Probability of Success 65%

6.6 STRUCTURAL, LIFE ANALYSIS, AND TEST TECHNIQUES FOR COATINGS

Turbine blades and vanes are now routinely coated for corrosion and oxidation protection. However, the influence of these coatings on component life is not understood very well. Figure 6.6-1 illustrates the influence of strain-temperature conditions on coating crack initiation for two different blades. Cracking of the coatings not only exposes the underlying metal to chemical attack, but may predispose it to earlier crack initiation and more rapid crack growth than a comparable uncoated part. Successful development of thermal barrier coatings will compound this problem. Success of the thermal barrier coating program will require an in-depth program to (1) develop the mechanical properties of coatings and coated metals, (2) develop the stress analysis and life prediction methods to incorporate these properties, and (3) accumulate the test data to make component life predictions. With the fundamental methods developed, computer programs will have to be written to apply these methods to components, and a verification program will have to be completed to establish confidence in the methods' predictions.

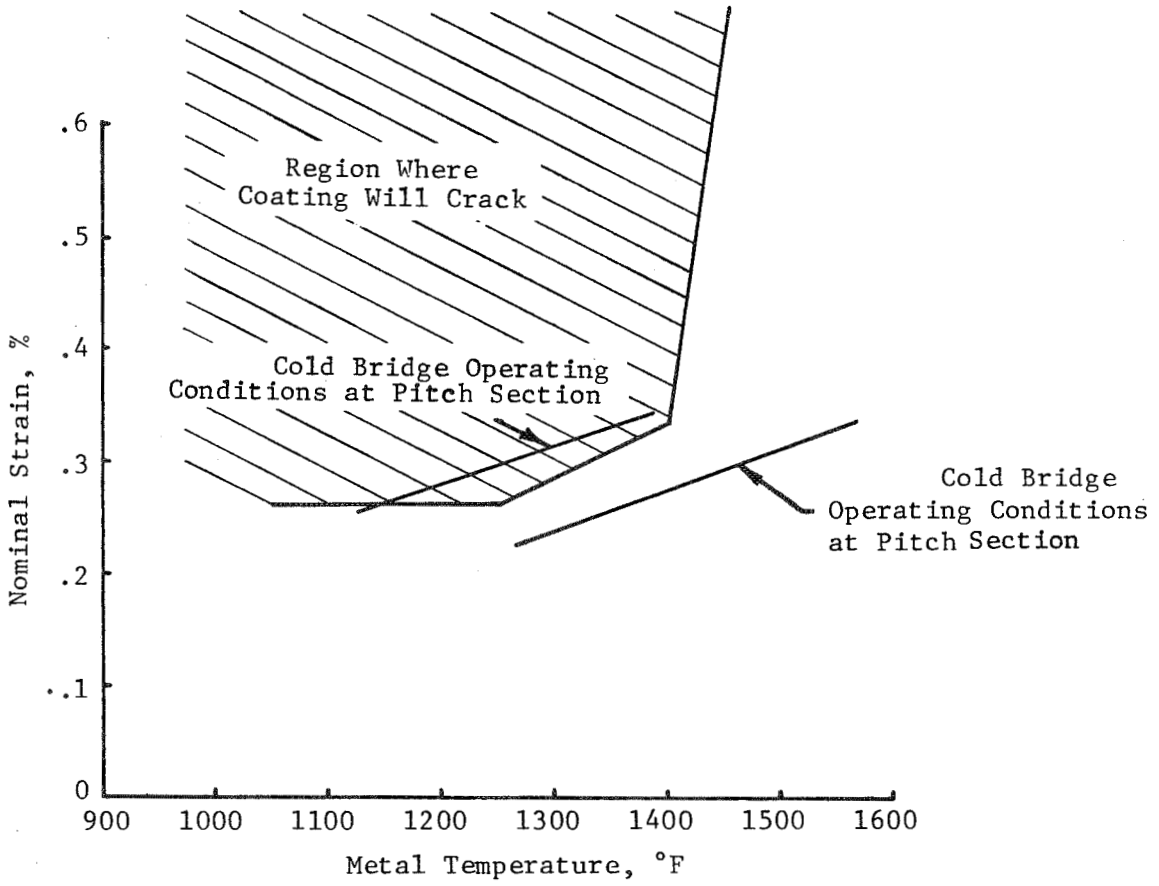

Figure 6.6-1. **Production Blades** – Cold Bridge Design Operating Strain-Temperature Conditions.

Identification Number 6.6

Program Title: Structural, Life Analysis, and Test Techniques of Coatings

Objective: Develop the necessary material property data and analytical tools to allow the efficient, deterministic use of coatings in aircraft gas turbine engines.

Tasks	Schedule, Months
• Develop testing techniques	12
• Accumulate material property data	18
• Develop theoretical analysis techniques	18
• Develop analysis computer programs	12
• Develop life prediction techniques	12
• Verify techniques and tools	12

Elapsed Time 36

Probability of Success 75%

6.7 ANISOTROPIC TURBINE BLADE AND VANE LIFE PREDICTION

The usual approach to service evaluation of a new gas turbine material is by a direct material substitution in an existing part, with little or no design change. For most material substitutions a new design is usually needed for optimal use of the new material's unique properties. Nowhere is this more true than for anisotropic materials such as directionally solidified (DS) monocrystal materials for turbine blades. A typical result from an analytical comparison between DS and conventionally cast Rene' 80 turbine blades shows a marked advantage for DS materials in the longitudinal (growth) direction but lower life in the transverse direction (Figure 6.7-1). An extensive technology program is therefore needed to support the successful introduction of anisotropic materials into gas turbine blades and vanes.

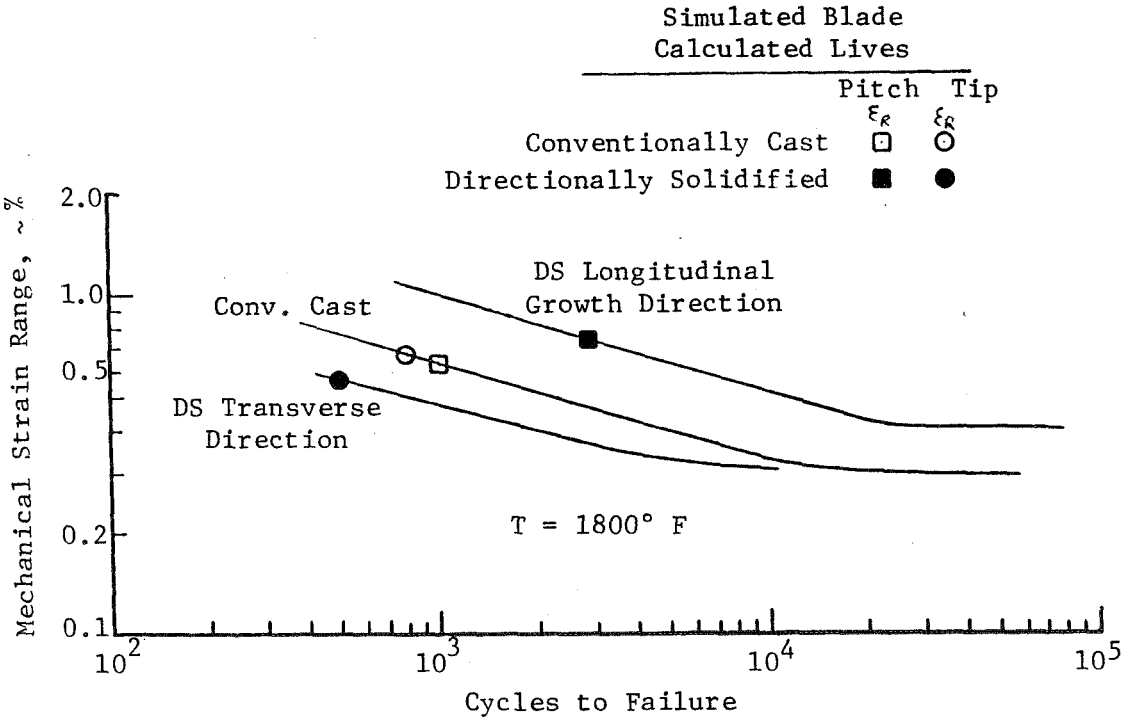

Figure 6.7-1. Low Cycle Fatigue of Conventionally Cast and Directionally Solidified Rene' 80 Alloys.

Program Title: Anisotropic Turbine Blade and Vane Life Prediction

Identification Number 6.7

Objectives: Develop structural-analysis and life-prediction technology for designing durable solidified and monocrystal turbine blades and vanes. This will improve engine efficiency by a 100^{0} F increase in turbine temperatures while maintaining adequate blade life.

Tasks	Schedule, Months
• Develop testing techniques for anisotropic materials	18
• Accumulate material property data	30
• Develop theoretical analysis techniques	18
• Develop analysis computer programs	24
• Develop life prediction methods	24
• Verify techniques and methods	15

Elapsed Time 60

Probability of Success 75%

6.8 COMPONENT FATIGUE AND RUPTURE DAMAGE ASSESSMENT

The high cost impact of current gas-turbine structural and life analysis arises from the very large uncertainty in the resulting component life predictions. This leads to a dilemma: premature failures can cause engine shutdowns, but premature part removals are costly. The dilemma is heightened when performance improvements have been achieved through the use of advanced mechanical design concepts: replacing parts is often costlier, yet to not replace them is to risk greater unknowns. This problem is felt throughout the engine, and, as shown in Table 6.0-1, bears upon eight of the eighteen advanced design concepts.

Four factors contribute to life uncertainty:

(1) Inherent scatter in material life test data
(2) Approximations and inaccuracies in design methods
(3) Engine usage variability: variable mission load, time and temperature spectra
(4) Multiple failure modes: high- and low-cycle fatigue (crack initiation), crack growth, creep, and rupture

Improvement of life prediction at the design stage is an ongoing effort. An additional and equally cost-effective approach would be to develop improved techniques to assess accrued damage and residual life in high-time parts. Parts nearing the end of their service life (measured in hours of use), which for commercial operation is one-third of the design life, are now being subjected to destructive testing to ascertain their residual life. The service life is then extended by one-half of the residual life. The approach used is strength and life testing to evaluate the residual life at critical locations in the component. This is time-consuming, costly, and inherently no more accurate than the original design-life prediction. If interpreted conservatively, it does, however, provide a basis for component life extension.

What is needed is a broader and more fundamental approach to residual life determination, one which would combine fundamental metallurgical and mechanics-of-materials ideas with currently used engineering approaches to evaluating fatigue and rupture damage accrued by high-time engine components. Figure 6.8-1 shows some preliminary results from this type of approach. Though this program would be on a high-risk level, the payoff would be extremely high - both directly, in cost savings through extended part usage, and indirectly, by allowing components to be designed to incorporate performance improvements without incurring structural life penalties.

Examples

Rene' 80 982C (1800F)
(Antolovich et al.)

- Oxidation Spike Length Correlates with Fatigue Life
- Coffin-Manson Exponent Derived from Oxidation Model

AISI 304 SS (649C, 1200F)
(Nahm)

- **Fatigue Life Correlates with Dislocation Cell Size**

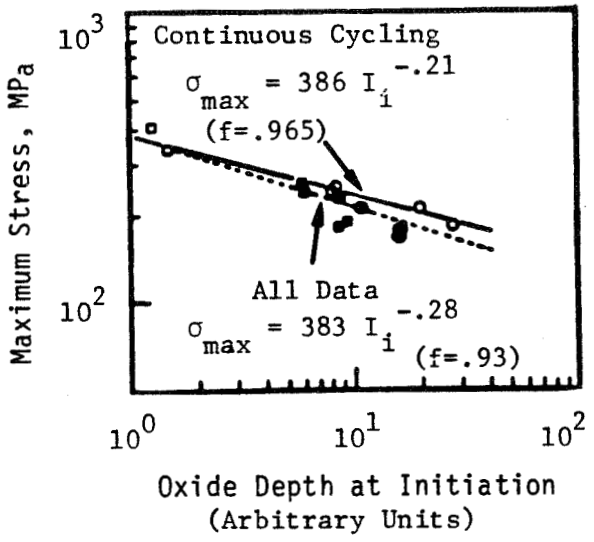

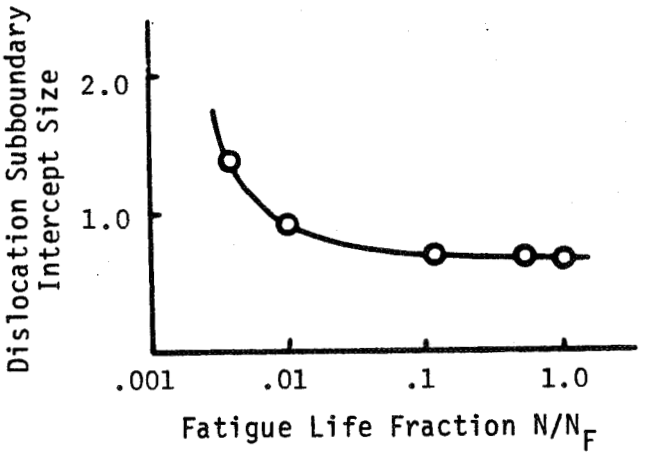

Figure 6.8-1. Microstructural Damage Assessment.

Program Title: Component Fatigue and Rupture Damage Measurement

Identification Number 6.8

Objectives: Establish quantitative microstructural measurements of fatigue and rupture damage in aircraft engine structural materials subjected to elevated temperature at high stress.

Tasks	Schedule, Months
• Acquire material (3 alloys)	5
• Manufacture test specimens	6
• Cyclic fatigue and stress rupture testing	12
• Metallographic assessment of damage	16
• Establish damage parameter	18
• Develop life management criteria	6
• Final report and recommendations	4

Elapsed Time 60

Probability of Success 50%

6.9 EXTEND MANSON - HALFORD DAMAGE-CURVE LIFE ANALYSIS METHODOLOGY TO AIRCRAFT GAS TURBINE PROBLEMS

A fundamental problem in predicting fatigue life of gas turbine components, as well as many other types of machinery and structures, is that the life of a part that will undergo a complex load history is predicted using fatigue-life data obtained from simple cycle tests. The accepted approach is to use a linear damage rule - Miner's rule - which predicts failure when

$$\sum_i \left(\frac{n_i}{N_i} \right) = 1$$

where: n_i = number of cycles imposed at stress (strain) range $\Delta \sigma_i$ ($\Delta \varepsilon$), and N_i = number of cycles to failure under stress (strain) range $\Delta \sigma_i$ ($\Delta \varepsilon_i$).

Experience has shown that failure may actually occur when the summation attains a value in the range 0.5 to 2.00. Recently S.S. Manson and G.R. Halford have succeeded in correlating bi-level stress range test data using the Damage-Curve concept shown on Figure 6.9-1 (NASA TM 81517, 1980). This approach allows for nonlinear damage accumulation, which includes a loading order or history effect. Though test data show this effect to be important, it is not included in linear damage theory. The Manson-Halford Damage Curve is a very promising beginning which needs to be extended to the many other effects which influence component life in gas turbines: multiaxial stresses, variable temperature loading, creep, and residual stress. As shown in Table 6.0-1. extension of the Damage-Curve approach will facilitate many advanced performance concepts without imposing undue penalties in structural weight and cost.

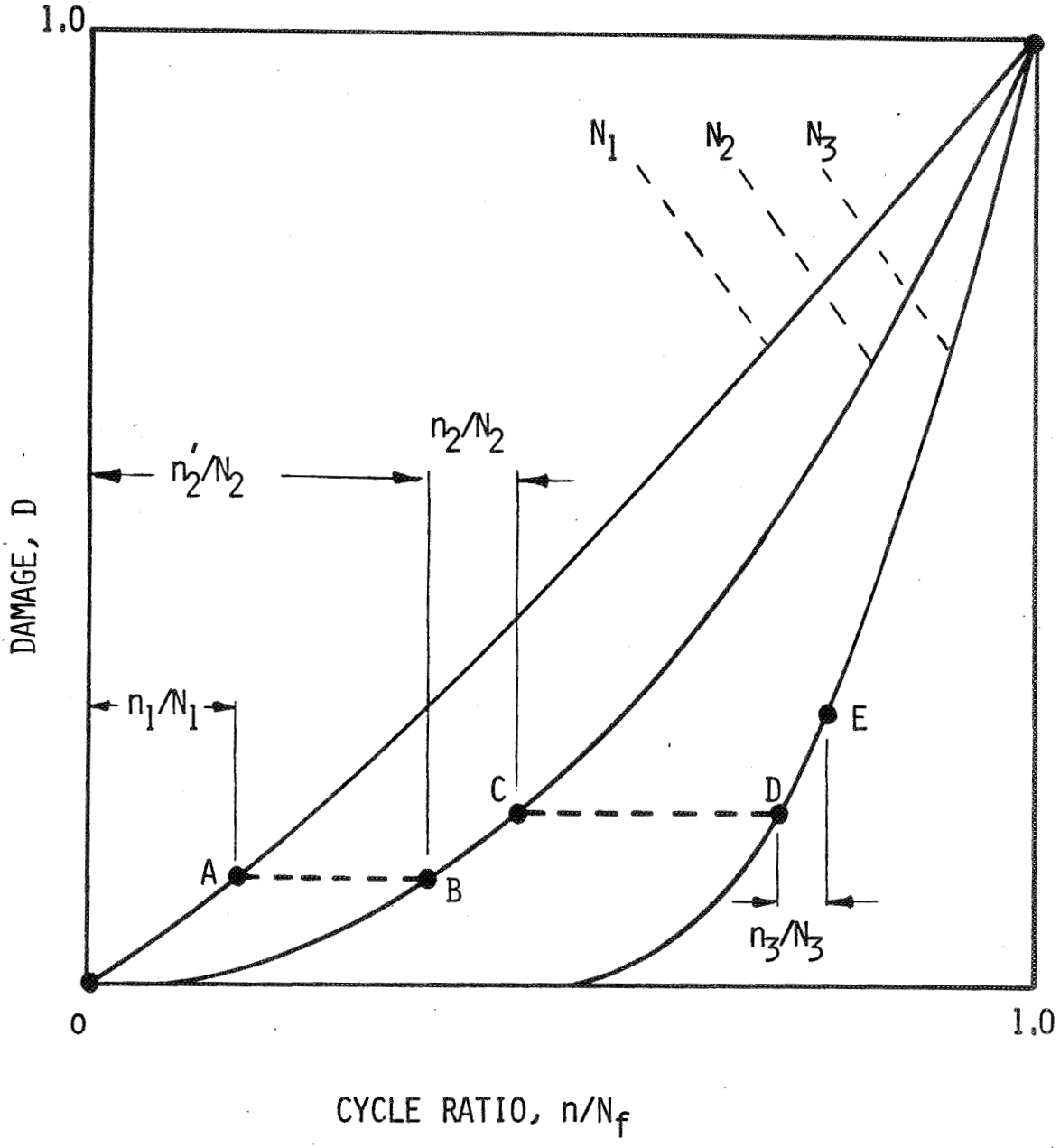

Figure 6.9-1. Manson-Halford Damage Curve.

Identification Number 6.9

Program Title: Extend Manson-Halford Damage-Curve Life Analysis Methodology to Aircraft Gas Turbine Problems

Objective: Incorporate additional complexities which occur in aircraft turbine engine life problems into the Manson-Halford Damage Curve methodology, thereby making it a powerful tool for aircraft gas turbine engine durability predictions.

Tasks	Schedule, Months
• Develop theoretical techniques for:	
- Residual stresses and strains	12
- Creep	16
- Multiaxial stresses and strains	12
- Multiple variable temperature loading	20
• Develop necessary test data	12
• Verify with complex testing	18

Elapsed Time 36

Probability of Success 80%

6.10 INCORPORATE DAMPING INTO VIBRATION ANALYSIS

Gas turbine fan blades must be shrouded to raise their resonant vibration frequencies and avoid blade flutter. This reduces the fan efficiency and imposes an engine performance penalty. The use of composite materials to eliminate blade shrouds is an approach that has floundered because of the low impact resistance of composites. An alternate approach now being investigated is a hollow blade with a superplastic-formed titanium core, with fiber-reinforced titanium outer surfaces (Figure 6.10-1). This type of structure is ideally suited to the incorporation of damping material. Structural analysis techniques do not exist today which would allow systematic study of possible damping concepts for this configuration. A combined-analytical-methods development program with experimental verification is needed.

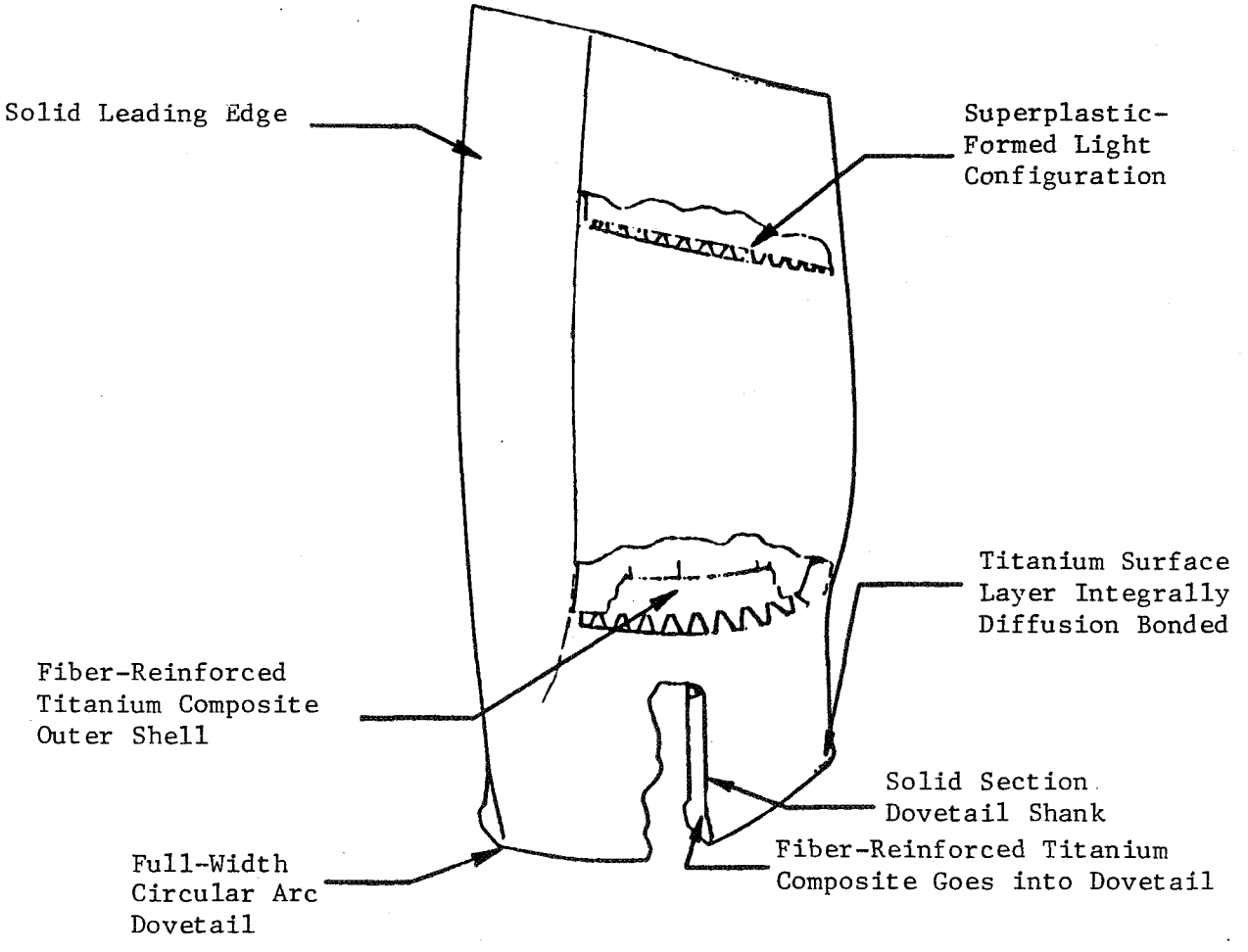
Solid Leading Edge
Superplastic-Formed Light Configuration
Titanium Surface Layer Integrally Diffusion Bonded
Fiber-Reinforced Titanium Composite Outer Shell
Solid Section Dovetail Shank
Fiber-Reinforced Titanium Composite Goes into Dovetail
Full-Width Circular Arc Dovetail

Figure 6.10-1. Proposed Conceptual Design Fiber-Reinforced Titanium Blade.

Identification Number 6.10

Program Title: Incorporate Damping into Vibration Analysis

Objective: Provide the verified analytical tools whereby it will be possible to design aircraft gas turbine engine blades (fan blades) in the engine excitation frequency range through the effective use of damping.

Tasks	Schedule, Months
• Accumulate damping data on proposed damped structures	18
• Develop theoretical analysis techniques	24
• Develop analysis computer programs to optimize damping	18
• Verify techniques and tools	12

Elapsed Time 48

Probability of Success 65%

6.11 TIME-SHARING COMPUTER PROGRAM FOR THE ANALYSIS OF TURBOMACHINERY VIBRATION

Whether a new gas turbine concept is aimed at performance improvement or structural life improvement, one of the major constraints on its application is the control of engine system vibration. Present-day practice yields very flexible engines in which, for two-spool engines, the frequencies of the first two rigid-body modes, and often the first shaft bending mode, are below the engine operating speed range. Control of the higher modes and frequencies then becomes a major design problem. Many iterations are usually needed to arrive at a satisfactory design. Because batch computer calculations of system vibration require a substantial turnaround time between runs, there is often a limitation on the number of analyses than can be made prior to a design decision. Development of a time-sharing interactive analysis would facilitate system vibration analyses for preliminary design of such concepts as the shortened fan flowpath. Development of this analytical tool by NASA would provide an economical common approach to system vibration analysis, which would be usable not only by the engine manufacturers, but also by contractors and users: NASA, the armed services, airlines, utilities, pipeline companies, etc.

- A COMBINED TRANSFER MATRIX-DIRECT STIFFNESS APPROACH FOR PRELIMINARY DESIGN AND TRADE-OFF STUDIES

- DIRECT SOLUTION APPROACH
  - PROHL-MYKLESTAD METHOD TO REDUCE THE DIMENSIONALITY
  - DIRECT STIFFNESS METHOD TO ADDRESS BRANCHED LOAD PATHS

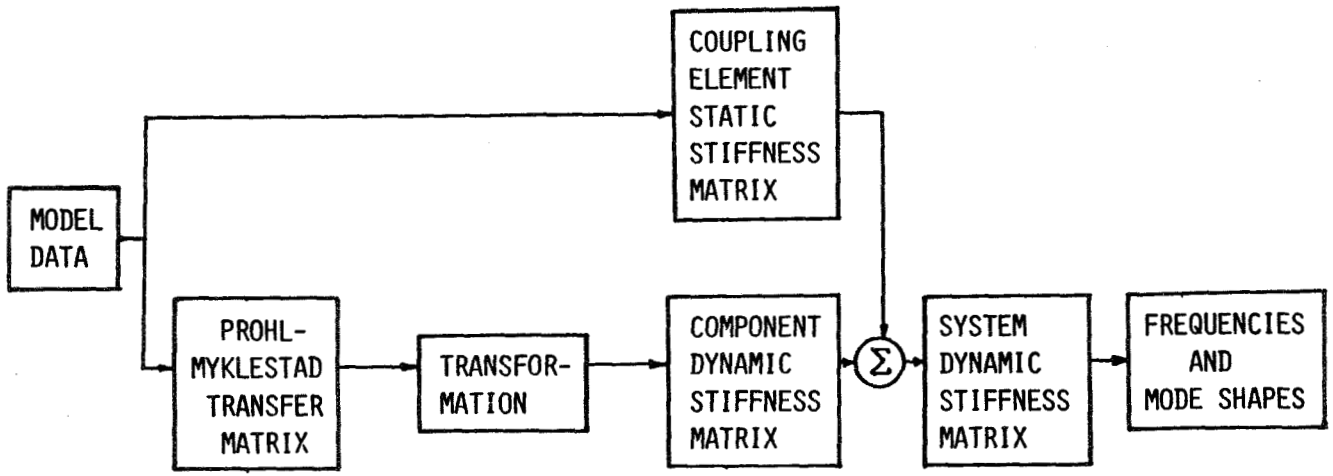

Figure 6.11-1. Time-sharing Computer Program for the Analysis of Turbomachinery Vibration.

Identification Number 6.11

Program Title: Time-Sharing Computer Program for the Analysis of Turbomachinery Vibration

Objective: Develop a time-sharing computer program for initial design analysis of turbomachinery vibration. The program to be developed would allow the quick examination of a wide range of possible rotor-system configurations in the early design phase.

Tasks	Schedule, Months
• Develop subsystem finite-element based on transfer-matrix direct-stiffness approach	3
• Develop generalized multi-point spring element stiffness matrix for use in subsystem coupling	3
• Develop assembly program to generate system dynamic stiffness matrix and develop frequency search algorithm	6

Elapsed Time 12

Probability of Success 100%

6.12 TRANSIENT BLADE-OUT MODAL ANALYSIS OF ADVANCED HIGH-BYPASS TURBOFAN ENGINES INCLUDING THE EFFECTS OF MULTIPLE RUBS

The unbalance caused by the loss of a fan or turbine blade can induce severe rubs and extensive secondary damage to engines. While the loss of a single blade can be tolerated, it is imperative that the engine design be evaluated for the likelihood that the engine will suffer secondary damage, which can cause an engine shutdown. The TETRA computer program, developed under NASA Contract NAS3-22053, makes it possible to analyze the problem.

This type of analysis is particularly needed for new structural concepts such as the shortened fan flowpath and the low-pressure-turbine flared flowpath. The program in its present form allows for multiple rubs. What is needed, however, is additional verification studies to establish blade-loss and multiple-rub event/time histories which simulate actual blade-out events. To support these analyses, system studies must be conducted to optimize the engine modelling in terms of modal representation of the subsystems which make up the overall engine model. This will ensure accurate and economical analysis of multiple engine rubs.

Identification Number 6.12

Program Title: Transient Blade-Out Modal Analysis of Advanced High-Bypass Turbofan Engines including the Effects of Multiple Rubs

Objectives: Using the TETRA component element program developed under NASA contract NAS3-22053, perform transient blade-out analyses addressing secondary damage resulting from a sequence of blade loss and rub events. The study will include an investigation of the effects of modal truncation.

Tasks	Schedule, Months
• Subsystem modeling of the E^3 Based upon the existing system vibration model	2
• Establish number of modes for each subsystem for effective linear simulation	2
• Establish blade loss and rub-event/time history for realistic simulation of turbofan behavior under abusive-vibration blade-loss conditions	3
• Perform studies investigating the number of of subsystem modes required to obtain convergent solutions for nonlinear blade-loss/rub simulation	6
Elapsed Time	12

Probability of Success 100%

6.13 TRANSIENT ANALYSIS AND DESIGN CRITERIA FOR ENGINE SEIZURE LOADS

The ability to withstand seizure loads is a design requirement for gas turbine engines. While present methods are based on absorption of the torsional rotational kinetic energy in the shaft, the actual dynamics of an engine seizure are much more complex. Thus, a more precise understanding of seizure dynamics is needed to ensure the success of some of the advanced structural concepts listed in Table 6.0-1.

The TETRA program developed by GE-AEBG for NASA allows this analysis to be developed. Figure 6.13-1 shows shaft deflections caused by fan unbalance both with and without blade-casing rubs, as calculated using TETRA. By assuming that seizure occurs after the initial rub encounter, the engine dynamics of seizure can be calculated with a minimum number of changes to TETRA. Table 6.13-1 shows (as filled circles) the degrees of freedom now included in the TETRA program. Since the engine case already includes torsional degrees of freedom, only two torsional degrees of freedom (represented in Table 6.13-1 by triangles) need to be added to each rotor. The end product will contribute to flight safety by providing a more complete model of engine rub/seizure dynamics.

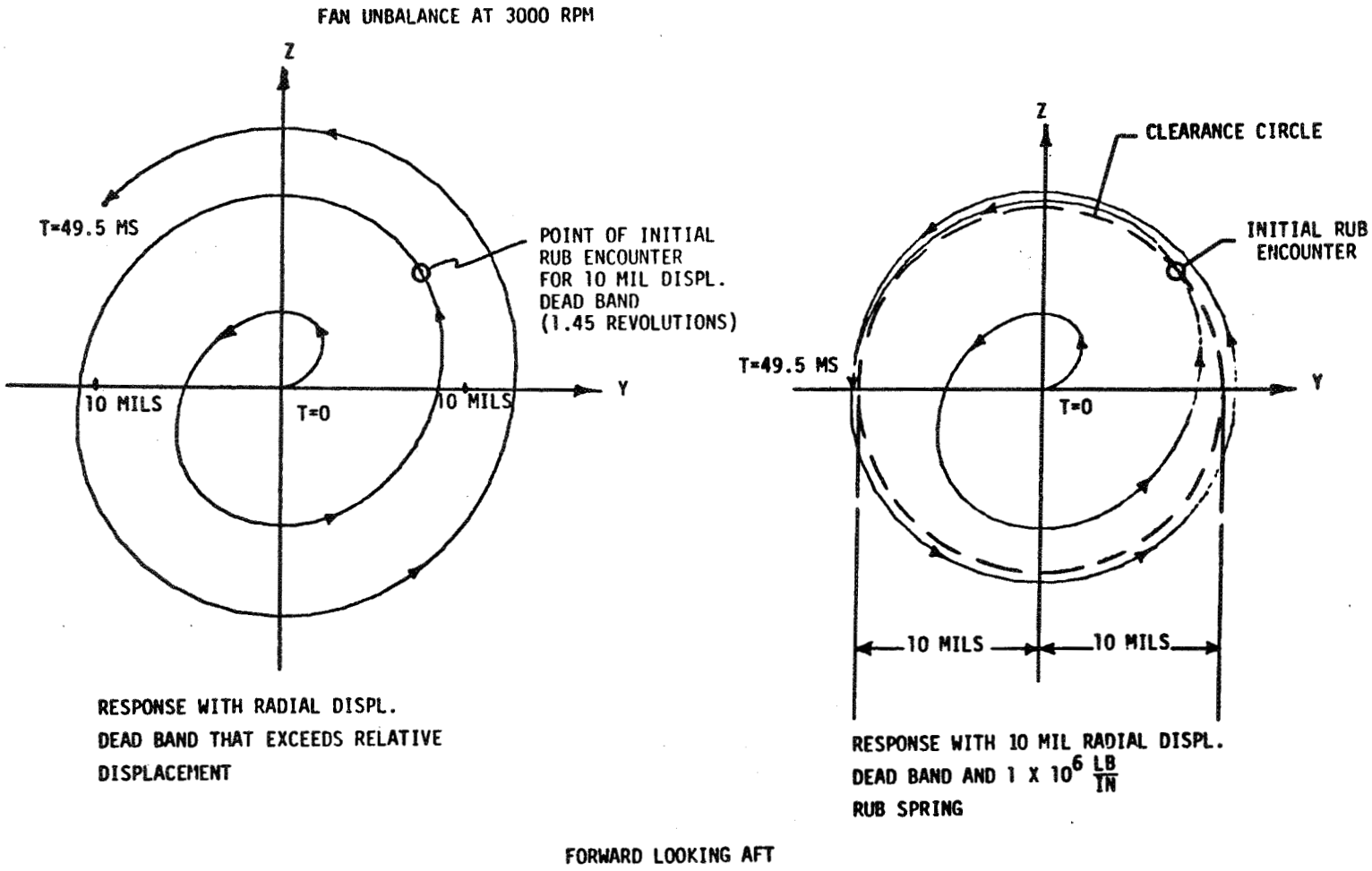

Figure 6.13-1. Locus of Relative-Displacement Vector Between the Fan Rotor and the Case for the Demonstrator Model for Sudden 100 gm-in. Fan Unbalance at 3000 rpm.

Table 6.13-1. Physical Global Degrees of Freedom and Direction Numbers for the Subsystems.

SUBSYSTEMS	GLOBAL DEGREES-OF-FREEDOM					
	Z	Θ_Y	Y	Θ_Z	X	Θ_X
	1	2	3	4	5	6
VERTICAL PLANE FLEXIBLE ROTOR (S)	●	●				
HORIZONTAL PLANE FLEXIBLE ROTOR (S)			●	●		
RIGID BODY ROTOR (S)	●	●	●	●	●	△
VERTICAL PLANE FLEXIBLE CASE	●	●				
HORIZONTAL PLANE FLEXIBLE CASE			●	●		
RIGID BODY CASE	●	●	●	●	●	●
TORSIONAL FLEXIBLE CASE						●
3D FLEXIBLE PYLON	●		●		●	
TORSIONAL FLEXIBLE ROTOR						△

● - Degree of Freedom now in TETRA

△ - Torsional Degree of Freedom Needed to be Added to Each Rotor

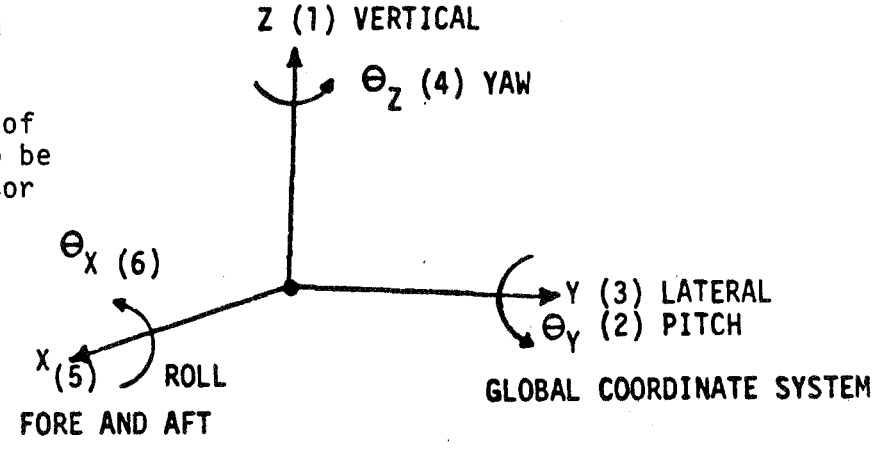

Program Title: Transient Analysis and Design Criteria for Engine Seizure Loads

Identification Number 6.13

Objectives: Incorporate seizure loads analysis capabilities into an existing engine-system transient analysis computer program and develop design criteria in order to replace empirical procedures for seizure loads design analysis.

Tasks	Schedule, Months
• Develop nonlinear-seizure-force finite element	2
• Incorporate the seizure element into an existing engine-system transient analysis program	4
• Check-out/refine the new analysis capability based on correlations with existing test data	3
• Develop design criteria	4

Elapsed Time 12

Probability of Success 95%

7.0 DISTRIBUTION

	Mail Stop	Copies
NASA Lewis Research Center 21000 Brookpark Road Cleveland, OH 44135		
Attn: Contracting Officer	501-11	1
Technical Report Control	5-5	1
Technology Utilization Office	3-19	1
AFSC Liaison Office	501-3	1
S and MT Div. Contract File	49-6	1
Library	60-3	1
J. A. Ziemianski	49-6	1
L. Berke	49-6	1
R. H. Johns	49-6	1
G. T. Smith	49-6	1
G. V. Brown	49-6	1
C. C. Chamis	49-6	1
L. J. Kiraly	49-6	20
N. T. Saunders	49-6	1
M. H. Hirschberg	49-6	1
L. P. Ludwig	23-2	1
C. C. Ciepluch	301-4	1
J. W. Schaefer	301-4	1
L. E. Macioce	86-3	1
F. D. Berkopec	301-2	1
National Aeronautics and Space Administration Washington DC 20546		
Attn: NHS-22/Library		2
RTM-6/L. A. Harris		1
RTM-6/S. L. Venneri		1
RTM-6/D. Weidman		1
NASA Ames Research Center Moffett Field, CA 94035		
Attn: Library	202-3	1
NASA Goddard Space Flight Center Greenbelt, MD 20771		
Attn: 252/Library		1
NASA John F. Kennedy Space Center Kennedy Space Center, FL 32931		
Attn: Library	AD-CSO-1	1
NASA Langley Research Center Hampton, VA 23365		
Attn: Library	185	2
Nasa Lyndon B. Johnson Space Center Houston, TX 77001		
Attn: JM6/Library		1
NASA George C. Marshall Space Flight Center Marshall Space Flight Center, AL 35812		
Attn: AS61/Library		1

	Copies
Jet Propulsion Laboratory 4800 Oak Grove Drive Pasadena, CA 91103 Attn: Library	1
NASA S and T Info. Facility P. O. Box 8757 Baltimore-Washington Int.Airport MD 21240 Attn: Acquisition Dept.	25
Air Force Systems Command Aeronautical Systems Division Wright-Patterson AFB, OH 45433 Attn: Library C. W. Cowie	1 1
Air Force Wright Aeronautical Laboratories Wright-Patterson AFB, OH 45433 Attn: I. Gershon L. Bailey F. Schmidt	1 1 1
Aerospace Corp. 2400 E. El Segundo Blvd. Los Angeles, CA 90045 Attn: Library-Documents	1
Air Force Office of Scientific Research Washington DC 20333 Attn: Library	1
Department of the Army U.S. Army Material Command Washington DC 20315 Attn: AMCRD-RC	1
U.S. Army Ballistics Research Lab. Aberdeen Proving Ground, MD 21005 Attn: Dr. Donald F. Haskell DRXBR-BM	1
Mechanics Research Lab. Army Materials and Mechanics Research Center Watertown, MA 02172 Attn: Dr. Donald W. Oplinger	1
Commanding Officer U.S. Army Research Office (Durham) Box CM, Duke Station Durham, NC 27706 Attn: Library	1
Bureau of Naval Weapons Department of the Navy Washington DC 20360 Attn: RRRE-6	1

	Copies
Commander U.S. Naval Surface Weapons Center Dahlgren, VA 20910 Attn: Library	1
Director, Code 6180 U.S. Naval Research Laboratory Washington DC 20390 Attn: Library	1
Denver Federal Center U. S. Bureau of Reclamation P. O. Box 25007 Denver, CO 80225 Attn: P. M. Lorenz	1
National Technical Information Service Springfield, VA 22151	1
Naval Air Propulsion Test Center Aeronautical Engine Department Trenton, NJ 08628 Attn: Mr. James Salvino	1
Naval Air Propulsion Test Center Aeronautical Engine Dept. Trenton, NJ 08628 Attn: Mr. Robert DeLucia	1
Naval Air Propulsion Test Center Aeronautical Engine Department Trenton, NJ 08628 Attn: Mr. G. J. Mangano	1
Federal Aviation Administration Code ANE-214, Propulsion Section 12 New England Executive Park Burlington, MA 01803 Attn: Mr. Robert Berman	1
Federal Aviation Administration DOT Office of Aviation Safety, FOB 10A 800 Indepdendence Ave., SW Washington DC 20591 Attn: Mr. John H. Enders	1
Federal Aviation Administration AFS-140 Washington DC 20591 Attn: Mr. A. K. Forney	1
FAA, AFS-140 800 Independence Ave., SW Washington DC 20591 Attn: Dr. Thomas G. Horeff	1

	Copies
FAA, ARD-520 2100 Second Street, SW Washington DC 20591 Attn: Cdr. John J. Shea	1
National Transportaion Safety Board 800 Independence Ave., SW Washington DC 20594 Attn: Mr. Edward P. Wizniak, TE-20	1
MIT Room 33-313 Cambridge, MA 02139 Attn: Professor John Dugundji Professor James Mar	1 1
MIT Room 33-207 Cambridge, MA 02139 Attn: Professor Rene H. Miller	1
MIT Room 41-219 Cambridge, MA 02139 Attn: Professor Emmett A. Witmer	1
MIT Room 6-202 Cambridge, MA 02139 Attn: Dr. David Roylance	1
Rockwell International Corp. Los Angeles International Airport Los Angeles, CA 90009 Attn: Mr. Joseph Gausselin D 422/402 AB71	1
Stevens Inst. of Technology Castle Point Hoboken, NJ Attn: Dr. F. Sisto	1
University of Illinois at Chicago Circle Dept. of Materials Engineering Box 4348 Chicago, IL 60680 Attn: Dr. Robert L. Spilker	1
Detroit Diesel Allison General Motors Corp. Indianapolis, IN 46206 Attn: Mr. Joseph Byrd Dr. Pete Tramm Dr. Lynn Synder N. Provenzano Library	1 1 1 1 1

	Copies
AVCO, Lycoming Division 550 South Main Street Stratford, CT 06497 Attn: Mr. Herbert Kaehler	1
AVCO, Lycoming Division 550 South Main Street Stratford, CT 06497 Attn: Mr. John Veneri	1
Beech Aircraft Corp., Plant 1 Wichita, KA 67201 Attn: Mr. M. K. O'Connor	1
Albany International Research Co. 1000 Providence Highway Dedham, MA 02026 Attn: James Blout	1
Boeing Commercial Airplane Co. Seattle, WA 98111 Attn: C. Lewis	1
Boeing Aerospace Co. Impact Mechanics Lab. P. O. Box 3999 Seattle, WA 98124 Attn: Dr. R. J. Bristow	1
Boeing Commercial Airplane Co. P. O. Box 3707 Seattle, WA 98124 Attn: Dr. Ralph B. McCormick Dr. Dirk Bower	1 1
Boeing Commercial Airplane Co. P. O. Box 3707 M.S. 73-01 Seattle, WA 98124 Attn: Dr. David T. Powell Dr. John H. Gerstle	1 1
Boeing Company Wichita, KA Attn: Mr. C. F. Tiffany	1
McDonnel Douglas Aircraft Corp. P. O. Box 516 Lambert Field, MO 63166 Attn: Library	1
Douglas Aircraft Co. 3855 Lakewood Blvd. Mail Code 36-41 Long Beach, CA 90846 Attn: Ron Kawai	1

	Copies
General Dynamics P. O. Box 748 Fort Worth, TX 76101 Attn: Library	1
General Dynammcs/Convair Aerospace P. O. Box 1128 San Diego, CA 92112 Attn: Library J. Jensen	1 1
Garrett Airesearch Mfg. Co. Box 5217 Phoenix, AZ 85010 Attn: Dr. L. Matsch E. Nelson	1 1
Grumman Aircraft Engineering Corp. Bethpage, Long Island, NY 11714 Attn: Library	1
IIT Research Institute Technology Center Chicago, IL 60616 Attn: Library I. M. Daniel	1 1
Lockheed California Co. P. O. Box 551 Dept. 73-31, Bldg. 90, PL. A-1 Burbank, CA 91520 Attn: Mr. D. T. Pland	1
Lockheed California Co. P. O. Box 551 Dept. 75-71, Bldg. 63, PL. A-1 Burbank, CA 91520 Attn: Mr. Jack E. Wignot	1
Northrop Space Laboratories 3401 West Bradway Hawthorne, CA 90250 Attn: Library	1
North American Rockwell, Inc. Rocketdyne Division 6633 Canoga Ave. Canoga Park, CA 91304 Attn: Library, Dept. 596-306	1
North American Rockwell, Inc. Space and Information Systems Div. 12214 Lakewood Blvd. Downey, CA 90241 Attn: Library	1

	Copies
TWA, Inc. Kansas City International Airport P. O. Box 20126 Kansas City, MO 64195 Attn: Mr. John J. Morelli	1
TRW Systems, Inc. One Space Park Redondo Beach, CA 90278 Attn: Technical Library	1
United Aircraft Corporation Pratt & Whitney Aircraft 400 E. Main Street East Hartford, CT 06108 Attn: Library J. Woodward R. Liss T. Cruse C. Platt E. Feder	1 1 1 1 1 1
United Aircraft Corporation Pratt and Whitney Group Government Products Division P. O. B2691 West Palm Beach, FL 33402 Attn: Library Mr. J. T. Dixon	1 1
United Technologies Research Center 400 E. Main St. East Hartford, CT 06108 Attn: A. V. Srinivasen	1
United Aircraft Corporation Hamilton Standard Division Windsor Locks, CT 06096 Attn: Dr. G. P. Townsend Library	1 1
Aeronautical Research Association of Princeton, Inc. P. O. Box 2229 Princeton, NJ 08540 Attn: Dr. Thomas McDonough	1
Teledyne CAE Box 6971 Toledo, OH 43612 Attn: T. Moyer H. Gaylord	1 1
Rensselaer Polytechnic Institute Troy, NY 12181 Attn: Professor R. Loewy	1

	Copies
Republic Aviation Fairchild Hiller Corp. Farmington, L. I., NY Attn: Library	1
Rohr Industries Foot of H Street Chula Vista, CA 92010 Attn: Mr. John Meaney	1